ALMA MATER STUDIORUM - UNIVERSITÀ DI BOLOGNA

SCUOLA DI INGEGNERIA E ARCHITETTURA

DIPARTIMENTO DI INGEGNERIA CIVILE, CHIMICA, AMBIENTALE E DEI MATERIALI

CORSO DI LAUREA MAGISTRALE IN INGEGNERIA CHIMICA E DEL PROCESSO

TESI DI LAUREA

in

Meccanica dei fluidi e fenomeni di trasporto

Preparation and characterization of grafted nonwoven membranes for bioseparations

CANDIDATO
Giulia Pierini

RELATORE:
Chiar.mo Prof. Ing.
Giulio Cesare Sarti

CORRELATORE
Prof. Ruben G. Carbonell

Anno Accademico 20015/16

Sessione II

Alla mia famiglia

ACKNOWLEDGMENTS

The list of people to whom I want to express my gratitude is quite long, I tried to synthetize as well as I could. They all, in different ways, have helped me to reach my goals and living new experience. They all deserve the most wholehearted “thanks”, I can express in writing. The order in which their names appear here does not reflect in any way a priority in my heart and thoughts. First, I want to thank my advisor, Dr. Ruben Carbonell and my Professor Giulio Cesare Sarti who gave me the chance to live this wonderful research experience in Raleigh. Both of them gave me important advice and suggestions. My thoughts go to an other professor in Bologna, in particular to Criatiana Boi, who helped me to solve various practical questions. My gratitude and affection go to Professore Stefano Menegatti, who had represented a key person, a person I could count on in every moment where I needed. He has introduced me in Raleigh (NC, USA) and I did not miss the Italian cuisine, due to his excellent ability to cook. The academic environment at NC State University has been my home for more than six months. I have become part a group of people who share with me the happiness, the moody day, the sadness for work, o for my personal life. I could not work with best people. My gratitude goes to each person who I worked with and supported me, proving patience and tolerability. I would like to name few as Tuhidul, Amith, Qian, Billy, Yang, Andrew, John, and the two Japanese guys.

A special thanks goes to Kate, a friend who used to work in lab. She made me the experience in Raleigh unforgettable. She was and is a special friend. Qian has joined later as post-doc to our research group. nevertheless I am very grateful for her help and the friend who is. I lived this experience in the best was thanks also to my boyfriend Fabio who came close to me (700 miles far) to develop a research study for his dissertation.

I can't say thank enough to my family. I am deeply grateful to the support, the patience, and the help that you always gave me.

ABSTRACT

La purificazione delle proteine ha un ruolo fondamentale nella industria biotecnologica e biofarmaceutica, ove i processi di separazione causano il 40-80% dei costi totali di produzione. Questo impegna le compagnie biofarmaceutiche a semplificare i processi di separazione, riducendo il numero di operazioni e sostituendo impianti costosi. In tal senso, membrane non-tessute di polibutilene terefatlato (PBT) sono state sviluppate come supporto cromatografico monouso. Le membrane non-tessute di PBT sono in grado di catturare la proteina target e ridurre i contaminanti mediante cromatografia a scambio ionico. Le membrane sono state modificate mediante grafting di uno strato di poli(glicidil-metacrilato) (GMA) ottenuto mediante polimerizzazione foto-indotta o termo-indotta. I gruppi epossidici del GMA monomero sono stati convertiti in gruppi di scambio ionico (ligandi) rispettivamente mediante reazione con acido solfonico o dietilammina (DEA). A seguito della formazione dei ligandi, i gruppi epossidici residui sono idrolizzati con acido solforico per ridurre la cattura non specifica di proteine.

Questa ricerca si è finalizzata allo studio di diversi parametri, in particolare l'effetto (i) della %-uale di modifica gravimetrica e (ii) della densità di ligando sulla capacità di legame statica delle membrane. Albumina di siero bovino (BSA) ed Immunoglobulina G umana (hIgG) sono state utilizzate come proteine modello negli studi di scambio anionico e cationico. Per la BSA, si è ottenuta una capacità di legame all'equilibrio di 673 mg/g di membrana a scambio anionico prodotta mediante grafting termo-indotto con una densità di ligando DEA di 1.54 mmol/g. Per la hIgG, si è ottenuta una capacità di legame all'equilibrio di 675 mg/g di membrana a scambio cationico prodotta mediante grafting termo-indotto con una densità di ligando di 0.47 mmol/g. Il rendimento delle membrane a scambio ionico prodotte mediante grafting termoindotto è stato studiato anche in condizioni di flusso. Spaziatori di poli(etilene tereftalate) (PET) rigido sono stati introdotti tra le membrane di PBT per aumentare la capacità di flusso totale della colonna cromatografica. Le perdite di carico delle membrane sono risultate dipendere dalla forza ionica della fase mobile, probabilmente a causa di un rigonfiamento parziale dello strato di modificazione, che ha causato un blocco dei pori. La capacità di legame dinamica misurata al 10% del punto di breakthrough (DBC10%) è risultata di 168mg/g per la BSA, con un tempo di residenza di 7.9 minuti. La DBC10% della hIgG è risultata di 100 mg/g, con un tempo di residenza di 3.9 e 7.9 minutes. La selettività di entrambe le membrane a scambio ionico e cationico è stata

misurata mediante assorbimento di BSA o hIgG da una miscela di proteine. Le membrane a scambio cationico non hanno riportato risultati soddisfacenti, mentre le membrane a scambio anionico prodotte mediante grafting termo-indotto hanno dimostrato di legare ed eluire la BSA ad elevata purezza e rendimento in un singolo passaggio di purificazione.

ABSTRACT

Protein purification plays a crucial role in biotechnology and biomanufacturing, where downstream unit operations account for 40%-80% of the overall costs. To overcome this issue, companies strive to simplify the separation process by reducing the number of steps and replacing expensive separation devices. In this context, commercially available polybutylene terephthalate (PBT) melt-blown nonwoven membranes have been developed as a novel disposable membrane chromatography support. The PBT nonwoven membrane is able to capture products and reduce contaminants by ion exchange chromatography. The PBT nonwoven membrane was modified by grafting a poly(glycidyl methacrylate) (GMA) layer by either photo-induced graft polymerization or heat induced graft polymerization. The epoxy groups of GMA monomer were subsequently converted into cation and anion exchangers by reaction with either sulfonic acid groups or diethylamine (DEA), respectively. After the ligand attachment, the unreacted epoxy groups were hydrolyzed using sulfuric acid to reduce nonspecific protein binding.

Several parameters of the procedure were studied, especially the effect of (i) % weight gain and (ii) ligand density on the static protein binding capacity. Bovine Serum Albumin (BSA) and human Immunoglobulin G (hIgG) were utilized as model proteins in the anion and cation exchange studies. An equilibrium binding capacity for BSA of 673 mg of protein/g of membrane was obtained for anion exchange heat grafted (HIG) nonwovens with a DEA density of 1.54 mmol/g. Equilibrium hIgG binding capacity as high as 675 mg/g was observed for cation exchange HIG, which showed a ligand density of 0.47 mmol/g. The performance of ion exchange PBT nonwovens by HIG was evaluated under flow conditions. Rigid Polyethylene terephthalate (PET) nonwoven spacers were used to separate individual PBT nonwoven membranes in order to increase the total flow porosity of HPLC columns. The pressure drops of the heat grafted PBT nonwoven ion exchangers was found to be dependent on the ionic strength of the mobile phase, likely due to a partial swelling of the grafted layer, causing the blocking of the pores. The dynamic binding capacities evaluated at 10% of break-through (DBC10%) for BSA capture, using anion exchange HIG nonwovens was achieved of 168 mg/g, with a residence time of 7.9 minutes. The DBC10% using cation exchange HIG nonwovens for hIgG binding was approximately 100 mg/g for residence time of 3.9 and 7.9 minutes. The anion- and cation- exchange HIG PBT nonwovens were

evaluated for their ability to selectively adsorb and elute BSA or hIgG from a mixture of proteins. Cation exchange nonwovens were not able to reach a good protein separation, whereas anion exchange HIG nonwovens were able to absorb and elute BSA with very high value of purity and yield, in only one step of purification.

TABLE OF CONTENTS

LIST OF FIGURES

LIST OF TABLES

Chapter 1

Introduction

1.1 Motivation

The high cost production of drugs based on antibodies, antibody fragments, and other proteins is due to the high purity required by these medicines which involves numerous steps in downstream protein purification in order to remove any host cell protein (HCP), pyrogens, endotoxins, prions or other contaminants. Steps required in downstream protein purification, which includes extraction, precipitation, electrophoresis and various modes of column chromatography (e.g. ion exchange, affinity) represent the 40%-80% of the overall cost of a bioprocess [1]. In order to reduce the cost many studies were carried out during recent years. At first, the strategy aimed to reduce the concentrations and the number of the contaminants modifying protein expression techniques and cell culture growth conditions, has been pursued [2], [3]. Secondly, the industries are trying to simplify the separation process reducing the number of steps and to substitute some separation devices with other more inexpensive (e.g. low cost affinity ligands that replace protein-A in affinity chromatography [4], [5] or novel inexpensive separation devices in chromatographic process). Recently, the development of membranes as novel support in chromatography separation has been a growing interest either for capturing contaminants or for capturing products [6], [7]. Since membrane chromatography is able to overcome the limits of conventional packed bed chromatography (bead-based) such as slow intraparticle diffusion, large pressure drops through the column, low throughput, high cost, and difficulty in scale-up, membrane chromatography show to be an attractive alternative [8], [9]. In order to further reduce the production costs of protein biotherapeutics, research is moving to disposable devices [10] which have a great benefit for adsorbing pathogens or toxins, to avoid the contamination. This dissertation deals with the development of PBT nonwoven as novel disposable membrane chromatography support able to capture product and reduce contaminant by ion exchange chromatography.

1.2. Overview of this dissertation

This study investigates the binding capacity and the ability to separate proteins of modified PBT nonwovens. This work has been developed at North Carolina State University in collaboration with the research group of Professor Ruben Carbonell.

Chapter 2 provides a review of the scientific literature, it gives information regarding the biopharmaceuticals market, principles of ion exchange chromatography and membrane chromatography (dealing in details nonwovens materials) and the grafting method as surface modification technique. In Chapter 3 the materials used and the procedure employed during the research project are described in detail. Results obtained from the experiments are discussed in Chapter 4. Chapter 5 summarizes the conclusions from the previous chapters and makes suggestions for future works.

.

Chapter 2

Literature review

2.1 Overview of biopharmaceuticals market

Biotechnologies are able to produce drugs that structurally mimics compounds found within the body. These drugs are named biopharmaceuticals. They include vaccines, monoclonal antibodies, recombinant hormones, recombinant growth factors, to name a few [11]. Since any drugs can be genetically modified for specific medical problems in different individuals, biopharmaceuticals have made the treatment of many diseases (e.g. diabetes, malignant disorders) more effective [12]. The biopharmaceutical industry is one of the most important sector in industrial biotechnology. The biopharmaceutical market, already represents 20% of global pharmaceutical revenue. The continuous growing of this industry is due to the increase of geriatric population, chronic diseases, technological advancements which permit to cure diseases with no available treatment. The global biopharmaceuticals market was estimated to be USD 162.8 billion in 2014, and it is expected to grow with a CAGR of 8.6%, during 2015-2020, reaching USD 267.8 billion by the year 2020. The biopharmaceuticals market can be divided geographically in North America (United States Canada), Europe (The United Kingdom, Germany, France, Italy, and Spain), Asia-Pacific (Japan, China, Australia, South Korea, and India), and the Rest of the World (all other countries). North America has holds the record with 44.5% of the share in the year 2015. the biopharmaceutical market can be segmented also into products and therapeutic area. Based on the product, the monoclonal antibodies market segment dominated the global biopharmaceuticals market in 2014 with about 37.31% share. Based on the therapeutic area, the oncology segment accounted for the highest share of 30.5% in the global biopharmaceuticals market in the same year [11].

These drugs are expressed in complex system (e.g. microbial systems, mammalian cell culture, insect cells) that may contain many potentially harmful components (e.g., DNA, RNA, endotoxins, host cell proteins, protein aggregates) that must be removed before their introduction into the body [13]. Therefore, downstream purification plays an essential role in the manufacturing of biopharmaceuticals. The high purity necessary in

the final products, to reach appropriate health and safety standards, requires several purification and separation treatments making the downstream process the bottleneck of the biopharmaceuticals production, accounting until the 80% of the overall cost of a bioprocess [1]. Chromatography is one of downstream process steps and it is by far the most widely used technique for high resolution separation and analysis of proteins [8]. Many different types of chromatographic techniques are used in biotechnology, due to the several possible interaction mechanisms (electrostatic, hydrophobic ect.). Several studies were carried out in this sector in order to develop alternative devices, such as inexpensive ligands or novel media used in the stationary phase, reducing the costs and the limits of the technique currently used.

2.2 Principle of ion exchange chromatography

Biomolecules are purified using chromatography techniques that can be classified on the base of the differences in their specific properties, as shown in Table 1 [14].

Table 1. Chromatography techniques base on different interaction principles between solute and media.

Property	**Technique**
Charge	Ion exchange chromatography (IEX), chromatofocusing (CF)
Size	Gel filtration (GF), also called size exclusion
Hydrophobicity	Hydrophobic interaction chromatography (HIC) Reversed phase chromatography (RPC)
Biorecognition (ligand specificity)	Affinity chromatography (AC)

One of the most frequently used chromatographic technique for the separation and purification of charged biomolecules like proteins (e.g. enzymes, antibodies) and nucleic acids (e.g. DNA), is ion exchange chromatography. This technique is based on the reversible interaction between ions in a solution and ions immobilized on a chromatography matrix [15]. In cation (anion) exchange chromatography positively (negatively) charged molecules are attracted to a negatively (positively) charged solid support [15]. The pH at which a molecule has no net charge is called its isoelectric point (pI). The choice of the pH of the environment permits to confer to a proteins a net

positive charge (pH<pI), a net negative charge (pH>pI), or no charge (pH=pI). Fundamental properties characterizing the ion exchanger are the type and strength of the charged groups (i.e. ligand) attached to the media. They are categorized in strong and weak ion exchangers. This distinction does not refer to the strength of binding, but to the limitation of weak exchangers to ionize in a narrower range of pH than the strong ion exchangers. Sulfonic acid groups and quaternary amines are normally strong cation and anion exchangers respectively, while weak anion exchangers usually contain primary, secondary or tertiary amines (anion) or carboxylic groups (cation).

Ion exchange experiments are commonly realized in the following steps: equilibration, loading, washing, elution, regeneration and re-equilibration. A schematic representation of this steps is illustrated in Figure 1 [16].

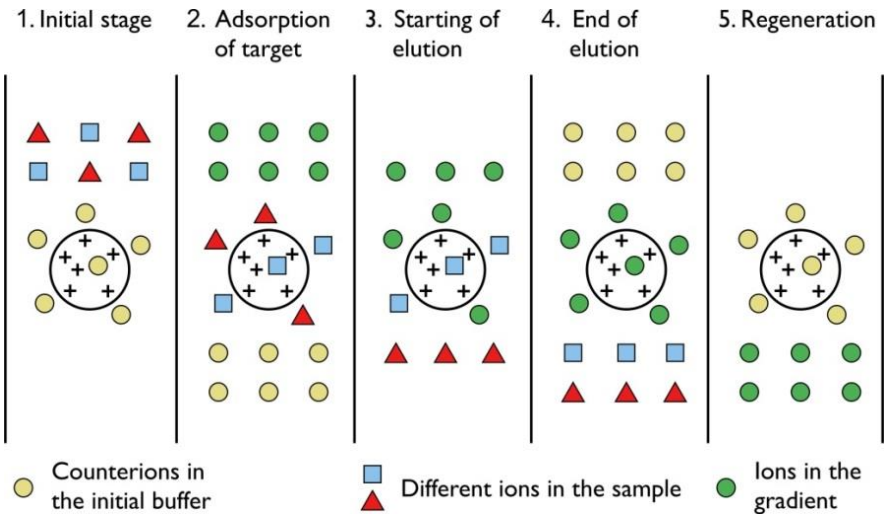

Figure 1. Phases of ion exchange chromatography (salt gradient elution).

Equilibration is necessary to bring the ion exchanger, in terms of pH and ionic strength, to a condition which allows the binding of the desired solute molecules. The solid matrix contains fixed functional groups of a given charge with counter ions of the opposing charge attached to each functional group. The loading step includes the feed and adsorption of the sample in which solute molecules, with the same charge as the counter ions, come in contact with the material displacing counter-ions and binding reversibly to the matrix due to the stronger electrostatic force. Unbound substances can be removed from the exchanger bed using equilibration buffer (washing step). Then, in the elution stage the bonds between the solute molecules and the matrix are broken by modifying the condition of the mobile phase that normally involves an increasing of the ionic strength (case of the Figure 1 where the recovery of the protein is achieved

increasing the salt concentration) or changing its pH. In order to remove from the column the molecules that had not been previously eluted and to restore the primitive conditions of the column, a regeneration step, using buffer normally characterized by acid or basic pH, and a re-equilibration step are realized respectively [16].

In chromatographic processes the feed is pumped through the adsorbent; then some effluent parameters, like UV absorbance, conductivity, pH and temperature are continuously monitored. Plotting the effluent concentration versus time or effluent volume, it is obtained the breakthrough curve (BTC), given by way of example in Figure 2 [17]. The chromatographic process is mainly evaluated by analysis of the BTC.

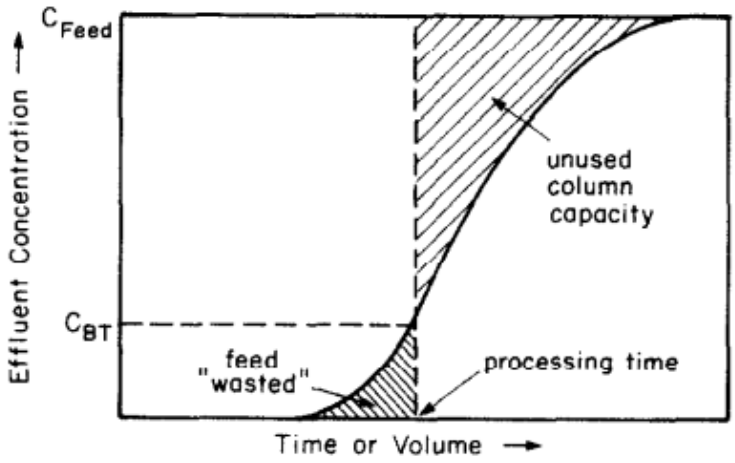

Figure 2. Qualitative profile of a breakthrough curve

In an ideal BTC, at short times the solute in the feed is completely adsorbed by the media, then its output concentration increases with the time until to become equal to the feed concentration (corresponding the point where the BTC achieves the value of one), when the adsorbent becomes saturated. The maximum capacity of the column for a given feed concentration is equal to the area behind the breakthrough curve, while the amount of solute which exits in the column is the area under this curve. In industrial process, in order to reduce the loss of product, the adsorption steps is usually terminated before column saturation, a specific solute concentration C_{BT}. Capacity and feed concentration are important parameters able to change the position of the breakthrough: it could be shift to the right increasing the capacity at a fixed feed concentration or decreasing the feed concentration at a fixed capacity, since the volume of feed increases. Through the analysis of the breakthrough curve it is possible to determine how much of the column capacity is exploited, how much solute is lost in the effluent and the processing time [17]. Other relevant information from washing and elution steps

are extracted. A qualitative profile of a complete chromatographic cycle is shown in Figure 3.

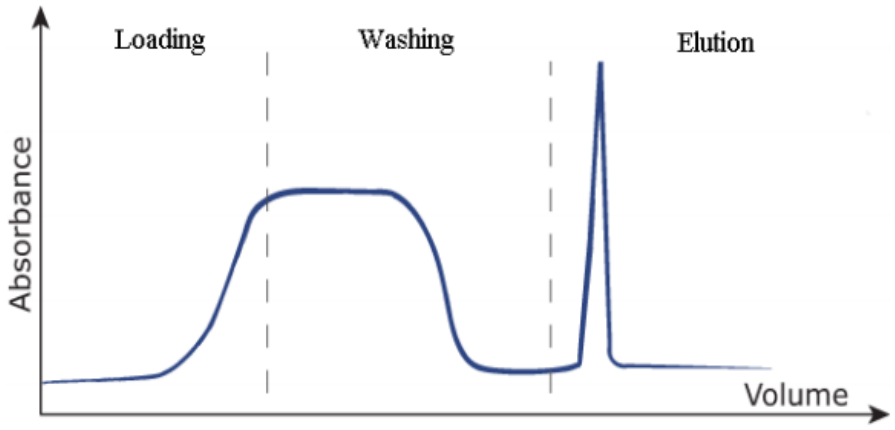

Figure 3. Qualitative profile of a complete chromatography cycle.

The concentration profile decreases over effluent volume during the washing step, due to the all unbound molecules are removed from the column. Integrating the area under the washing curve it is possible to calculate the amount of solute flow out in this step, data to be considered in the solute mass balance. The area of the characteristic peak obtained during the elution is equal to the mass of protein recovered. In ion exchange chromatography it is possible to decide if binding the substances of interest and allow the contaminants to pass through the column, or if binding the contaminants and allowing the substance of interest to pass through. Generally, the first method is more useful since it allows a greater degree of fractionation and concentrates the substances of interest.

2.3 Membrane chromatography

Several chromatographic supports are employed in the chromatographic protein separation. Packed-bed chromatography is an ubiquitous method in the protein purification process due to the high binding capacity, high resolution ability and the mature understanding of the process. However packed bed chromatography exhibits various limitation as high pressure drops, high material cost, low throughput and complicated scale-up. In addition the mass transfer of molecules to their binding sites in the inner pores of resins, is dominated principally by slow diffusive transport. The consequent increase of the process time and the increase of elution volume may produce

the denaturation of the solute due to the long exposition to aggressive conditions. Additionally, the relatively small pores of the resin are ineffective at capturing large biomolecules due to size exclusion (molecular weight >200 kDa) [8]. Further problem to consider is the channeling, i.e the possible formation of flow passages due to cracking of the packed bed, that leads to poor bed utilization caused by short-circuiting of material flow. Furthermore, the complexity of the transport phenomena makes scale-up of packed bed chromatographic processes complicated [8], [18]. In order to overcome these limitations, membranes are being investigated as potential replacements for packed bed chromatography.

In membrane chromatographic process the mass transfer is mainly dominated by convection, thanks to the large interconnected pore structure of this media (pore sizes of 0.45 – 3.0 μm in conventional chromatographic membranes [19]), permitting to achieve a binding time ten times lower that one required for the bed packed chromatography and a elution volume considerably reduced. The different type of mass transfer in chromatographic resins and membrane are illustrated in Figure 4 [8].

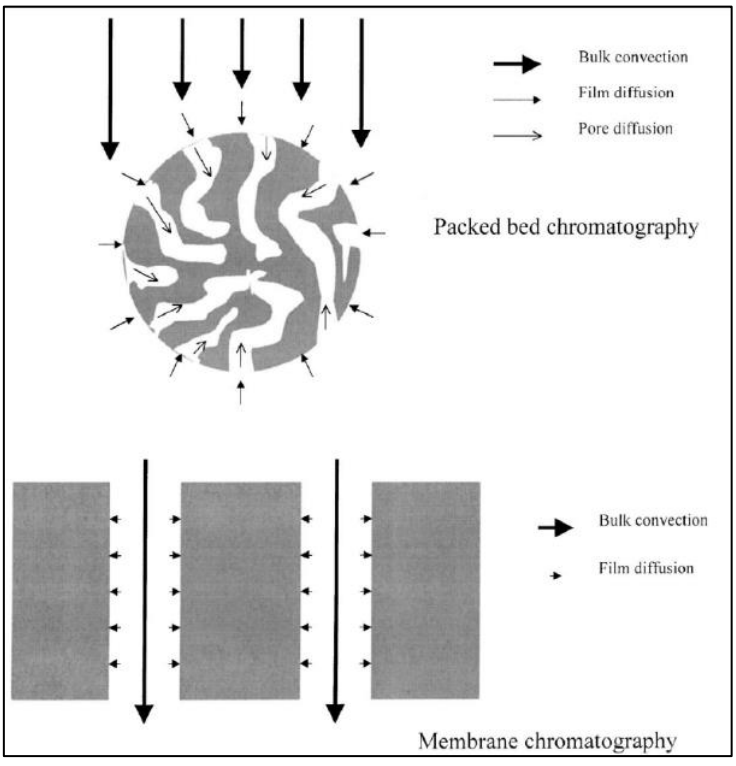

Figure 4. Principal solute transport mechanisms in packed bed chromatography and membrane chromatography [8].

The pore structure of the membrane results in a lower pressure drop than packed column and it is possible to use high flow rate since the binding efficiency is generally

independent from the feed flow rate. Other important advantages are the easier scale-up and the lower cost of these membrane that make them a disposable stationary phase for chromatography [20]. In addition, membrane is particularly suitable to bind large proteins (molecular weight > 250 kDa) which are not able to enter in pores presented in conventional resins, therefore forced to bind only in the external surface area of such media. Since one main advantage of resins is the significantly higher binding capacity than membranes support, this property is not exploited for large proteins [8].

However, membrane chromatography are not yet fully utilized in the bioprocess industry [8]. There are various challenges and limitations that must be considered in membrane chromatography. An issue is associated to the inlet flow distribution due to the significantly larger frontal area than the height of the membrane column. The sections between the tubing and the module inlet generally has a considerable widening. Since a uniform inlet flow distribution is necessary to avoid the broadened break through curves and a decrease of the system performance, an accurate design of inlet distribution for specific membrane configurations is required [21]. In addition, the flow distribution is also influenced by the pore size distribution and thickness of the membranes. The pore diameter in microporous and macroporous membranes is not uniform, they are characterized by a pore size distribution will result in preferential flow through the largest interstices, leading to a decrease of the column performance. In order not to register a drastic effect, the difference between the outmost value of pore size distribution and the average is suggested not exceed the 1% of the average value [21]. To overcome this issue it is recommended to use a stack of several membrane sheets.to avoid the formation of a preferential flow [8]. However, the main limitation of membrane is the low biomolecules binding capacity due to its inherent low specific surface area [8], [22]. Therefore membrane supports are suited for low target molecules concentrations in large production volume as the production of therapeutic antibodies is. In this case ion exchange membrane are used for polishing after primary capture, the product is passed through the column in a flow through mode of operation [22]. For using membranes in a primary protein capture step, an increase of the binding capacity of such media is required. The options to achieve this target may be increase the surface area of the support or introduce a three dimensional binding environment inside the pores of the support. Methods to increase biomolecule adsorption capacity of membranes and their applications in bioseparations constitute the focus of this dissertation and will be discussed extensively in future sections.

2.4 Nonwoven membranes

2.4.1 Properties

Nonwoven fabrics are broadly defined as web structures, wherein the random fibers and filaments are bonded together mechanically, thermally or chemically with different techniques such as mechanical interlocking, thermal bonding or entanglement [23] [24]. Nonwoven fabrics are used in numerous applications from medical field to electronic field. These fabrics can be made by a large variety of materials and produced using different technique permitting to control different characteristics such as porosity, fiber diameter and pore sizes [25]. The fibers may be of natural origin, such as cellulose, cotton, silk and wool, or made from synthetic thermoplastic polymers such as polyolefin, polyesters, polyamides, polycarbonate, polyvinyl chloride, polysulfone, polystyrene (to list few of them) [26]. Since the majority of chemical and mechanical properties derives from the fiber polymer, the choice of the raw material for a given application results important. The production costs of nonwoven fabrics are very low and the materials are relatively cheap (e.g. polypropylene, poly(butylene terephthalate) and nylon to name a few of them.). For this reason, nonwovens show a promising potential as disposable devices for application as downstream protein purification [27].

2.4.2 Manufacturing processes

All nonwoven fabrics are based on a fibrous web. The characteristics of the web determine the physical properties of the final product and they can be controlled through the process used for forming nonwovens. The production of nonwovens can be described in three stages: web formation, web bonding and finishing treatments.

The different web formation technique of nonwoven fabrics can be divided in three major methods: drylaying, wetlaying and melting or direct spinning (meltblown, spunbond, flashspun, polymer-laid or spunmelt) [28]. In drylaid web formation, fibers are carded or aerodynamically formed (airlaid) and then bonded by mechanical, chemical or thermal methods. Wet-laid procedure derives from a modification of papermaking process. Fibers of relatively short length are passed through water or some other medium, which provides to form a continuous web of desired structure integrity for down-stream processes. Specialized paper machines are used to separate the water from the fibers to form a uniform sheet of material, which is then bonded and dried.

Melt/direct spinning nonwovens are manufactured with processes developed from polymer extrusion [24]. In this category spunbonding and melt blowing production techniques are interesting to make nonwovens with useful properties for the bioseparations. The continuous nature of these processes, provides opportunities for increasing production and reduction of cost compared to other techniques.

Spunbonding technique consists in depositing, in uniform random manner, molten polymer extruded (spun filaments) onto a collecting belt where fibers subsequently are bonded in order to impart strength and integrity to the web. The fibers are separated during the web laying process by air jets or electrostatic charges [24], [29]. A diameter range between 20-500 µm is possible to obtain by using a spunbonding process, through new methods is possible to achieve smaller diameters [30]. In melt blowing process, similar to the spunbonding, molten polymer is extruded to form fibers through a linear spinneret containing small orifices though which a hot air jet flows from top to bottom of the spinneret, converging at the orifice in the direction of the extrusion. The use of the hot air blow, permits to reach finer diameters (fibers with diameters in the range of 1–50 µm) comparing to traditional spunbonding [28], [31], [32]. A representative meltblown process is shown in Figure 5.

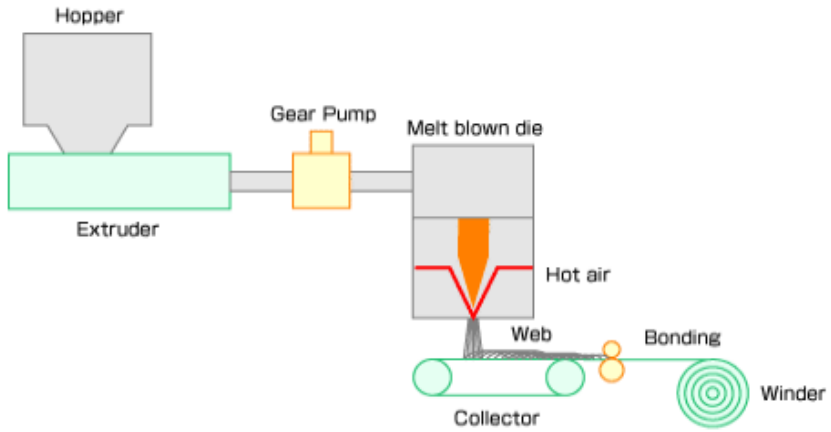

Figure 5. Meltblown nonwoven manufacture process [33]

Through the variation of melt blowing or spunbonding processing parameters, which control properties as fiber diameter, spatial orientation of the filaments and basis weight of nonwoven, is possible to regulate properties as porosity, pore size and specific surface in nonwoven fabrics [34]. These features are important in bioseparation purposes where a low specific surface, results in a low binding capacity. The relation

between the specific surface area as a function of the PET fiber diameter is reported in Figure 6 as an example [35].

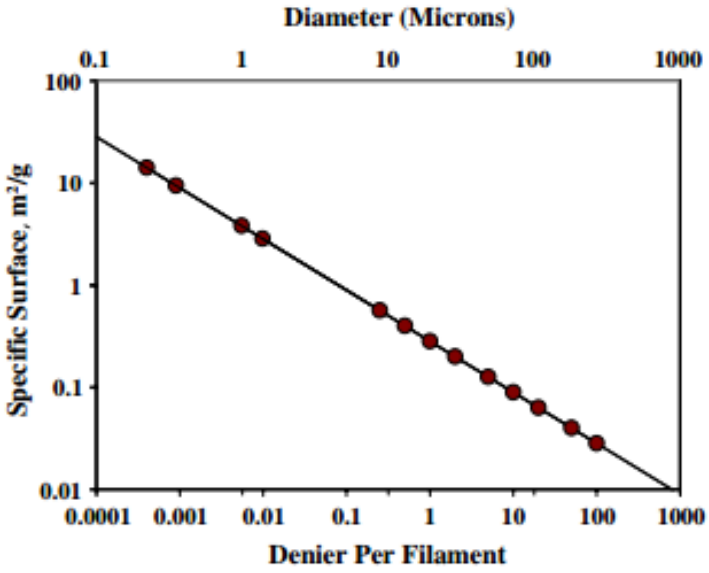

Figure 6. Specific surface area as a function of fiber diameter for PET nonwoven [35].

In order to have higher surface area in nonwovens, in attempt to achieve higher binding capacity, fiber with smaller diameter should be used, as showed in Figure 6. A novel technology has been developed and permits to reach fiber diameter smaller than 100 nm (40 to 2000 nm): electrospinning [32]. Nevertheless the resulting membranes from this process show low mechanical integrity and are highly compressible resulting in flow issue and high pressure drops if used liquid flows. Moreover the procedure is slower and more expensive compared to the one used in melt blowing and spunbonding [30]. In this dissertation a meltblown polybutylene terephthalate (PBT) nonwoven was investigated for bioseparation application. The physical properties deriving from the industrial process are reported in Table 2 [36].

Table 2. Physical properties of meltblown PBT nonwovens

Fiber diameter (μm)	3.0±0.7
Mean flow pore size (μm)	8.0±0.5
Membrane thickness (μm)	300±30
Basis weight (g/m^2)	52
Apparent density (g/cm^3)	0.17
Porosity (%)	87

2.4.3 Nonwoven applications and their limits in bioseparation process

Nonwovens offer economical solutions for a wide application range thanks to numerous and different qualities that derive from the large range of materials and techniques used to produce them. The field applications are multifold: personal care and hygiene, healthcare, clothing, home, automotive, geotextiles, construction, filtration [28]. The continuous development of nonwovens in biotechnology is due to the ability to control porosity, fiber diameter and pore size using specific manufacturing technologies. The chemical and physical properties of the nonwovens strongly depend from the raw material used during the manufacturing process. Nonwovens based on cellulose are characterized by high density of hydroxyl groups on the fiber surface, making it hydrophilic and chemically active for the ligand attachment [37]. Unfortunately, a wide number of these polymers such as polypropylene, polyester, polyethylene, are hydrophobic and inert. Therefore surface modification techniques, including physical and chemical processes, are used to make a hydrophilic and active surface [38]. Physical processes can involve radiation of electromagnetic waves, segregation and oxidation with gases. Chemical modifications can include wet-treatment, blending, coating, and metallization. Polymer surface grafting is a method of surface modification widely diffused which can be achieved via the combination of physical and chemical processes [38]. Grafting is an easy method for the introduction of graft chains on the fiber surface maintaining the bulk properties unchanged, but increasing the surface area of the fibers [38]. This technique is discussed in more detail in the subsequent section. The attention and the desire to develop the properties of nonwovens in filtration and chromatography device, notwithstanding the limits to overcome, is due to their disposable nature, resulting from their low production cost. When pathogens, toxins or viruses have to be adsorbed, disposable membrane are useful to prevent cross contamination for chromatographic processes, limiting also the costs [39]. Some barrier need to be overcome before to achieve a routine successful process-scale production, such as the low binding capacity [40].

2.5 Polymer grafting

The grafted polymer chains on the membrane surface play an important role to minimize undesired properties or introduce additional functions for a polymer

separation membrane [41]. The advantages of using grafting method are various. It is an easy and controllable process that lead to introduce a high density of graft chains maintaining the bulk polymer properties unchanged and it allows to achieve a long-term chemical stability thanks the covalently bounds of the graft chains onto a polymer surface that avoid the delamination, issue presented in other coated technique [38]. Grafting methods can be divided in "grafting-from" and "grafting-to" processes. In "grafting-to method", preformed polymer chains carrying reactive groups are covalently coupled to the surface, resulting in a uniformity in length and properties of the polymer chains attached. Notwithstanding, this procedures are not straightforward enough for industrial applications. "Grafting-from" method utilizes active species existing on a membrane surface to initiate the polymerization of monomers from the surface toward the bulk phase. Therefore active sites are required for "grafting from" process, and they are typically realized using initiators or special treatments [41], [38]. This dissertation is focused in "grafting from" method that will be solely discussed from here on.

Plasma treatment, ozone treatment, high energy radiation such as x-rays, γ-rays and energy rich particle rays, are some examples of methods used to modify the surfaces of polymeric materials. These complicated polymerization methods are rarely used industrially due to the high cost experimental setups required and the stringent reaction conditions. The UV-light technique and heat technique are other methods used in polymer surface modification and they do not require very expensive and complex equipment (comparing with methods previously named) which is relatively easy to operate and maintain. The performance and the properties of modified material are considerably influenced by the grafting technique used, the degree of grating, the grafting density, the structures of grafted layer and the environment conditions [38], [41].

In hydrophobic and inert polymer without active grafting sites, it is an efficient technique to generate a grafted layer with reactive groups that can be chemically modified introducing appropriate functional groups, with an additional reaction step, to realize ion exchange membranes [42] or affinity membranes [36]. To achieve this purpose, glycidyl methacrylate (GMA) monomer has been widely used to modify surface polymer such as PBT, PP [36], [27]. The GMA monomer has the peculiarity to have both a vinyl group for polymerization and reactive epoxy groups ready to functionalized by covalent attachment of appropriate ligand such as amines, hydroxyls,

carboxylic acids, sulfonic acids, thiols, peptides. Examples of possible chemical conversion of epoxy groups are showed in Figure 7 [43].

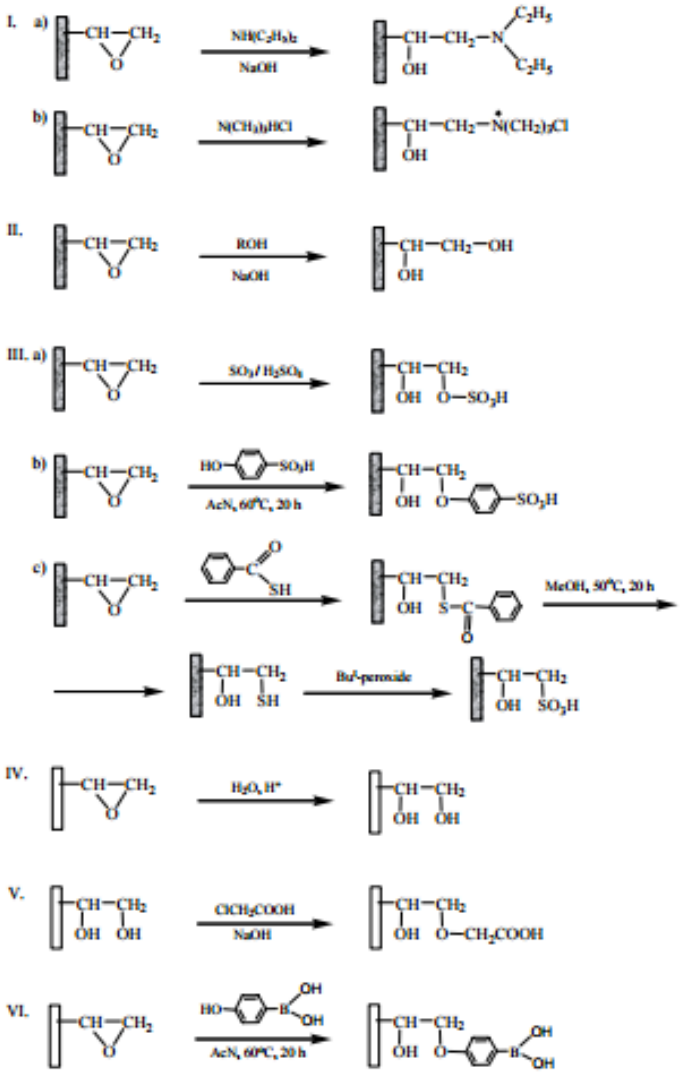

Figure 7. Examples of chemical conversion of epoxy groups [43].

2.6 Focus of this dissertation

In this study commercially available polybutylene terephthalate (PBT) meltblown nonwoven membrane has been developed as novel disposable membrane chromatography support able to capture product and reduce contaminant by ion exchange chromatography. The features of PBT nonwoven are the low production cost, the thermal stability and the high tensile strength.

Poly(glycidyl methacrylate) were successfully grafted on the PBT nonwovens using both UV-light and heat as energy source in the radical polymerization reaction. Grafted layer was activated by reaction with diethylamine, and sulfonic acid groups in order to produce anion- and cation- exchange membranes respectively. As already investigated in previous studies [44], [30], the structural differences, obtained using these two different techniques, affect the performance in protein capture of nonwovens. This work is focus on the optimization of the procedure used in the modification of PBT nonwovens in order to improve the protein binding capacity and the ability to separate proteins from complex mixtures.

Chapter 3

Materials and methods

3.1 Introduction

In this chapter the material and the experimental method during the research project are described. This chapter discusses the two different techniques for surface grafting of PBT nonwovens: heat induced polyGMA grafting and UV induced polyGMA grafting. The functionalization methods to create weak anion exchangers and strong cation exchangers are also described. The description of SBC and DBC study and purification of protein mixture are reported. *Surface Modified Nonwoven Membranes for Bioseparation* of Haiyan Liu [44] and *Polymer Grafted Nonwoven Membranes for Bioseparations* of Michael Leonard Heller [30] were used as principal references for the develop of this research.

3.2 Experimental

3.2.1 Materials and reagents

Commercially available PBT nonwovens, with a density of 52 g/m^2, a mean pore size of 8 µm and a porosity of 87%, were provided by Marcopharma (Tourcoing, France). PET nonwoven spacer fabric was provided by the Nonwovens Coperative Center (NCRC, North Carolina State University, Raleigh, NC). Glycidyl methacrylate (GMA) monomer was purchased from Pflatz & Bauer (Waterbury, CT).

Benzophenone (BP) was purchased from Sigma Aldrich (St. Louis, MO). Benzoyl peroxide (70% wt.) (BPO), N,N-dimethylformamide (DMF), sodium hydroxide, 1-butanol, isopropyl alcohol, tris base, hydrochloric acid, beta-mercaptoethanol, sodium chloride and sodium acetate trihydrate were purchased from Fisher Scientific (Fairlawn, NJ). Tetrahydrofuran (THF), methanol, sulfuric acid and acetic acid were purchased from BDH (West Chester, PA). Diethylamine (DEA) was purchased from Alfa Aesar (Ward Hill, MA). Sodium sulfite was purchased from Acros Organics (Fairlawn, NJ).

Solid phase extraction tubes (SPE) were purchased from Supelco (Bellefonte, PA). Amicon Ultra centrifugal concentrator filters with a 3,000 NMWL were purchased from Fisher Scientific (Farilawn, NJ). Mini-PROTEAN TGX precast SDS-PAGE gels, 2x Laemmli sample buffer, 10x TGS running buffer, Brilliant Coomasie Blue stain and Precision Plus Protein Standard were purchased from BioRad (Hercules, CA). Albumin from bovine serum (BSA) and egg white lysozyme were purchased from Sigma Aldrich (St. Louis, MO). Human immunoglobulin G (hIgG) was purchased from Equitek-Bio Inc. (Kerrville, TX). A 10 mm inner diameter adjustable piston OmniFit column was purchased from Diba Industries (Danbury, CT).

3.2.2 Grafting of polyGMA on PBT nonwoven membrane

At first, the surface modification of PBT nonwovens membranes was realized using grafting technique (grafting "from" the surface). Grafted Membranes were realized by free radical polymerization reaction of GMA monomer, started by the activation of suitable initiators. In this dissertation, energy sources, such as thermal heat and UV irradiation , were used to activated the free radical initiator, creating a active polyGMA grafted layer on the surface of PBT nonwovens.

3.2.2.1 Heat induced grafting (HIG) of polyGMA on nonwoven fabrics

Samples of PBT nonwoven membranes were cut (75 x 50 mm) and weighed before the grafting treatment (size corresponding approximately at 200 mg).

Benzoyl peroxide (BPO) was used as the initiator in the grafting polymerization of GMA monomer from the PBT fiber by heat method. Samples were immersed in 20 ml of 75 mM BPO in DMF and kept in the thermal initiator solution for 1 hour at room temperature to allow the adsorption of BPO to the surface of samples. After 1 hour, samples were laid across a towel to remove the excess of initiator solution from the pores of the membrane. The difference between BPO in the initiator solution and BPO in both initiator and grafting solution was investigated. Approximately 400 mg of samples were rolled together and placed in 20 ml of GMA grafting solutions, prepared using DMF as solvent with a GMA concentration of 30% (v/v). During the reaction the polymerization temperature was kept constant by using a hot water bath (Isotemp 115, Fisher Scientific, Fairlawn, NJ). Polymerization temperatures of 60, 70, 80, 90 °C were

investigated. After a reaction time in a range from 0.5 to 8 hours, the unreacted and untethered GMA was removed by soaking samples with THF (25 ml for each 200 mg of nonwoven) for 30 minutes in an ultrasonic bath (Bransonic 3510R-MT, Branson Ultrasonics Corporation, Danbury, CT) at room temperature. Each 15 minutes fresh THF was replaced. To remove the THF from the nonwoven, samples were washed for 10 minutes with methanol (25 ml for each 200 mg of nonwoven). Following methanol, nonwoven samples were left to dry in air overnight.

The grafting efficiency of the monomer on the fabrics was reported as a function of weight increase of the sample, calculated using the Eq.1:

$$\text{Degree of polyGMA grafting (\% weight gain)} = \frac{W_f - W_0}{W_0} \qquad \text{Eq. 1}$$

where W_0 and W_f is the weight of nonwoven samples prior to and after grafting, respectively.

3.2.2.2 UV induced grafting (UVG) of polyGMA on nonwoven fabrics

The nonwoven samples were cut into 75 x 50 mm samples, corresponding about 200 mg of weight. Samples were weighed prior and after the grafting procedure. The grafting solution was prepared with 20% v/v polyGMA monomer in 1 butanol solvent. Benzophenone was added to the grafting solution as a photoinitiator in a BP:GMA molar ration of 1:20 (mol:mol). Samples were sprayed by a syringe with 1.5-2 ml of grafting solution and placed between two borosilicate glass slides of the samples with the same size. The free radical polymerization was started by exposure to UV lamp (model EN-180L, Spectronics Corporation, Westbury, NY) with a wavelength of 395 nm and intensity of 5 mW/cm^2. Samples were placed at 3 mm of distance from the light source. Reaction times were investigated from 5 to 60 minutes. After the exposure to UV light, the unreacted and untethered monomer was washed off with sonication treatment in an ultrasonic bath (Bransonic 3510R-MT, Branson Ultrasonic Corporation Danbury, CT) in tetrahydrofuran (THF) for 30 minutes, followed by sonication treatment in methanol of 10 minutes. The samples were dried completely overnight and weighted to calculate the grafting percentages in terms of % weight gain (see Section 3.2.2.1).

3.2.3 Functionalization of grafted nonwovens with DEA and sulfonic acid groups

Heat and UV grafted PBT nonwovens were functionalized to create weak anion exchangers and strong cation exchangers. The weak anion exchangers were realized using diethylamine (DEA) in aqueous solution and creating a tertiary ammine on the polyGMA brushes. Approximately 100 mg of samples were immersed in a 50 ml of solution. The DEA solution consisted in various volume concentration (between 2% and 60%) of secondary ammine in water. The reaction was kept at 30°C under shaking condition at 100 rpm using an incubator shaker (Certomat® RM, B. Braun Biotech International, Melsungen, Germany) contained an incubator hood (Certomat® RM, B. Braun Biotech International, Melsungen, Germany) overnight.

The activation of the epoxy groups to create strong cation exchangers were realized by attaching sulfonic acid groups to the polyGMA brushes. Approximately 100 mg of PBT grafted nonwovens (PBT-pGMA) were immersed in 25 ml of sodium sulfite solution and sulfonated at 80°C in the incubator (Isotemp 115, Fisher Scientific, Fairlawn, NJ) for 8 hours. The solutions were prepared with sodium sulfite, isopropyl alcohol (IPA) and water in a variable mass ratio of Na_2SO_3:IPA:H_2O=x:15:75 %wt. where x ranges between 0.1 and 12, while the mass ratio of IPA and H_2O is constant. At the end of the reactions, the samples, PBT-pGMA-DEA and PBT-pGMA-SO_3, were repeatedly washed in DI water to remove the functional solution. Samples were immersed in 100 mM sulfuric acid solution and incubated at 50 °C overnight to hydrolyze any unreacted epoxy groups. After hydrolyzation, samples were repeatedly washed with DI water to remove excess sulfuric acid and then air dried overnight.

3.2.4 Material characterization

The surface morphology of nonwoven samples was observed using a Hitachi S-3200N variable pressure scanning electron microscope (VPSEM) (Hitachi High Technologies America, Inc., Schaumburg, IL). The SEM was available through the Analytical Instrumentation Facility (AIF). A scanning electron microscope (SEM) is a type of electron microscope that produce a three-dimensional image of the sample on the cathode-ray tube by moving a beam of focused electrons across an object and reading both, the electrons scattered by the object and the secondary electrons produced by it. After grafting and functionalization modification, nonwovens were analyzed to evaluate the differences in uniformity, conformity and performance. Nonwoven samples were

fixed onto a sample holder by carbon tape and sputtered with Pd/Au alloy in argon gas before they were put into the microscopy chamber. The accelerating voltage was 5 kV with a working distance around 22 mm.

3.2.5 Protein adsorption under static conditions

The static binding capacity (SBC) study was carried out for PBT nonwovens grafted using both method, heat and UV. Adsorption and desorption of proteins on the PBT-GMA-DEA and PBT-GMA-SO_3 membranes were performed through anion and cation-exchange mechanisms respectively. Membranes with various % weight gain and functionalized using a solution with different ligand concentrations were investigated.

3.2.5.1 Anion exchange

Approximately 20 mg of samples were placed into SPE (Solid Phase Extraction) tubes. All samples were equilibrated in 3 ml of 20 mM Tris-HCl pH 7 for at least 30 minutes and 10 mg/ml of Bovine serum albumin (BSA) solution was prepared in 20 mM Tris-HCl pH 7. Any residual of tris solution was removed from the membranes and 3 ml of BSA solution were added into the SPE tube, placed onto a rotator and incubated for overnight at room temperature. Then, samples were rinsed with an additional 3 ml of 20 mM Tris-HCl pH 7. The flow-through fraction, a total volume of 6 ml, was collected in a 15 mL centrifuge tube. Samples were washed for 5 times to remove the unbound protein completely. The protein elution fraction was performed by adding 3 mL of 20 mM Tris-HCl, 1M NaCl, pH 7 to the nonwovens and the samples were incubated in mild shaking for 30 min at room temperature, then was collected the fraction together with additional 3 ml of wash using the same buffer (with salt). All fractions, i.e. flow-through and elution, were collected and analyzed by spectrophotometer at λ = 280 nm to determine the BSA content using the Lambert-Beer law:

$$C = \frac{A_\lambda}{\epsilon_\lambda \, l} \qquad \text{Eq. 2}$$

where C is the protein concentration in solution (mg/ml), A_λ is the absorbance value corresponding to the wavelength λ = 280 nm, l is the path length (thickness of the cell where the solution is positioned), and ϵ_λ is the proportional coefficient at the

wavelength λ called also extinction coefficient ($\epsilon_\lambda$depend on the protein and buffer used due to the pH and ionic strength can be modify the protein configuration). The linearity of Lambert-Beer law is valid for solutions that are enough diluted to have a molarity M < 0.01 mol/L due to electrostatic interactions between molecules in close proximity.
The value of binding capacity can be calculated measuring the bound protein from the flow through (indirect approach, Eq. 3) or from the elution (direct approach, Eq. 4)

$$SBC_{indirect} = \frac{C_0 - (C_{UP} * V)}{W} \quad \text{Eq. 3}$$

$$SBC_{direct} = \frac{C_{BP} * V}{W} \quad \text{Eq. 4}$$

here SBC is the value of the binding capacity in static condition expressed as mg of bound protein per grams of dry membrane; C_0 is the initial protein concentration before binding (10 mg/ml), C_{UP} correspond to the unbound protein concentration in the flow-through fraction, C_{BP} is the bound protein concentration measured in the elution fraction, V is the volume of the solution (ml), W is the mass of samples (g).

3.2.5.2 Cation exchange

Approximately 20 mg of samples were placed into SPE (Solid Phase Extraction) tubes. All samples were equilibrated in 3 ml of 20 mM Acetate pH 5.5 for at least 30 minutes and 10 mg/ml of human immunoglobulin G (hIgG) solution was prepared in 20 mM Acetate pH 5.5. Any residual of acetate solution was removed from the membranes and 3 ml of hIgG solution were added into the SPE tube, placed onto a rotator and incubated for overnight at room temperature. Then, samples were rinsed with an additional 3 ml of 20 mM Acetate pH 5.5. The flow-through fraction, a total volume of 6 ml, was collected in a 15 ml centrifuge tube. Samples were washed for 5 times to remove the unbound protein completely. The protein elution fraction was performed by adding additional 3 ml of 20 mM Acetate, 1M NaCl, pH 5.5 to the nonwovens and the samples were incubated in mild shaking for 30 min at room temperature, then was collected the fraction together with additional 3 ml of wash using the same buffer (with salt). All fractions, i.e. flow through and elution, were collected and analyzed by spectrophotometer at λ = 280 nm to determine the hIgG content, used to calculate the SBC as well as done for the anion exchange (see section 3.2.5.1).

3.2.5.3 Kinetics of protein adsorption

The kinetics of protein adsorption were studied to evaluate the rate of protein adsorption on the grafted and functionalized PBT nonwovens. In this experiment, the commercial PBT nonwovens which were thermally grafted at 28% weight gain and 29% weight gain, were functionalized to be an anion- and cation- exchanger, respectively. The study was carried out for the samples functionalized with a solution composed by different ligand concentrations. Concentrations of 30%, 40%, 50% v/v DEA in aqueous solution for anion exchange and 21 (Na_2SO_3:IPA:H_2O=2:15:75 %wt.), 52 (5:15:75 %wt.) and 102 (10:15:75 %wt.) mg/ml of Na_2SO_3 for cation exchange were investigated. Same study was executed for UVG nonwovens at 20% weight gain for anion and cation exchange. The concentrations of ligand in the functionalized solution of 30%, 50% and 70% v/v DEA in aqueous solution for anion exchange and 21 (Na_2SO_3:IPA:H_2O=2:15:75 %wt.), 52 (5:15:75 %wt.), 102 (10:15:75 %wt.) mg/ml Na_2SO_3 for the cation exchange were investigated. The same procedure used for the SBC study (see section 3.2.5.1), was performed using various exposure times granted to the protein to bind (range between 2 and 900 minutes).

3.2.6 Protein adsorption under dynamic conditions

The two heat grafted PBT nonwovens that gave the highest static binding capacities in anion and cation exchange were chosen for further characterization in pulse experiments, permeability measurements, dynamic binding capacity measurement and dynamic separation of protein mixtures.

Two 10 mm I.D OmniFit adjustable volume chromatography columns were packed with 40 layers nonwovens punched into 10 mm discs. The first column was packed with 20 layers of anion exchange PBT nonwovens thermally grafted at 28% weight gain functionalized with aqueous solution containing 30% v/v DEA. PBT nonwovens discs were alternated with 20 layers of PET nonwoven spacer (column height = 0.6 cm). Similarly the second column was packed with 20 layers of cation exchangers PBT nonwovens thermally grafted at 29% weight gain functionalized with a solution characterized by a mass ratio of Na_2SO_3:IPA:H_2O=2:15:75 %wt., that were alternated with 20 layers of PET nonwovens spacer (column height = 0.6 cm).

3.2.6.1 Pulse experiments and flow permeability measurement

The porosity of the column was measured by first absolute moment analysis using pulse experiments. Pulse experiments for the cation exchange PBT-pGMA-SO_3 column (Column volume 0.471 ml) were carried out at room temperature (22°C) on AKTA Avant 150 system (GE Healthcare) with a 20 µl sample loop. Experiments were performed under nonbinding conditions using acetone as a tracer in order to avoiding the interaction with media and disturbances of the fluid flow. An injection of 20 µl of aqueous acetone 2% (v/v) was made to sample column at 7 different flow rates from 0.2 to 2 ml/min corresponding to superficial velocities from 0.25 to 2.54 cm/min. The mobile phase for this experiment was a 20 mM Na-acetate, 1 M NaCl, pH 5.5. The contribution from the system volumes to the measured first moment, were accounted for by performing the same analysis with the column packed with 20 layers of PET nonwovens spacer.

The pressure drop across the PBT-pGMA-SO_3 column was measured to evaluate the flow permeability of the modified nonwovens under flow conditions. The packed column was tested on AKTA Avant 150 system (GE Healthcare) with pressure sensors integrated into the column valve. Pressure drop along the column was measured at different flow rates between 0.2 ml/min (0.25 cm/min) and 4 ml/min (5.1 cm/min). The effect of the different ionic strength was investigated using mobile phase with low to high salt concentrations. Same experiment was performed with column packed with 20 layers of PET nonwovens spacer in order to calculated the permeability of cation exchange PBT nonwovens.

3.2.6.2 Protein adsorption under dynamic condition

The OmniFit packed columns (see Section 3.2.6) were tested on a Waters 616 HPLC system integrated with a Waters 2487 UV detector. A 5000 µl sample loop was used to inject the sample, the retention of sample into membrane was monitored by measuring absorbance at 280 nm. For BSA binding, the column (column volume: 0.471 ml) containing 20 layers of PBT-pGMA-DEA (HIG at 28% weight gain, functionalized using 30% v/v DEA in aqueous solution) and 20 layers of PET spacer (height of 0.6 cm) was equilibrated in 20 mM Tris-HCl pH 7.0. Once equilibrated, 5 ml of 10 mg/ml of BSA in 20 mM Tris-HCl pH 7 (corresponding to binding buffer) were injected into the column at superficial velocities of 0.076, 0.15 and 0.25 cm/min. Then column was

washed with 20 column volumes (CV) of binding buffer. Bound BSA protein was eluted 32 CV with 20 mM Tris-HCl, 1 M NaCl, pH 7. The column was regenerated with 13 CV of 20 mM Tris-HCl, 1 M NaCl, pH 10, washed using 13 CV of 20 m M Tris – HCl,1 M NaCl, pH 7 to reduce the pH faster, and re-equilibrated with 8 CV of 20 mM Tris-HCl pH 7. The experimental protocol is reported in Table 3.

Table 3. Experimental protocol of the chromatographic runs with 5 ml of 10 mg/ml BSA loaded for PBT-pGMA-DEA column.

Chromatographic step	**Buffer**	**Flow rate (ml/min)**	**Amount (CV)**
Equilibration	20 mM Tris-HCl pH 7	0.2	20
Loading	20 mM Tris-HCl pH 7	0.06, 0.12, 0.2	12
Washing	20 mM Tris-HCl pH 7	0.2	20
Elution	20 mM Tris-HCl, 1 M NaCl, pH 7	0.5	32
Regeneration	20 mM Tris-HCl, 1 M NaCl, pH 10	0.2	13
Conditioning	20 mM Tris-HCl, 1M NaCl, pH 7	0.2	13
Riequilibration	20 mM Tris-HCl pH 7	0.2	8

Dynamic binding studies for hIgG absorption were also performed on a column (column volume: 0.471 ml) packed with HIG nonwovens at 29% weight gain and functionalized using a mass ratio of Na_2SO_3:IPA:H_2O=2:15:75 %wt. The column was packed with 20 layers of nonwovens punched at 10 mm discs, alternated with 20 layers of 10 mm PET discs, obtaining a height column of 0.6 cm. At first the column was equilibrated with binding buffer (20 mM Acetate pH 5.5) and then 5 ml of 10 mg/ml of hIgG in 20 mM Acetate pH 5.5 were injected into the column at different superficial velocities (0.076, 0.15 cm/min). The column was washed with 20 column volumes (CV) of binding buffer. Bound hIgG protein was eluted with 32 CV of higher ionic strength buffer (20 mM Acetate, 1 M NaCl, pH 5.5). The column was regenerated with 20 mM Tris-HCl, 1 M NaCl, pH 10, 13 CV, then washed by 20 mM Acetate, 1 M NaCl, pH 5.5, 13 CV, to reduce the pH faster, and re-equilibrated with 20 mM Acetate pH 5.5. The experimental protocol is reported in Table 4.

Table 4. Experimental protocol of the chromatographic runs with 5 ml of 10 mg/ml hIgG loaded for PBT-pGMA-SO_3 column.

Chromatographic step	**Buffer**	**Flow rate (ml/min)**	**Amount (CV)**
Equilibration	20 mM Acetate pH 5.5	0.2	20
Loading	20 mM Acetate pH 5.5	0.06, 0.12	12
Washing	20 mM Acetate pH 5.5	0.2	20
Elution	20 mM Acetate, 1M NaCl pH 5.5	0.5	32
Regeneration	20 mM Tris-HCl, 1 M NaCl, pH 10	0.2	13
Conditioning	20 mM Acetate, 1M NaCl, pH 5.5	0.2	13
Riequilibration	20 mM Acetate pH 5.5	0.2	8

All solutions were filtered with 0.2 µm membrane filter (Whatman Inc, Piscataway, NJ) before use. The flow through-washing and the elution fractions were collected and the volume was measured to calculate the protein concentration using UV spectrometry to evaluate the dynamic binding capacity at saturation ($DBC_{100\%}$), and the recovery of the protein. The breakthrough curves of chromatograms, measured at 280 nm, recorded using Waters Empower Pro Software (Waters Corporation, Milford, MA) were used to determine the dynamic binding capacity at 10% of the maximum breakthrough height ($DBC_{10\%}$). These parameter were defined in the following way:

$$DBC_{100\%} = \frac{m_{ads,100\%}}{W} = \frac{C_0 V_{loaded} - m_{lost,100\%}}{W}$$ Eq. 5

$$DBC_{10\%} = \frac{(V_{10\%} - V_0) C_0}{W}$$ Eq. 6

$$Recovery = \frac{m_{elu}}{m_{ads,100\%}}$$ Eq. 7

where C_0 is the initial protein concentration (10 mg/ml), V_{loaded} is the volume of the protein solution loaded to the system (5 ml), $m_{lost,\ 100\%}$ is the mass of protein lost measured analyzing with UV spectrometry the loaded-wash step fraction collected (mg), W is the dry weight of PBT membranes packed in the column (g) (weight of PET layers was not considered in DBC calculation), $V_{10\%}$ represent the volume passed through the column at 10% breakthrough (ml), V_0 is the void volume (ml) calculated by a chromatogram obtained in nonbinding conditions, m_{elu} is the mass of protein eluted (mg) and $m_{ads,100\%}$ is the mass of protein adsorbed (mg) at saturation.

3.2.7 Dynamic separation from protein mixture

The PBT-GMA-DEA and PBT-GMA-SO_3 packed columns were described in Section 3.2.6. The PBT-GMA-DEA column was used for the separation of BSA from protein mixtures containing:

- BSA (5 mg/ml) and hIgG (5 mg/ml);
- BSA (5 mg/ml) and lysozyme (5 mg/ml);
- BSA (3.3 mg/ml), hIgG (3.3 mg/ml) and lysozyme (3.3 mg/ml);

The protein mixture was prepared in binding buffer, 20 mM Tris-HCl pH 6. After equilibration with binding buffer, 1 ml of the protein solution was loaded with a superficial velocity of 0.076 cm/min (0.06 ml/min). After protein binding, the column was washed with 13 CV of binding buffer to remove any unbound or loosely bound proteins. Then elution was performed with 32 CV of 20 mM Tris-HCl, 1M NaCl, pH 7. A regeneration step was performed with 13 CV of 20 mM Tris-HCl, 1 M NaCl, pH 10 to restore the primitive conditions of the column, followed by washing with 20 mM Tris-HCl, 1 M NaCl, pH 6 (13 CV) in an attempt to decrease the pH to 6 more rapidly. The effluent was monitored by absorbance at 280 nm. The flow-through, wash, elution and regeneration were collected and analyzed by SDS-PAGE.

The purification of hIgG from a protein mixture containing hIgG and BSA was performed with the PBT-GMA-SO_3 column. The mixture was prepared with a total protein concentration of 10 mg/ml in binding buffer and a mass ratio between proteins of 1. Different values of pH (5.0, 5.5, 6.0, 6.5) of the binding buffer (20 mM Acetate) were investigated. After equilibration with binding buffer, 1 ml of protein solution was injected with a superficial velocity of 0.076 cm/min (0.03 ml/min). After protein binding the columns were washed with 13 CV of binding buffer to remove any unbound protein. The bound proteins were then eluted using 20 mM Acetate, 1M NaCl, pH (5.0, 5.5, 6.0, 6.5) (32 CV). A regeneration step was performed with 20 mM Tris-HCl, 1 M NaCl, pH 10 (13 CV) to restore the primitive conditions of the column, followed by washing with 20 mM Acetate, 1M NaCl, pH 5.5 (13 CV) in attempt to decrease the pH to 6 more rapidly and then re-equilibrated with 20 mM Acetate at desired pH. The effluent was monitored by absorbance at 280 nm. The flow-through, wash, elution and regeneration were collected and analyzed by SDS-PAGE.

Prior to run the SDS-PAGE, all collected fractions were concentrated five times by centrifugation at 4 °C using an Amicon® Ultracentrifuge filter (3000 MWCO, Ultracel®, Millipore, Billerica, MA, USA) and diluted to obtain an estimated total protein concentration of 0.5 mg/ml. Samples were prepared under reducing condition. The preparation was done by adding 25 µl of each sample (protein load mixture, flow-through, elution, regeneration, pure proteins) with 23.75 µl of BioRad 2x Laemmli sample buffer + 1.25 µl of β-mercaptoethanol, and heated to 90 °C for 10 minutes in a hot water bath. SDS-PAGE was performed with Mini-PROTEAN TGX precast gel, 40 µl of the reduced samples and 20 µl of molecular marker (Biorad precision plus protein dual color standard) were loaded onto the gels. The gels were run at 200 V for 35 minutes and stained with Brilliant Comassie Blue. Images of the gels were captured using a BioRad Gel Doc XR + system (BioRad, Hercules, CA) with ImageLab software (BioRad, Hercules, CA). Densitometry analysis was performed using ImageJ 1.50i (National Institute of Health, USA) software to calculate the relative purities of the samples.

Chapter 4

Experimental Results

4.1 Introduction

In this chapter the experimental results obtained during the research period at North Carolina State University are described. At first the variation of some grafting reaction parameters, as thermal initiator and polymerization temperature, were evaluated in order to optimize the grafting procedure for HIG nonwoven. Then the effect of the ligand concentration, used in the epoxy activation step, and the % weight gain, on the protein binding capacity were investigated. Modified PBT membranes which show the best performance in static binding studies were further investigated in their ability to bind protein under flow conditions and to separate proteins from complex mixture.

4.2 Results and discussion

4.2.1 PolyGMA grafting on PBT nonwovens by HIG and by UVG

By variation of the reaction conditions, it is possible to have easy control over the degree of GMA grafting on the commercial PBT nonwovens and hence the membrane properties [36], [30], [27]. HIG of polyGMA on nonwovens using a constant concentration (75 mM) of the heat initiator BPO monomer in DMF as initiator solution, and 30% v/v of GMA in DMF as grafting solution, at different temperatures ranging from 60 °C to 90°C were investigated. The degrees of polyGMA grafted over the time at different polymerization temperatures are presented in Figure 8.

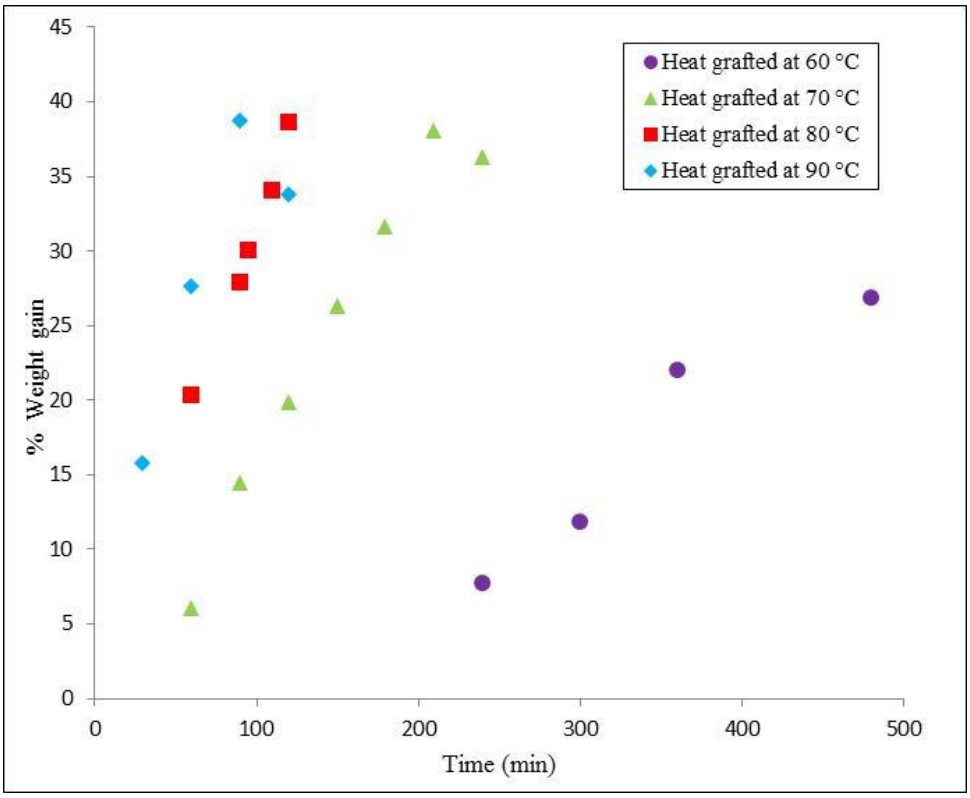

Figure 8. Comparison of the degree of polyGMA thermally grafted at different polymerization temperatures over reaction times.

As can be seen from Figure 8, the degree of GMA grafting on PBT nonwovens increase linearly with the time of exposure for all temperature investigated, which indicated that the number of terminations increases with the time producing a growing of the grafted layer on the nonwovens.

As is evident from the graph, the temperature has a wide effect on the radical polymerization reaction: the higher polymerization temperature caused the higher degree of grafting considering the same time of exposure. No grafting was observed earlier than 4 hours using 60 °C as polymerization temperature and the overall extent of grafting was less than 30% weight gain after 8 hours; this value is obtainable within 2 hours of reaction with higher temperatures. The rate of decomposition of BPO depend, in fact, on the solvent and the temperature [43]. Rate of decomposition of BPO in organic solvent at 60, 78, 100°C correspond respectively to $2 \cdot 10^{-6}$, $2.3 \cdot 10^{-6}$, $5 \cdot 10^{-4}$ [45]. The data were founded for benzene as solvent and used to have a general idea of the behavior of BPO. It is possible to observed that the rate of radical formation growth of two orders of magnitude with the increase of the temperature from 60 to 100 °C. This explain the fast rise of the grafting rate with the increase of the temperature. BPO as thermal initiator is commonly used at 80-95 °C [46].

The effect of the presence of the initiator benzoyl peroxide (BPO) in the initiator solution (IS) or in initiator and grafting solution (IGS) on the grafting at a polymerization temperature of 80 °C is showed in Figure 9.

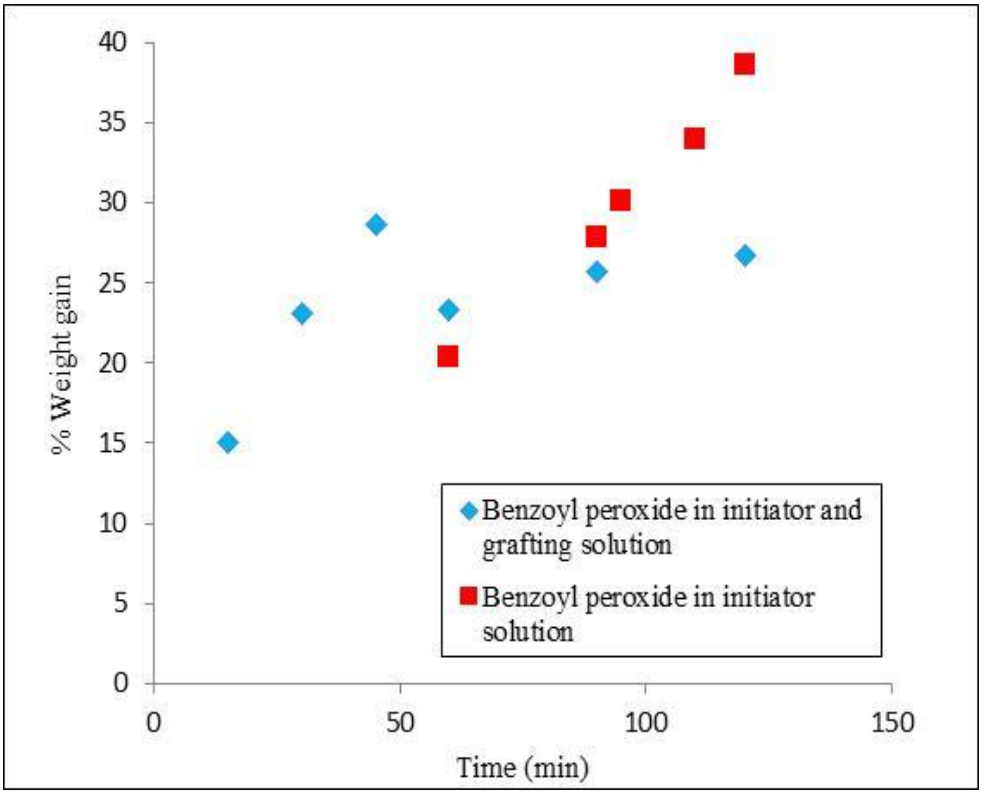

Figure 9. Comparison of the effect of the presence of the benzoyl peroxide in IS and in IGS on the degree of polyGMA thermally grafted on PBT fibers at 80 °C.

From Figure 9, it is clear that the presence of BPO in IGS results shows higher polyGMA grafting chain densities in short time. The higher amount of BPO in grafting solution results in the larger number of radical sites on the fiber surface. The decreasing of degree of grafting after 50 minutes it might be attributed to two factors: BPO which is not absorbed from the nonwovens can initiate the formation of GMA homopolymer in solution, causing the subtract of the polymer on the fibers. A similar behavior was observed by Liu *et al.* [36] and by Ma *et al.* [47]. Other aspect to be considered is that, the higher the amount of initiator in solution (case of BPO in IGS) the higher the production of free radicals.

Since the rate of termination goes to square of radical concentration, the larger number of radical tend to terminate more polymer chains instead of growing the chains on the fibers [48]. The resulted grafting structure is characterized by shorter and denser brushes compared to that one produced using lower amount of BPO (IS).

The surface morphologies of the PBT nonwoven before and after polyGMA grafting were observed using scanning electron microscope (SEM). Figure 10 shows SEM images of blank PBT (row A), and PBT-GMA thermally grafted at different reaction time resulting in different weight gain, 20% (row B) and 28% (row C). Grafting conditions of 80 °C (polymerization temperature), 70 mM BPO in DMF (initiator solution) and 30%v/v GMA in DMF (grafting solution) were used. Images in second column have a higher magnification to observe the details of the fiber surface.

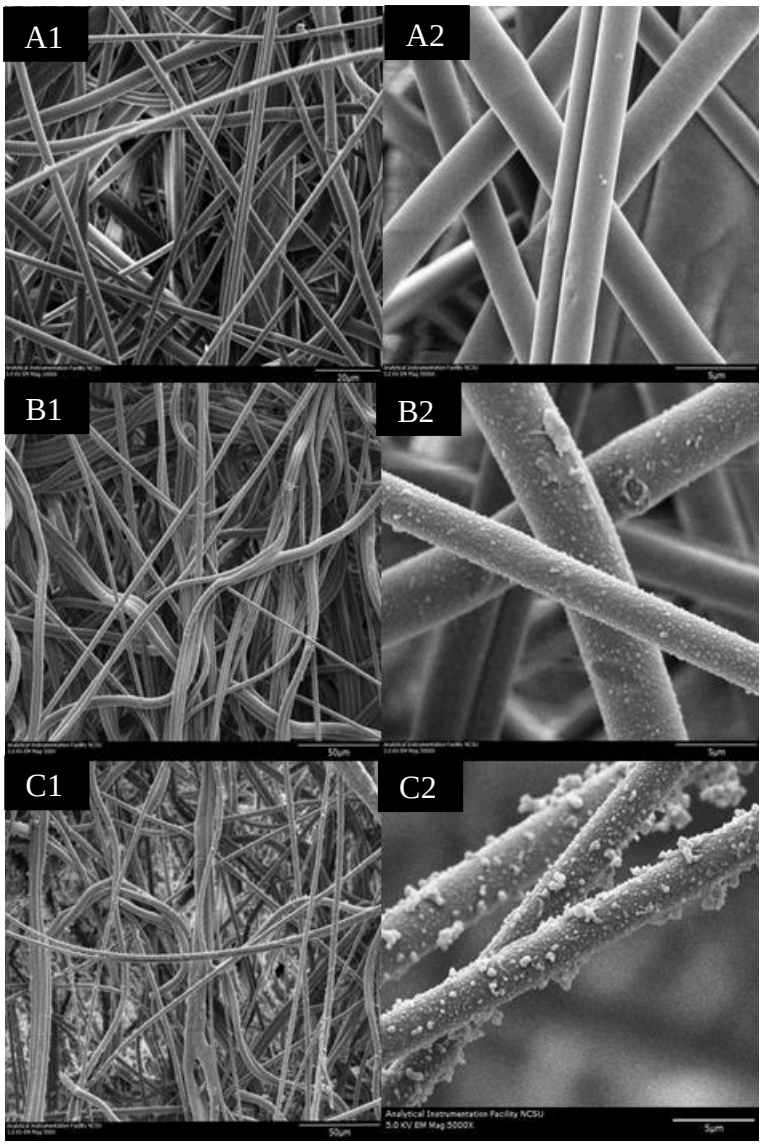

Figure 10. SEM images of membranes. (A): blank PBT, (B): heat induced polyGMA grafting on PBT fibers at 20% weight gain, (C): heat induced polyGMA grafting on PBT fibers at 28% weight gain. (Left: x500, Right: x5,000).

Blank PBT nonwovens (rows A) show a smooth surface. The fibers characterized by a low % weight gain, as 20% (row B) display homogenous polyGMA grafted layer

around the PBT fibers. Increasing the amount of polyGMA grafted, the roughness of the fibers increase even though the pore morphology of hydrophilized PBT membranes is very similar to that of unmodified PBT membrane.

Further parameter that can influence the surface morphology is the polymerization temperature as displayed in SEM images in Figure 11. Both samples are characterized by grafting at 28% weight gain with the different reaction temperature of 80 °C and 70 °C for samples in row A and B respectively.

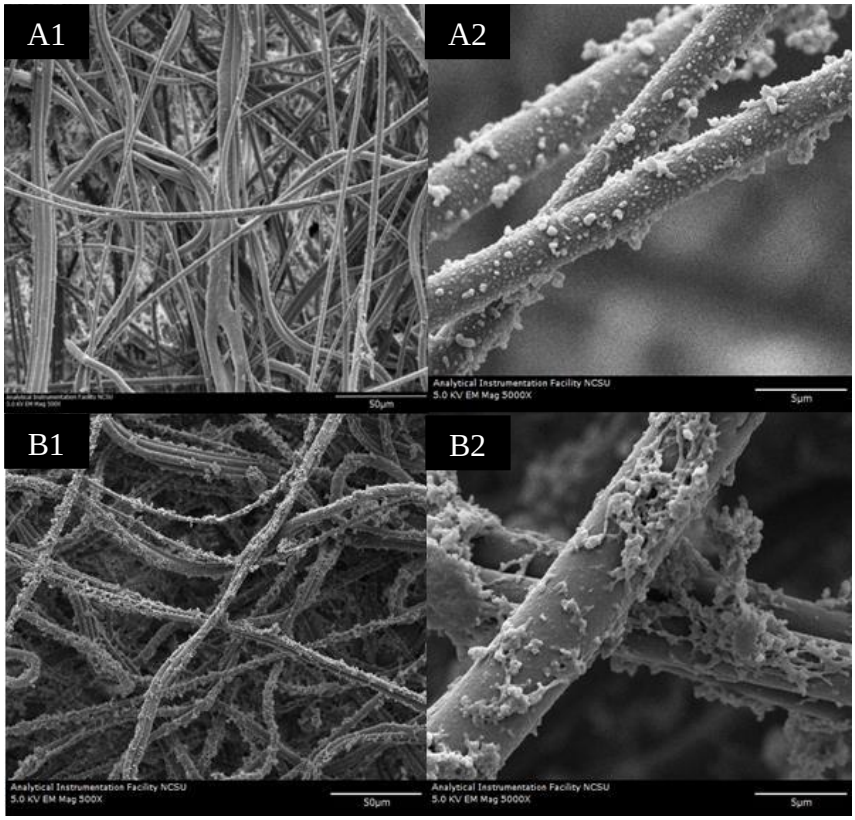

Figure 11. SEM picture of heat induced polyGMA grafting on the PBT nonwoven at different polymerization temperature: (A) 80 °C, (B) 70 °C. Both nonwovens grafted at 28% weight gain. (Left: x500, Right: x5000)

UV induced polyGMA grafting on PBT nonwovens was investigated. The trend of the % weight gain over the time is presented in Figure 12. The data shows that altering the exposure time to UV light of the nonwovens can be a useful method to control the grafted layer thickness: the free radical number seems to be proportional with the exposure time. After 35 minute of reaction, corresponding to 20% weight gain, it observed a plateau due to probably of the depletion of available GMA monomer in solution. No change in the degree of polyGMA grafting was registered by turning the side of the PBT nonwoven exposed to UV light during the polymerization process.

Same result was obtained by Liu *et al*. [36] and Zheng *et al*. [27]. This is produced by the fact that in porous system part of the incident light is reflected and scattered in different directions from all surfaces [49].

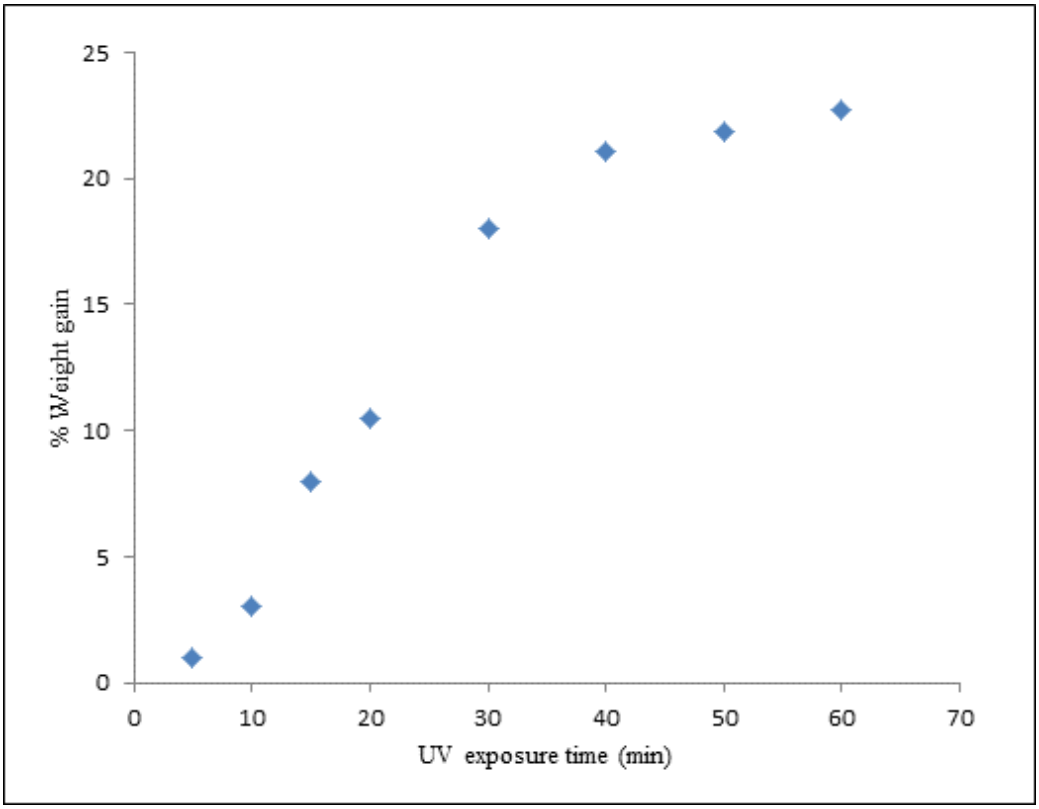

Figure 12. UV induced grafting evaluated by % weight gain over the polymerization time.

SEM images of PBT nonwoven before and after grafting, using UV method, are shown in Figure 13. Row A contains blank PBT, rows B and C contain modified nonwoven at 23% weight gain coming from two different parts of the sample; images in the right column have higher magnification. It seems that UV activation enables to have more uniform and conformal grafting on the fiber surface compared to use heat treatment.

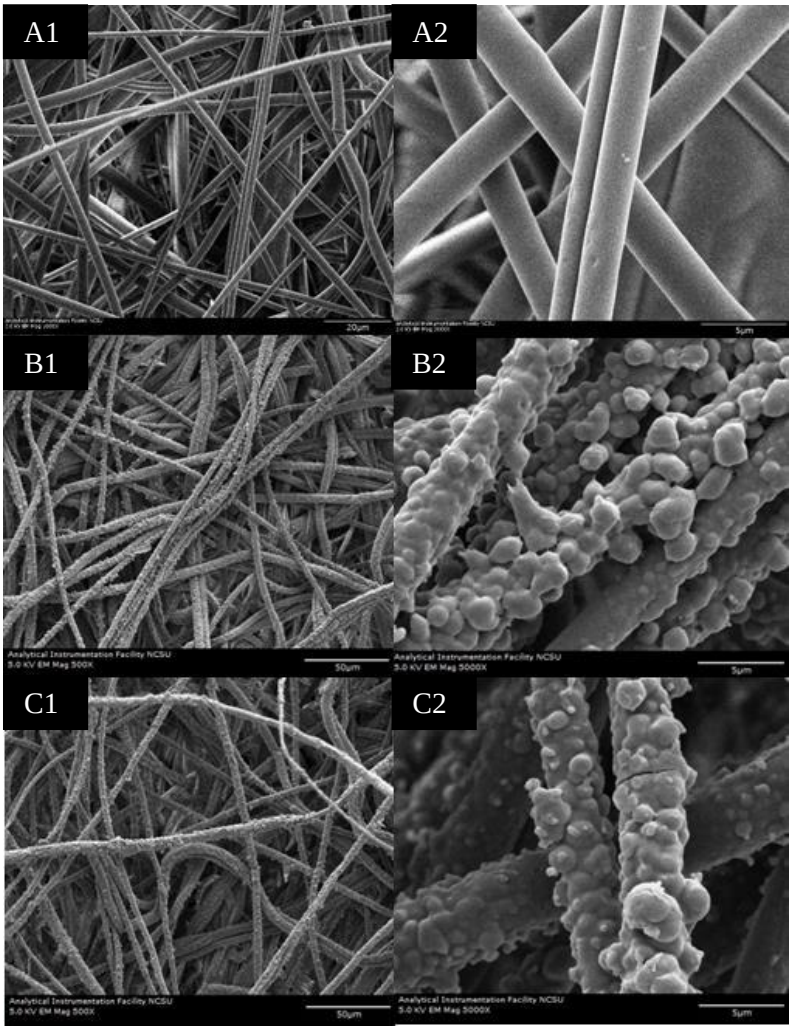

Figure 13. SEM images of PBT nonwoven. (A) Blank PBT, (B) and (C) UV induced polyGMA grafting on PBT nonwoven at 23% weight gain (corresponding to an exposure time of 60 minutes) comes two different part of the sample. (Left: x500, Right: x5000).

4.2.2 Effects of %weight gain and ligand density on static binding capacity

A schematic surface modification procedure to induce grafting on the membranes by heat and UV approach and the following functionalization to form weak anion exchangers and strong cation exchangers is showed in Figure 14. The first step is the polyGMA grafting on the PBT nonwoven fabrics in order to achieve PBT-GMA structure that includes reactive epoxy groups.

Ionic groups located on the surface of the fibers are required for ion exchange chromatography. These epoxy groups were then converted into cation and anion exchangers by nucleophilic reaction with sulfonic acid groups and diethylamine (DEA)

respectively. After ligand attachment, the unreacted epoxy groups were hydrolyzed with sulfuric acid to reduce nonspecific protein binding [50].

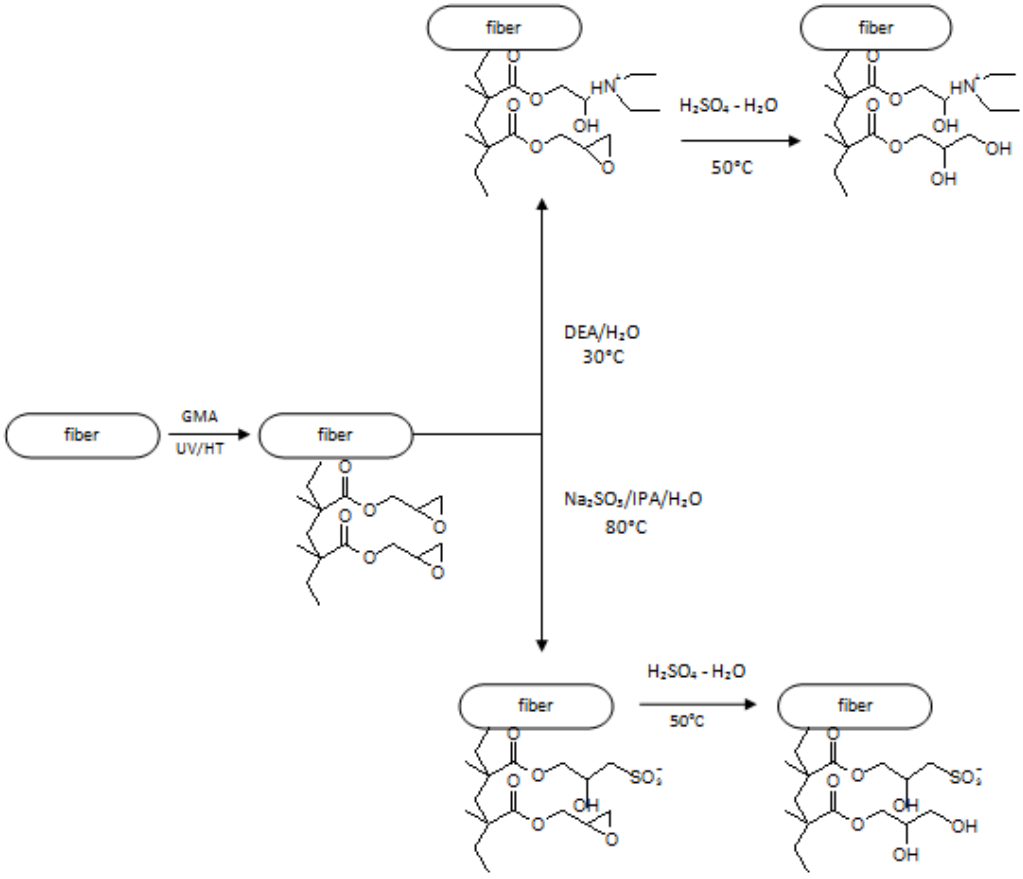

Figure 14. Schematic representation of the procedure used to create anion and cation exchange PBT nonwoven membranes. Following the HIG or UVG of polyGMA on nonwoven fabrics, membranes were functionalized to be weak anion exchangers, by DEA attachment, and strong cation exchangers, by attaching sulfonic acid groups. A last treatment with sulfuric acid, to convert the unopened ring to diol, was realized.

BSA and hIgG were used as model proteins for anion exchange binding and cation exchange binding respectively.

In primary studies, PBT grafted nonwoven was functionalized as anion exchanger using 50% v/v DEA in aqueous solution and as cation exchanger using sodium sulfite in a solution with IPA and water with a ratio of 10:15:75 =Na_2SO_3:IPA:H_2O %wt [30], [42]. The data of the amounts of BSA and hIgG bound over the % weight gain, of grafted PBT nonwovens functionalized according the conditions just mentioned, are showed in Figure 15.

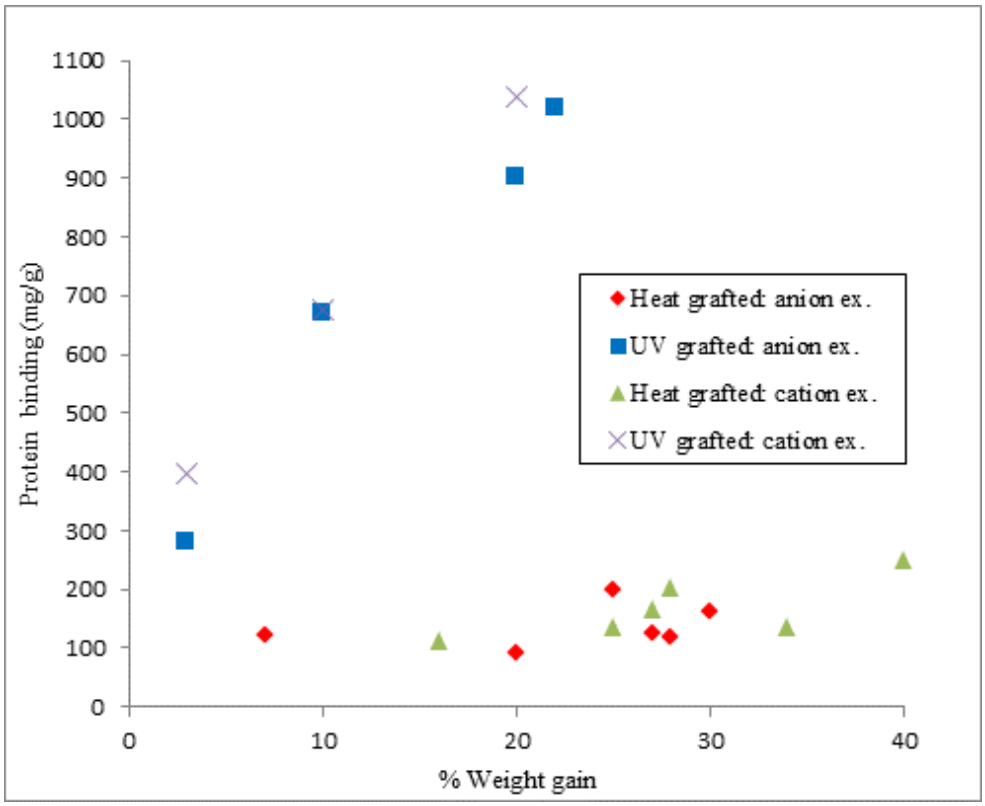

Figure 15. Comparison of equilibrium binding capacity of UV and heat grafted membranes functionalized either using a to be a cation (Na_2SO_4:IPA:H_2O=10:15:75) and anion (50% DEA v/v) exchanger to bind hIgG and BSA respectively, at various degrees of polyGMA grafting.

As is evident from the Figure 15, using UVG grafted or HIG nonwovens produce considerable difference in static binding capacity (SBC).

A direct proportionality between the equilibrium binding capacity and % weight gain is more obvious for UVG membranes than HIG membranes. A maximum value of 249 mg/g of binding capacity is obtained with HIG nonwoven in contrast to a value of 800-1000 mg/g with UVG nonwovens. These data match with results from a previous study of other author [30] in which this behavior, different in amount of protein adsorbed, was explained by a different structure of GMA induced by the two different method of grafting. As showed in the figure the UV approach creates a grafting structure capable to accommodate a larger number of proteins than the heat grafting approach. Since the reaction of free radical polymerization induced by UV light produces linear and flexible polyGMA brushes anchored on the nonwovens. UVG membranes are able to accommodate a large amount of protein due to the capacity of brushes to expand and rearrange. Contrarily, the high rate of chains transfer using the heat as activation of reaction, produces a highly branched polymer chain and a highly cross-linked polymer network. These effects determine a higher density of the grafted polyGMA layer that

causes a smaller volume to accommodate proteins and more rigid structure due to the highly cross-linked polymer network that prevents protein diffusion into the depth of grafted layer. Figure 16 shows a schematic representation of the two different grafting structure, Figure 16 is an adaptation from Heller *et al.*'s article [30].

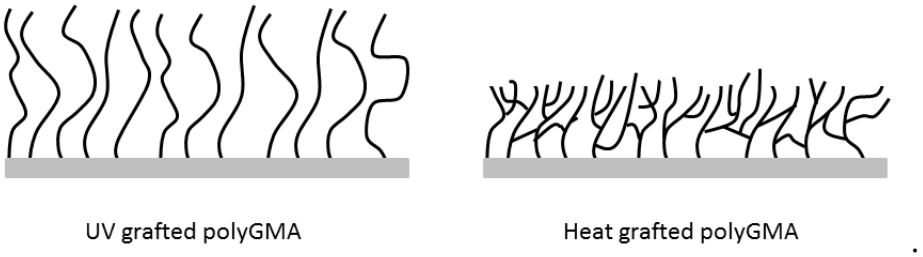

Figure 16. Schematic representation of the different grafting structure induced by UV light and heat [30].

In order to optimize the equilibrium binding capacity of HIG nonwovens, the effect of grafting conditions were investigated. The effect of the presence of thermal initiator BPO in initiator and grafting solution, and only in the initiator solution, for HIG membranes at 22 % weight gain were reported in Figure 17. Polymerization temperature of 80 °C were used.

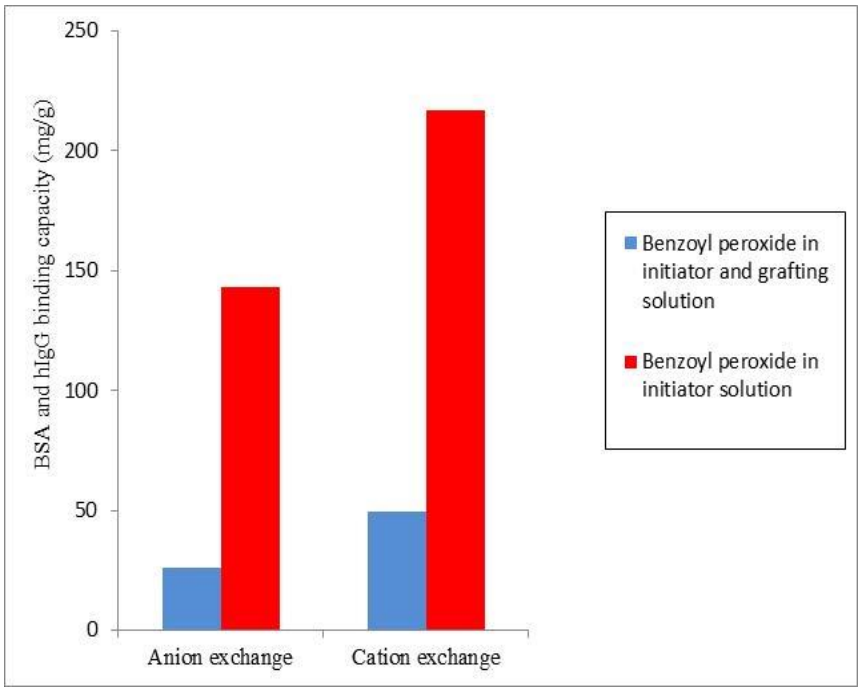

Figure 17. Effect of the thermal initiator BPO in grafting solution and initiator solution on the protein binding capacity of anion- and cation- exchange PBT nonwovens. Samples were grafted at 22% weight gain with polymerization temperature of 80 °C.

From Figure 17 it is apparent that using the thermal initiator in both solution results no protein binding-efficient. As anticipated in *4.2.1 PolyGMA grafting on PBT nonwovens*, the higher concentration of BPO the higher the concentration of the radicals and the rate of termination reaction during the polymerization. The probably resultant grafting structure, with higher density of shorter brushes compared on equal % weight gain , increases the steric hindrance causing low value of protein binding capacity.

The effects of the polymerization temperature and the DEA concentrations on the BSA binding capacity were also investigated. Results are shown in Figure 18.

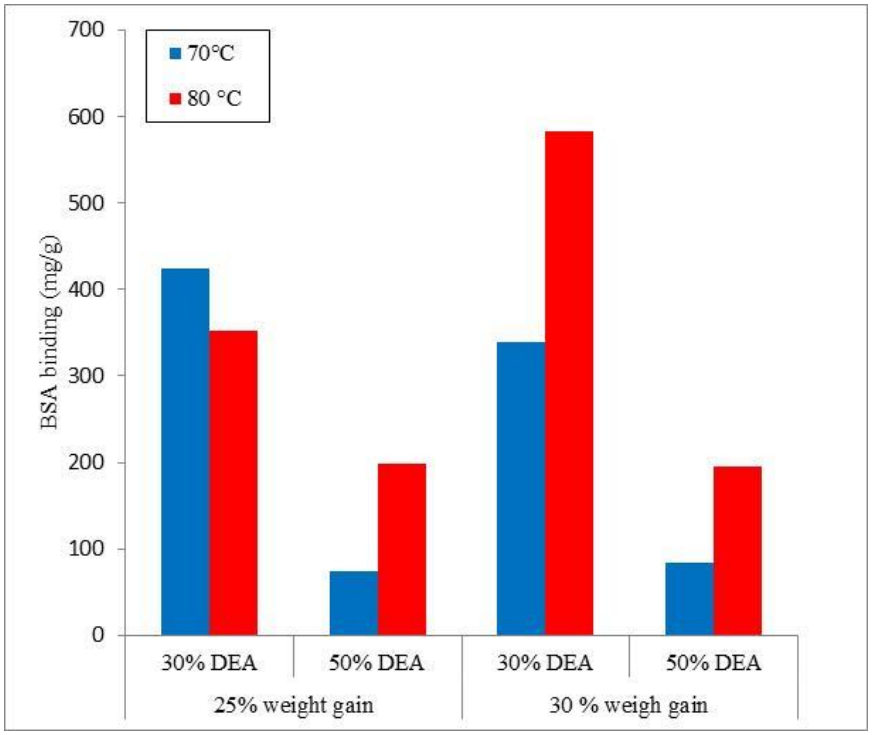

Figure 18. Effect of the DEA concentration in functionalization solution and the polymerization temperature on the equilibrium BSA binding capacity. Studies carried on for anion exchange thermally grafted PBT nonwovens at 25% and 30% weight gain.

Equilibrium BSA binding capacity is higher by using a polymerization temperature of 80 °C and a lower amount of DEA in functionalization solution for almost all condition investigated.

Results reported in this section demonstrate a strong dependence of the protein adsorption on the polyGMA grafted layer and the functionalization conditions [51], [46]. The study of these parameter permit to optimize the accessibility of the binding protein. HIG nonwovens with excellent results were prepared with a polymerization temperature of 80 °C and adding the thermal initiator only in the initiator solution.

In this work, various DEA or Na_2SO_3 concentrations were investigated to activate the epoxy groups on grafted PBT membranes. Anion and cation exchange membranes were functionalized using concentrations between 2 and 60 % v/v of DEA in aqueous solution and a mass ration between Na_2SO_3:IPA:H_2O=0.1:15:75 %wt and 12:15:75 %wt of sodium sulfite, respectively.

4.2.2.1 Heat induced polyGMA grafting on PBT nonwovens functionalized as anion exchangers

The activation of epoxy groups on the grafted nonwovens were achieved by reaction with diethylamine (DEA) forming a tertiary ammonium positively charged on PBT nonwovens. BSA was chosen as the model protein to evaluate how the various DEA concentrations in the functionalization solution affect the overall static binding capacity when these materials work as anion exchangers. Considering that the isoelectric point (pI) of BSA is 4.7 [52] a binding buffer at pH 7 (20 mM Tris-HCl pH 7) was applied aiming to make BSA, negatively charged, adsorbing to the membrane. In Figure 19 BSA binding values, expressed in mg of protein per g of samples, are reported for various volume concentrations of DEA in aqueous solution at different degree of polyGMA grafting thermally induced.

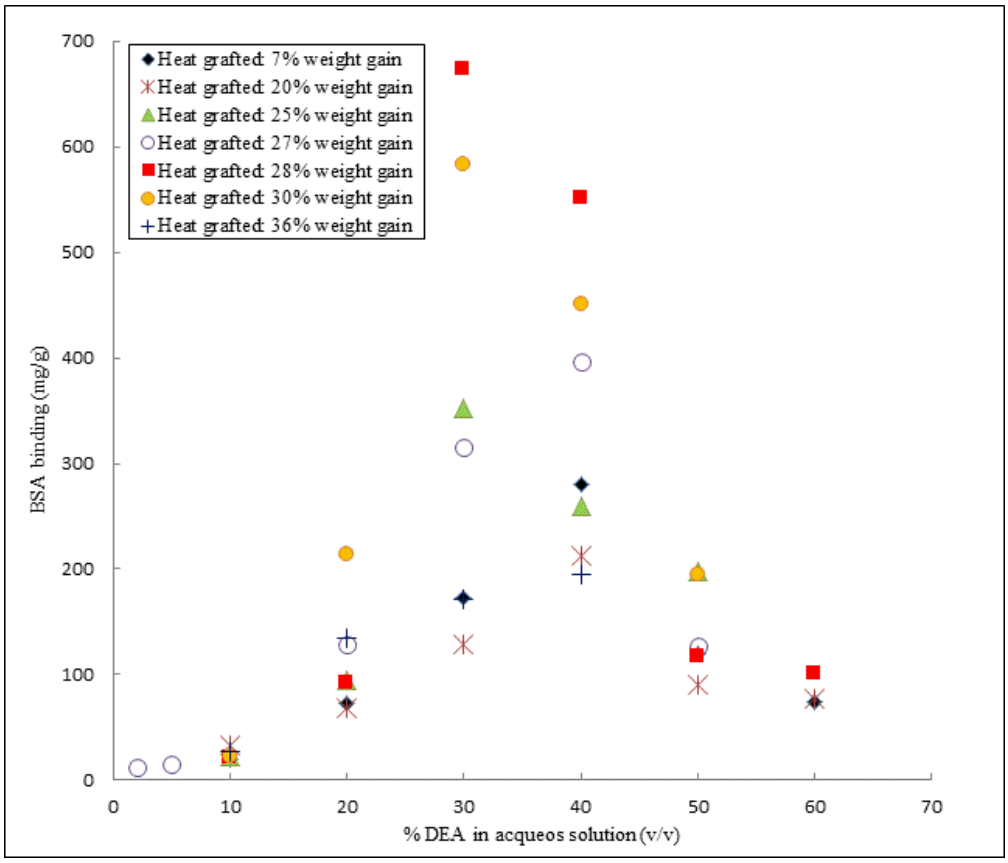

Figure 19. Equilibrium BSA binding of PBT nonwovens at various extents of polyGMA grafting, with different % (v/v) DEA in aqueous solution. HIG at 7%, 20%, 25%, 27%, 28%, 30% and 36% weight gain. All experiments were done in batch system for a binding time of 15 hours.

For DEA concentrations tested, BSA binding capacity display a peak when the % v/v DEA ranging between 30% and 40%, for all the % weight gain investigated. It also clear that the amount of protein adsorbed is strongly influenced by the degree of polyGMA grafting, which is getting more obvious in the range of 30-40% DEA. The highest values of BSA binding capacity, 673.6 mg/g and 583.14 mg/g, were achieved for membranes grafted at 28% and 30% weight gain respectively, both functionalized using 30% v/v DEA.

It is interesting the decline of amount of protein bound with an increase more than 30% weight gain, reaching with samples grafted at 36% weight gain a value of 171 mg/g (30%DEA), almost four times less than the maximum obtained (670 mg/g). The explanation of this phenomena is due to the particular structure of the heat induced polyGMA grafted nonwovens. The high % weight gain leads to the dense grafted layer and lots of cross-linked structure. This causes a more rigid and less flexible structure with the increase of the % weight gain, impeding the protein diffusion along the grafted layer due to the size exclusion phenomena [30].

Elemental analysis on the samples used in BSA binding study, HIG nonwovens functionalized as weak anion exchangers with DEA attachment, was performed in order to determine the ligand density of membranes functionalized under various conditions. To determine if the DEA concentration, used in the functionalization solution, is correlated with DEA density, the data of elemental analysis of membranes at different degree of grafting, are reported in Figure 20.

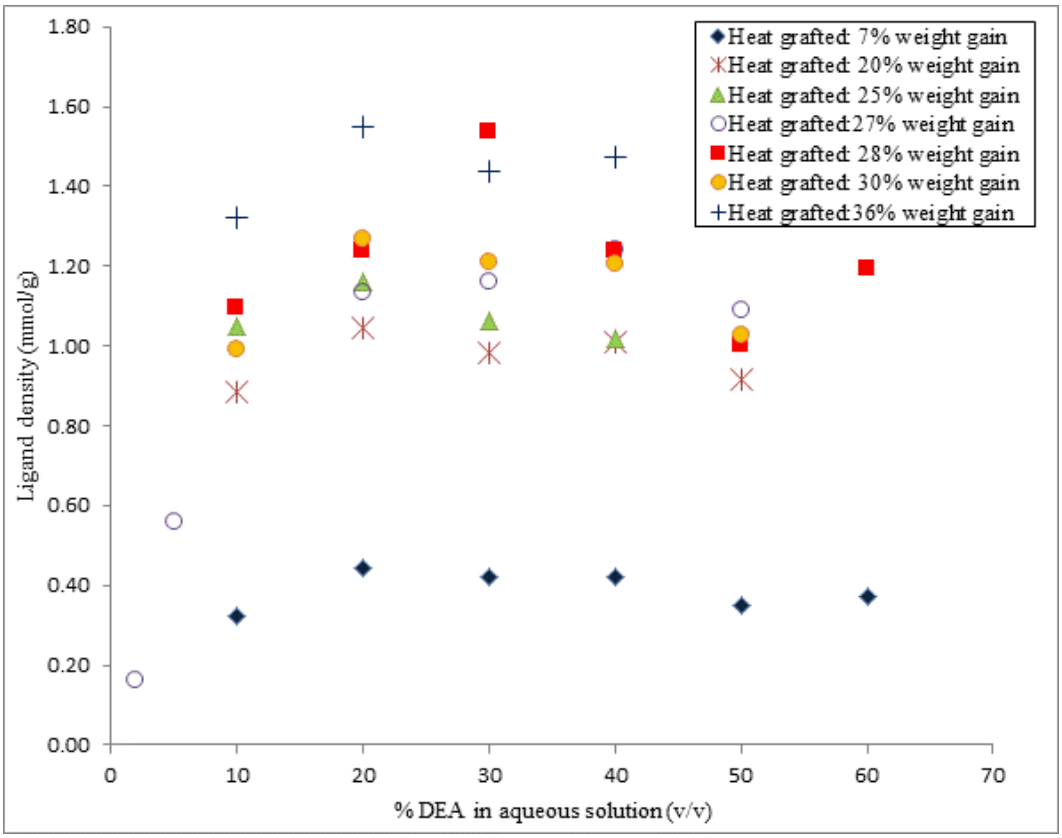

Figure 20. Relation between DEA ligand density and volume concentration of DEA in aqueous solution for different degree of grafting thermally induced. Densities determined via elemental analysis.

Few effect of % v/v DEA on ligand density is observed, contrarily controlled varying the degree of polyGMA grafted. It shows a growing of ligand density between 2% and 10% v/v DEA (27% weight gain), amount of ligand for which no binding was observed. It is possible to hypothesize for such plateau that at a specific % weight gain, when a DEA volume concentration is over 10%, the number of epoxy groups converted would not be changed by increasing the DEA volume concentration. Ligand density data of Figure 20 were plotted in function of the % weight gain in order to observe the linear nature of the function that exists between the two variable, as shown in Figure 21. The

direct proportionality between the degree of grafting and ligand density on the PBT nonwovens, using HIG and UIG, is confirmed also in other works [30], [42].

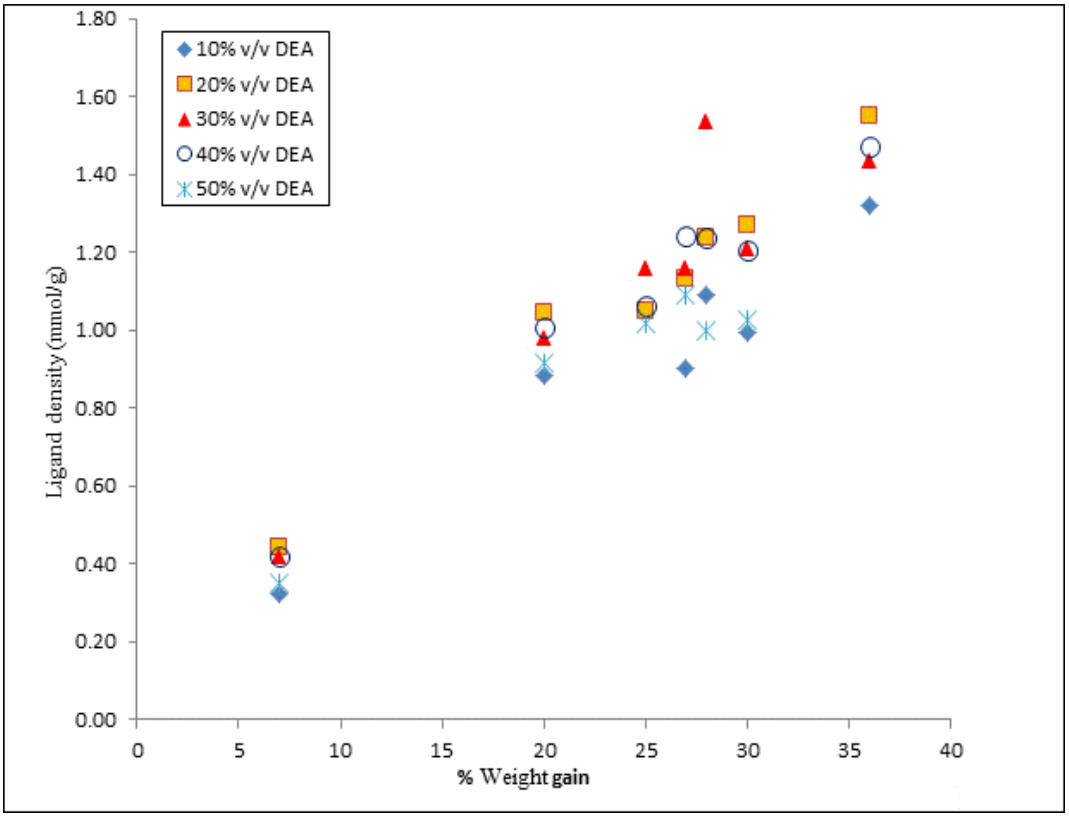

Figure 21. Relation between DEA ligand density and degree of polyGMA grafting on PBT nonwovens by HIG. DEA attachment is realized using different volume concentrations in aqueous solution (10% to 50%v/v DEA). Densities determined via elemental analysis.

The highest value (673 mg/g) of binding capacity, obtained for HIG nonwovens at 28% weight gain functionalized with 30%v/v DEA in aqueous solution, was achieved with ligand density of 1.54 mmol/g. Focusing on this, the higher the ligand density on the nonwovens, the higher the capacity to bind proteins. Unfortunately this not seems to be a general phenomenon: the increase of ligand density is not often connected with an increase of binding capacity. Considering high values of binding capacity (450, 550 and 583 mg/g), achieved for HIG at 28-30% weight gain, using 30%-40% DEA, was registered a medium ligand density of 1.2 mmol/g. It is important to underline that samples with same DEA density and % weight gain and different in DEA concentration used in the functionalization solution, reach values of BSA binding 2.4-5 times lower.

It supposes that using a DEA concentration to functionalize membranes between 30% and 40% v/v allows a more favorable distribution of ligand on the brushes of the nonwovens, parameter that can show an important effect on the binding capacity [53]. It

presumes that the favorable ligand distribution allows, during the BSA binding step, the reducing of the steric hindrance and repulsion effect between the protein negatively charged allowing to the penetration of protein inside the layer. Additionally, the best distribution of the ligand could permit to reduce the number of ligand molecules involved in bind of the same protein molecule due to of the non-null size of the protein. Therefore, the high ligand density is not always connected to the proportional higher protein binding capacity, due to the limitation of steric hindrance and repulsive effect that do not allow the protein to bind inside the grafted layer, as already reported in previous studies [54] [55].

SEM images of the nonwovens thermally grafted at 28 % weight gain are shown in Figure 22. Samples in row (A), (B), (C) and (D) correspond to PBT-pGMA functionalized using 0% (only grafted), 10% (ligand density: 1.09 mmol/g), 20% (1.24 mmol/g), 30% (1.54 mmol/g), 40% (1.24 mmol/g), 50% (1.00 mmol/g) v/v DEA in aqueous solution to see how the concentration of the ligand affects the surface morphology of the membrane. For each samples are showed two images with one at low magnification to show overall pore structure and one at high magnification.

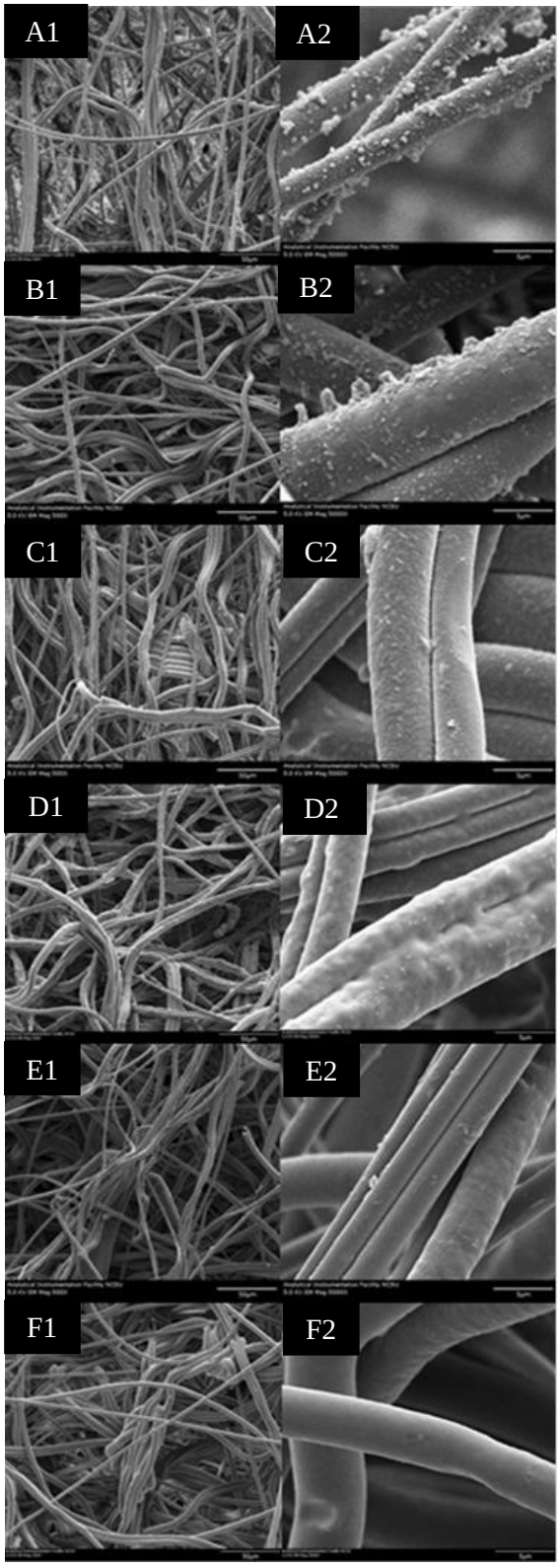

Figure 22. SEM micrographs of heat induced grafting on PBT nonwovens. Heat grafted membrane at 28% weight gain (A), heat grafted membrane at 28% weight gain functionalized with 10% (v/v) DEA (B), 20% (v/v) DEA (C), 30% (v/v) DEA (D), 40% (v/v) DEA (E) and 50% (v/v) DEA (F) in aqueous solution. (Left: x500, Right: x5,000)

The surface of the fibers becomes smoother and the particles on the surface disappear after the introduction of the N group functionalities probably due to the expansion of the polymer chains after ligand attachment [56]. The original pore structure is maintained. From SEM images seems that the complete and uniformly coverage of the fibers is achieved with the high ligand density of 1.54 mmol/g which is realized using 30% v/v DEA in aqueous solution. For others condition seems that ligand density is not enough to uniformly cover all fibers of the nonwoven.

4.2.2.2 Heat induced polyGMA grafting on PBT nonwovens functionalized as cation exchangers

During the sulfonation procedure, the epoxy ring of the GMA monomer is opened and a sulfonate functional group is formed.

Since Human polyclonal antibodies have the isoelectric point (pI) varying from 6 to 9 [57] [58], they can be captured by cation exchange chromatography at an acidic pH where they gain positive charge. In this study a binding buffer at pH 5.5 (20 mM Acetate pH 5.5) was applied aiming to make cation exchange membranes adsorbing positive hIgG. The functionalization of membranes with sodium sulfite was performed by immersing the membrane in a solution containing Na_2SO_3, IPA, and distilled water. The investigation of sodium sulfite (Na_2SO_3) concentrations, ranging between 1 mg/ml (Na_2SO_3:IPA:H_2O=0.1:15:75 %wt) and 122 mg/ml (12:15:75 %wt), provides very interesting effect on the static adsorption capacity. The mass ratio IPA:H_2O of 15:75 was fixed in functionalization solution for all Na_2SO_3 solutions investigated. Figure 23 shows the correlation between hIgG static binding capacity and Na_2SO_3 concentration for various % weight gain. The factor X, in abscissa in Figure 23, represents the variable of Na_2SO_3 in mass ratio Na_2SO_3:IPA:H_2O=X:15:75 %wt.

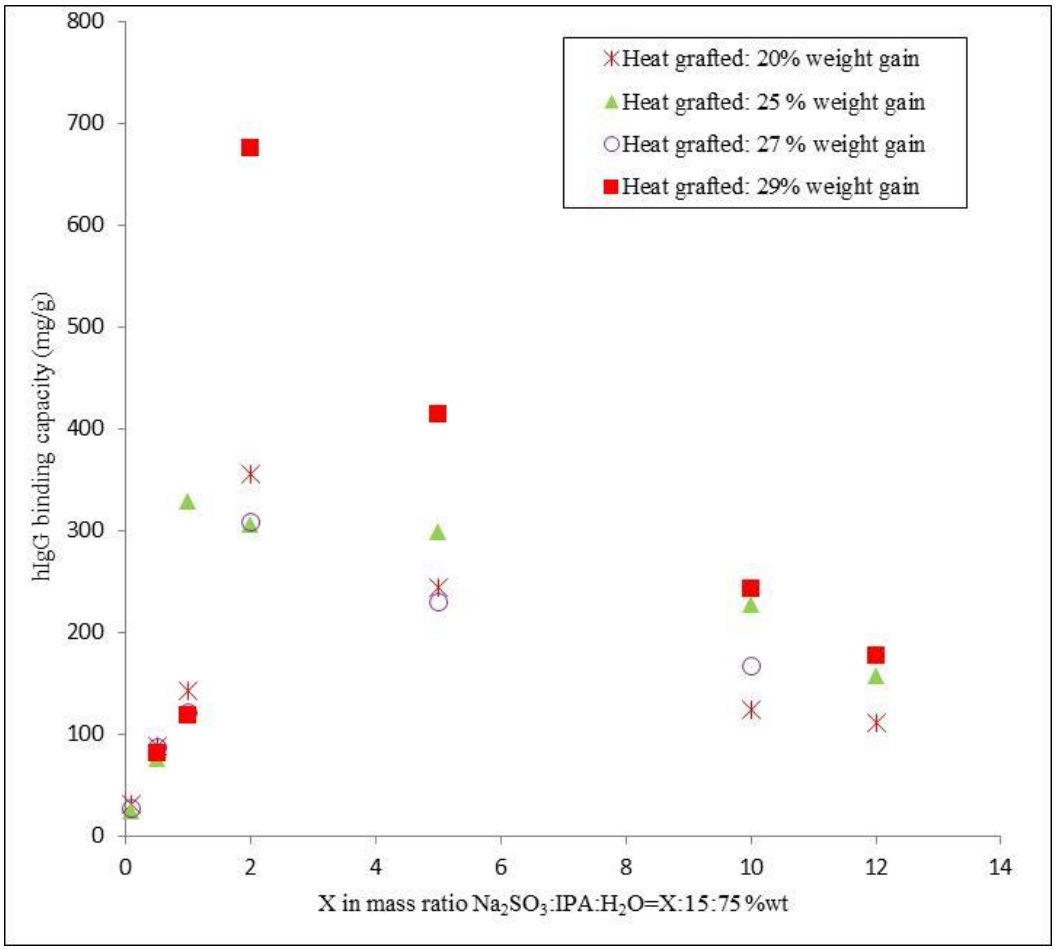

Figure 23. hIgG adsorbed amounts (in static condition) on heat grafted GMA nonwovens at different sodium sulfite concentrations, in terms of mass ratio, for various % weight gain. Factor X represents the variable in the mass ratio Na_2SO_3:IPA:H_2O=X:15:75 %wt.

The cation exchange nonwovens shows an evident relation between the Na_2SO_3 concentration used in the functionalization solution and ligand density obtained by element analysis, as presented in Figure 24. The ligand density was obtained, measuring the amount of sulfur groups on the membrane after functionalization.

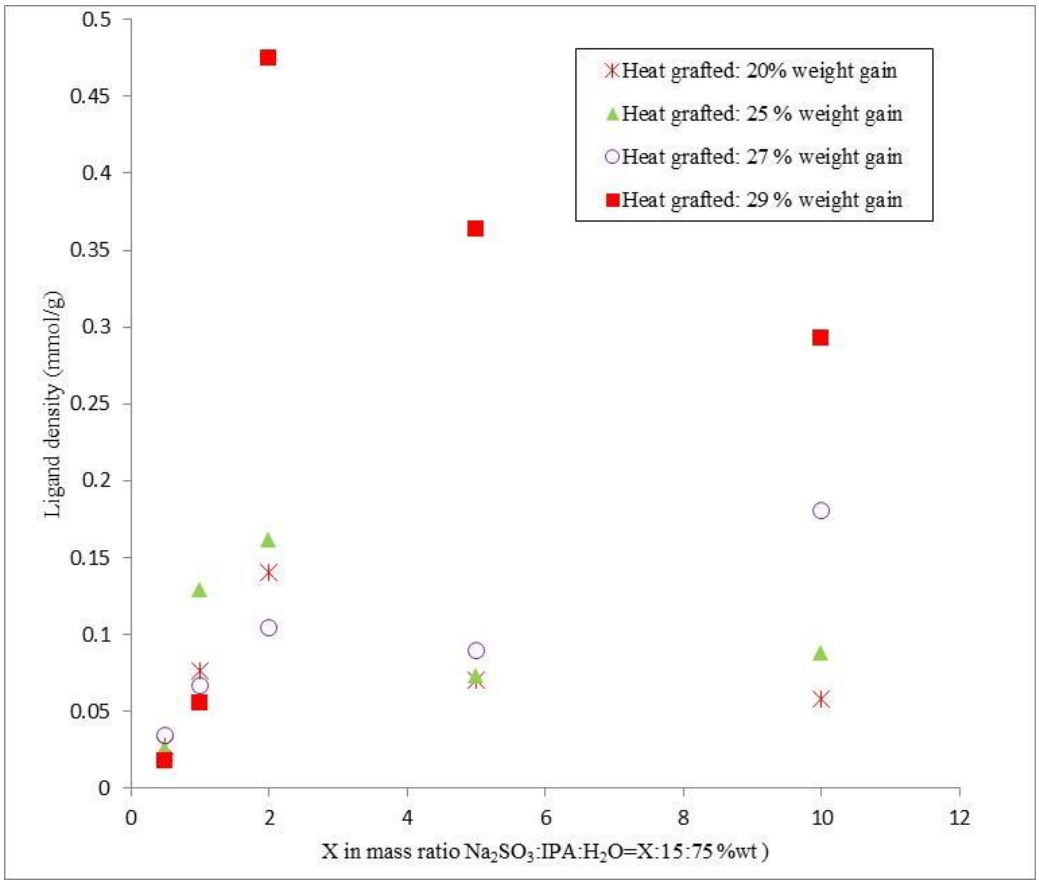

Figure 24. The relation between SO_3 ligand density and sodium sulfite concentration, in terms of mass ratio, at different % weight gains. Factor X represents the variable in the mass ratio Na_2SO_3:IPA:H_2O=X:15:75 %wt.

Highest ligand density is achieved using a mass ratio of Na_2SO_3:IPA:H_2O=2:15:75 %wt. for all % weight gain investigated (Figure 24).

The maximum of adsorption capacity, high value of 675 mg/g, was found for HIG nonwovens at 29% weight gain characterized by a ligand density of 0.47 mmol/g. It deduces that it is possible to control SO_3 density on the nonwovens by varying % weight gain and the concentration of the Na_2SO_3 in the functionalization solution. An approximately proportional relation between the amount of hIgG bound and the concentration of SO_3 groups on grafted layer is present in Figure 25.

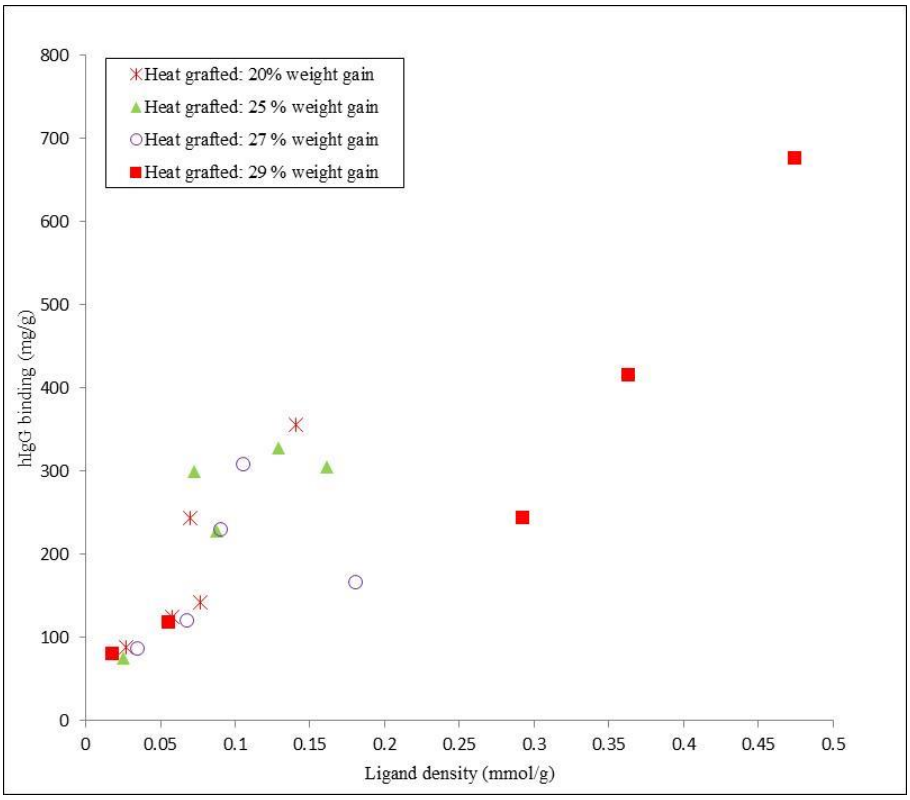

Figure 25. Correlation between the hIgG equilibrium binding capacity and the ligand density for cation exchange heat grafted nonwovens at various % weight gain.

The higher number of active sites causes the higher capability to host proteins. The approximately linear increase of ligand density at low values of SO_3 concentration could mean that the ligand attached on the samples is proportional the amount of ligand initially available in solution, until to reach an optimum at a mass ratio of Na_2SO_3:IPA:H_2O=2:15:75 %wt, for all % weight gain investigated, corresponding to a ligand density ranging between 0.10 and 0.47 mmol/g, based on the degree of polyGMA grafted considered. A further increase of sodium sulfite concentration results in a decrease of the SO_3 density and consequentially in a decrease of amount of protein bound. The larger number of molecules negatively charged in solution leads to the stronger repulsive electrostatic interaction. Recalling the inflexible nature of the HIG membrane structure it is possible that at high concentrations, the repulsion effect between molecules obstruct the attachment of ligand along the brushes of grafting, resulting in a decrease of ligand density. Concluding a sodium sulfite concentration of 21 mg/ml (Na_2SO_3:IPA:H_2O=2:15:75 %wt) permit to realize a good ligand accessibility and low repulsion resulted in a highest conversion of epoxy groups with the sulfonic groups. SEM images were used to study surface morphology before and after functionalization of the PBT nonwovens. Figure 26 shows SEM images of PBT after

polyGMA grafting at 29% weight gain. Rows A show SEM images of heat polyGMA grafted nonwovens at 29% weight gain, rows C, D, E contain SEM images with a SO_3 ligand density of 0.29, 0.36, 0.47 respectively. Images in the left have low magnification to show overall pore structure and Images in right column show high magnification to observe detailed fiber surface morphology.

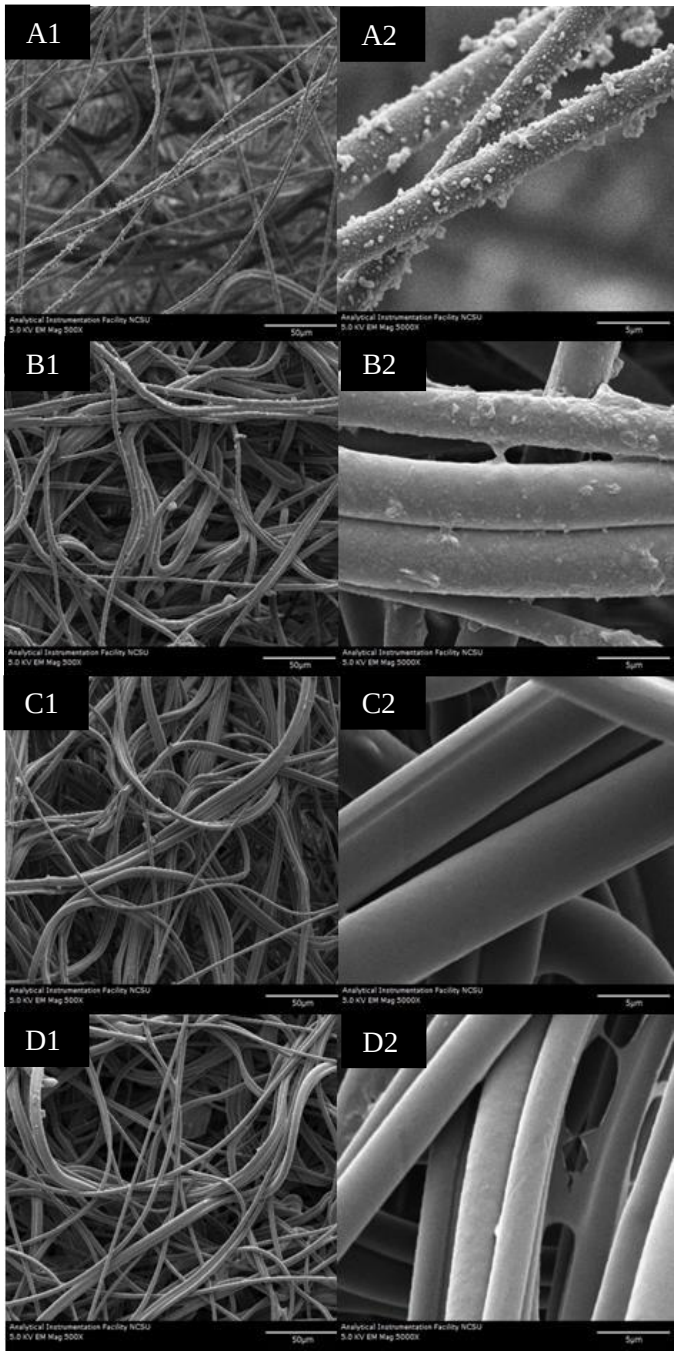

Figure 26. SEM micrographs of heat induced grafting on PBT nonwovens. (A) PBT nonwoven grafted at 29% weight gain, (B), (C), (D) heat grafted membrane at 29% weight gain with a ligand density of 0.29 (Na_2SO_3:IPA:H_2O=10:75:15 %wt.), 0.36 (5:75:15 %wt.), 0.47 (2:75:15 %wt) respectively. (Left: x500, Right: x5,000).

As illustrated by SEM analysis in Figure 26, the surface of the fibers became smother after attachment of sulfonic acid groups. Although the ligand density investigated ranging in a very limited space out, the minor value of ligand density of 0.29 mmol/g seems to be not enough to cover equally all fiber, observing the higher uniformity of the layer of the other samples.

4.2.2.3 UV induced polyGMA grafting on PBT nonwovens functionalized as cation and anion exchangers

Commercial PBT nonwovens were grafted at various % weight gain by exposure for different time to UV light and their equilibrium protein binding capacities for both, anion exchange capture of BSA and cation exchange capture of hIgG, were determined. The effect of DEA or Na_2SO_3 concentration in the functionalization solution on the SBC was also studied. The results of these experiments are reported in
Figure 27 (anion exchange) and Figure 28 (cation exchange).

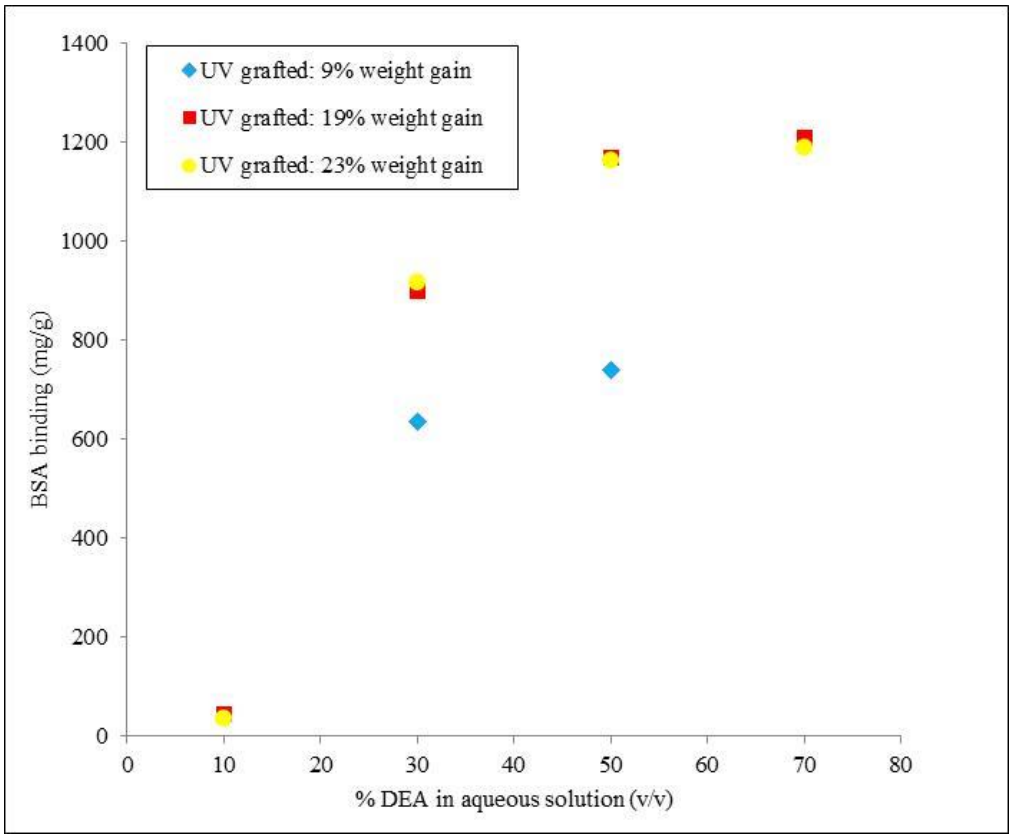

Figure 27. BSA adsorbed amounts (in static condition) on UV grafted polyGMA nonwovens at different volume concentrations of DEA in aqueous solution for various percentages of grafting. All experiment were done in batch system using a binding time of 15 hours.

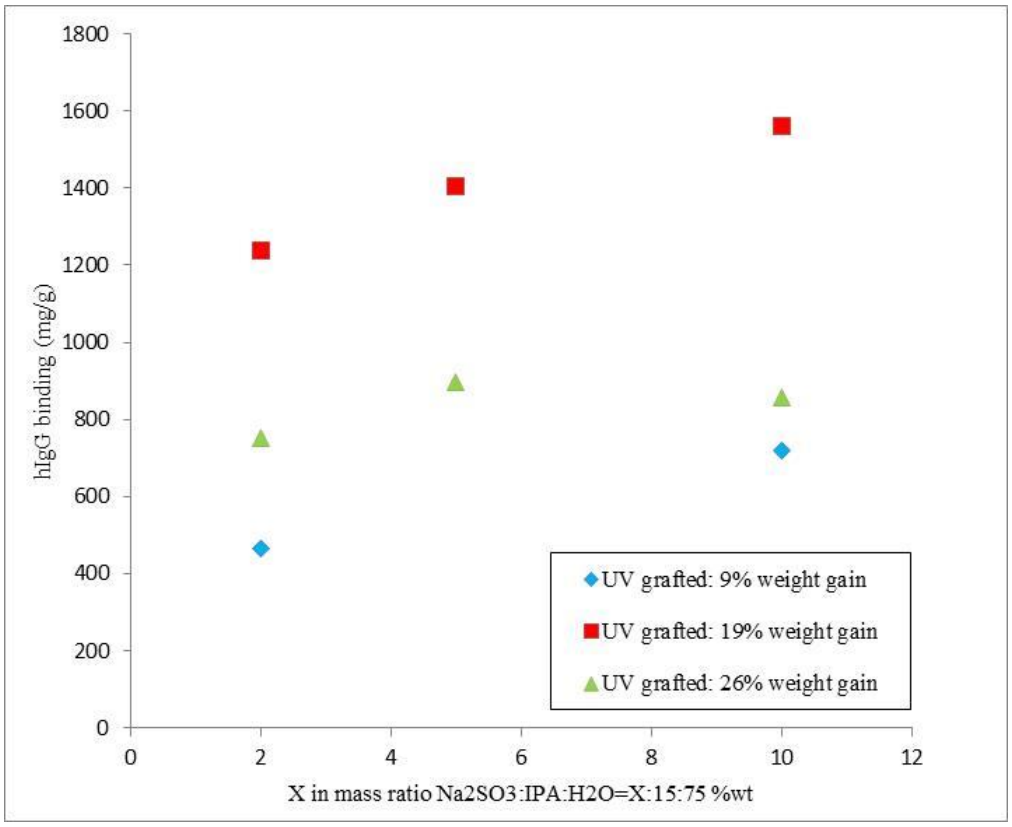

Figure 28. Equilibrium hIgG binding with different concentrations of sodium sulfite, in terms of mass ratio, for varying extents of polyGMA grafting: UV grafted at 9%, 19%, 26% weight gain. All experiment were done in batch system using a binding time of 15 hours.

Equilibrium binding capacity increases with the increased degree of polyGMA grafting, for both anion and cation exchangers, and for all of the ligand concentrations investigated. A decrease of hIgG adsorbed is shown at a high value of grafting as 26%, probably due to an increase of the pore blockage phenomena that seems to be already present at low weight gain by observation of a thin film connecting between fibers as shown in SEM images in Figure 29. Protein binding capacity grows with increased DEA or Na_2SO_3 concentrations. The discrepancy in behavior between materials grafted by heat approach and UV approach is most likely due to the difference in polyGMA grafted structure. UV grafted layer is characterized by independent free moving brushes capable to rearrange, permitting to accommodate a large amount of protein molecules, reducing simultaneously steric hindrance and repulsion effect phenomena. In previous work, it was demonstrated that UVG nonwovens and HIG nonwovens have similar ligand density for a given % weight gain, both functionalized with DEA aqueous solution at 50% v/v [30]. Since HIG nonwovens are characterized by networks of highly cross-linked polymers, polymer chains are more inflexible and not able to rearrange, and even if the ligand density is high as in UVG membranes, the SBC is lower.

Therefore, HIG nonwoven structure necessitates to optimize parameters such as ligand distribution in order to maximize the amount of protein accommodated.

Figure 29 shows representative SEM images of UV grafted PBT nonwovens at 20% weight gain (row A), PBT-pGMA-DEA membranes functionalized using DEA aqueous solution with 30% v/v DEA (row B) and 50% DEA (row C), PBT-pGMA-SO_3^- membranes functionalized using Na_2SO_3 solution with a mass ratio Na_2SO_3:IPA:H2O=2:15:75 %wt. (row D) and 10:15:75 %wt (row E). Images in right column have higher magnification to observe the detail of the fiber surface.

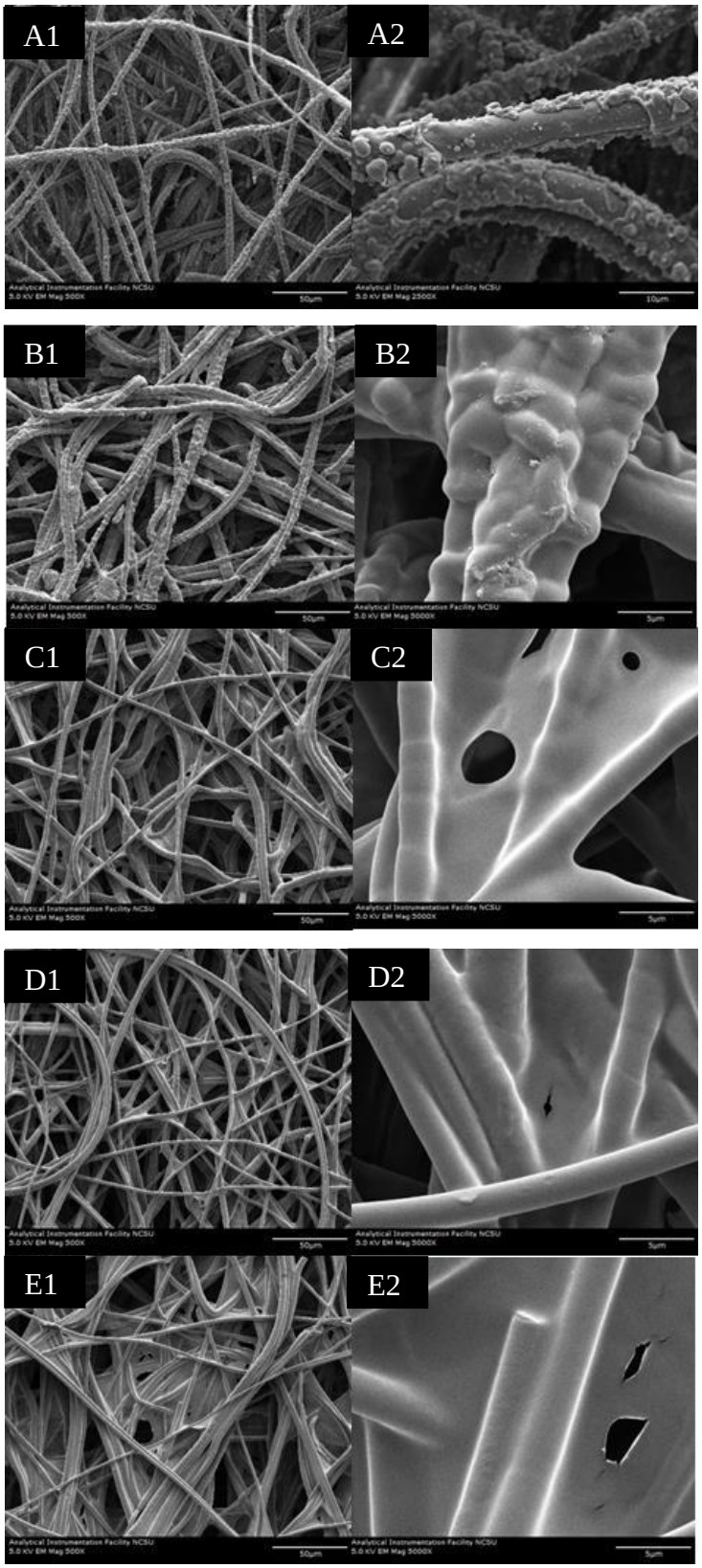

Figure 29. SEM micrographs of UV induced grafting on PBT nonwovens. PBT nonwoven after UV induced grafting at 20% weight gain (A), anion exchange UV grafted membrane at 20% weight gain functionalized with DEA aqueous solution at 30% v/v DEA (B) and 50% v/v DEA (C), cation exchange UV grafted membrane at 20% weight gain functionalized using a mass ratio Na_2SO_3:IPA:H_2O=2:15:75 %wt (D) and 10:15:75 wt% wt.(E). (Left: x500, Right: x5,000)

The rough fiber surface of grafted membranes becomes significantly smoother after DEA and Na_2SO_3 reaction, probably due to the rearrangement of the polymer chain provoked by the electrostatic repulsion between charged groups during the functionalization step. Additionally, a thin film interconnecting between fibers may cause the pore blockage phenomena, which is increased with the ligand concentration used in the functionalized solution. The interconnecting thin film between fibers might be one of the explanation of the very high pressure drop measured in previous work [30]. Permeability coefficient on the order of 10^{-13} cm^2 were have been calculated using Darcy's law, for UVG nonwoven at 20% weight gain [30].

4.2.3 Effect of protein size on static binding capacity

Lysozyme (14.3 kDa) and hIgG (150 kDa) were adsorbed to the cation exchange HIG nonwovens to compare the binding environment characterized by various ligand density. Target molar binding capacities are plotted as a function of target molecular weight at two different % weight gain in Figure 30.

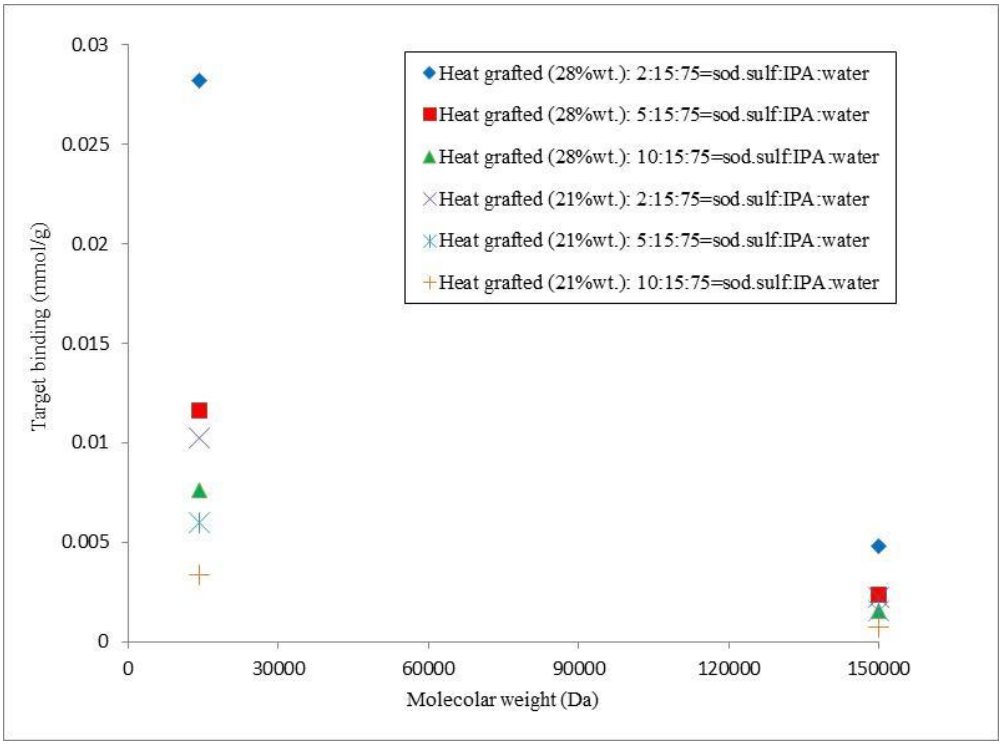

Figure 30. Equilibrium binding capacity of two target molecules (hIgG and lysozyme) as a function of the target molecular weight for heat grafted PBT nonwovens at 21% weight gain and 28% weight gain functionalized to be cation exchangers using different concentration of sodium sulfite.

In Figure 30 is illustrated that with increase of the target molecular weight, the equilibrium molar capacity decreases. Considering the best functionalization condition (Na_2SO_3:IPA:H_2O %wt.=2:15:75), lysozyme which is 10 times smaller than hIgG, binds on average 5 times more. The amount of target bound on the cation exchangers increases with the ligand density (Figure 24), which is manipulated through the % weight gain and the sodium sulfite concentration. Equilibrium molar binding capacity (mmol/g) depends on the size of protein bound for all conditions investigated. An increasing molecular weight, results in a decline of equilibrium molar binding capacity. Generally, at a given binding volume, the bigger size of the protein results in the lower number of protein capable to be bound due to the steric effect. Comparing the ratio of equilibrium molar capacity between the two targets, at given functionalization condition (e.g. 28% weight gain, 5:15:75=Na_2SO_3:IPA:H_2O %wt.), and the same ratio at other functionalization condition (e.g. 28% weight gain, 10:15:75=Na_2SO_3:IPA:H_2O %wt.), these are not affected by significant variation. It means that the equilibrium binding capacity is reduced under some conditions because the lower ligand density makes the lower number of binding sites available. Heller *et al.* [30] has carried out similar studies in order to compare different binding environments characterized by two different grafting techniques, by UV light and by heat, confirming the rigid and cross-linking structure belonging to heat grafted PBT nonwoven. It results more size exclusive effect for heat grafting than UV grafting nonwovens. The results of targets binding capacity, as a function of the target molecular weight, in his study were expressed wrongly in mmol/g. The correct unit of measure is μmol of target protein per grams of membranes in his publication.

4.2.4 Kinetics of adsorption

In order to evaluate the effect of the concentrations of DEA and Na_2SO_3, used in the functionalization solutions, on the rate of protein adsorption, nonwovens grafted using heat grafting and UV grafting method, were exposed to BSA and hIgG respectively at varying contact times and calculated the amount of protein bound. Figure 31 and Figure 32 present the results for protein binding capacity over varying contact times for heat grafting anion- and cation- exchanger respectively, Figure 33 shows the corresponding data for UV grafted nonwovens at 20% weight gain.

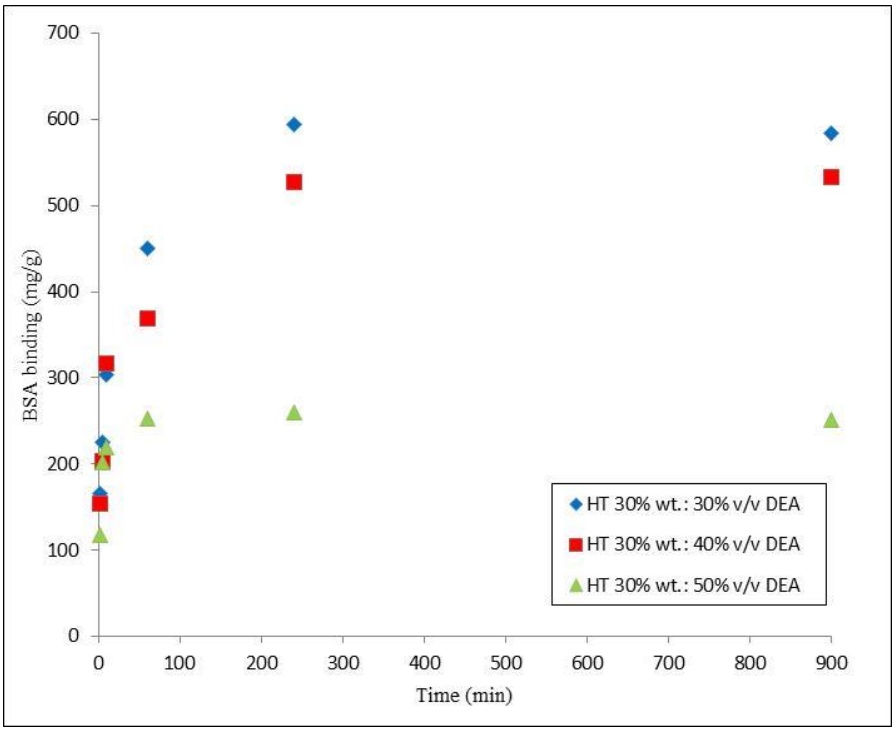

Figure 31. BSA absorbed amount at various contact times on heat grafted nonwovens functionalized to be anion exchangers with different DEA concentration (%v/v) in aqueous solution.

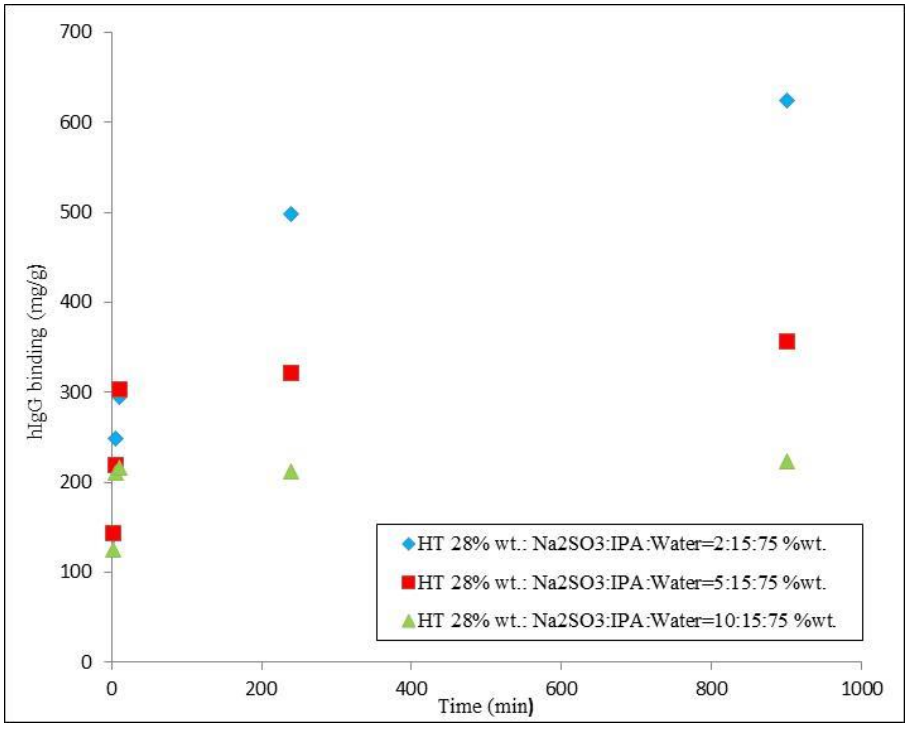

Figure 32. hIgG absorbed amount at various contact times on heat grafted nonwovens functionalized to be cation exchangers with different Na_2SO_3 concentrations.

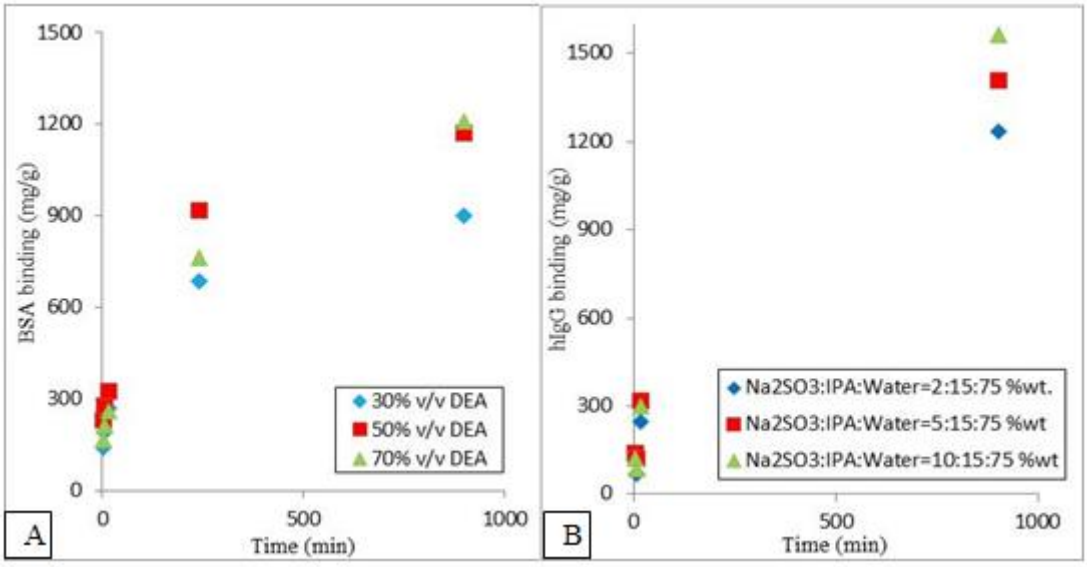

Figure 33. Protein binding at various contact times for UV induced polyGMA grafting on PBT nonwovens at 20% weight gain. (A) UV grafted nonwovens functionalized as anion exchangers for capture of BSA using different volume concentration of DEA in aqueous solution. (B) UV grafted nonwovens functionalized as cation exchangers for capture of hIgG using different concentration of sodium sulfite (Na_2SO_3).

It is already known that HIG nonwovens exhibit much faster (hours earlier) binding kinetics compared to UVG nonwovens [30]. This phenomenon is explained by structural differences induced by the two grafting methods. The flexible UVG nonwoven is capable to rearrange in order to accommodate large number of protein that spread in the depth of the brushes, resulting in a slow rates of protein adsorption. Therefore, the diffusion limitation is responsible of the slow rate of protein binding. Contrarily, the rigid and denser structure of HIG nonwovens is not able to rearrange for accommodating more protein, provoking inaccessible pores in the matrix. The rate of binding seems to be ruled principally by convective mass transport [30].

Figure 31 and Figure 32 show the effect of different ligand concentrations on the rate of adsorption for HIG nonwovens. It is clear that the time needed to reach protein binding equilibrium rises with the decrease of ligand density (corresponding to a decrease of % v/v DEA and Na_2SO_3 concentration in anion- and cation- exchangers, respectively) for heat grafting. It takes 1 hour (5 minutes) to saturate a membrane functionalized using 50%(v/v) DEA (Na_2SO_3:IPA:H_2O=10:15:75 %wt.) and around 4 hours using 40% and 30 % (v/v) DEA (4 hours for Na_2SO_3:IPA:H_2O=5:15:75 %wt. and more than 4 hours for Na_2SO_3:IPA:H_2O=2:15:75). Anion and Cation exchange nonwovens characterized by high binding capacity due to higher ligand density (with 30% v/v DEA and

Na_2SO_3:IPA:H_2O=2:15:75 %wt. respectively) need four hours or more to reach equilibrium since more binding time is required to saturate membranes with high protein binding capacity. The variation of ligand concentration in UVG nonwovens not seem to affect significantly the rate of adsorption, which can be seen from Figure 33. Same time is required to reach the equilibrium binding capacity for all the conditions investigated.

4.2.5 Porosity measurement of HIG nonwovens

The two type of ion exchange heat polyGMA grafted membranes that gave the highest static binding capacity (28% weight gain functionalized with 30% v/v DEA and 29% weight gain functionalized with Na_2SO_3:IPA:H_2O=2:15:75 %wt.) were chosen for further characterization in dynamic binding studies. As described in Section 3.2.6, 20 layers of modified PBT and 20 layers of PET spacers were used to pack each column. A summary of column features is reported in Table 5.

Table 5. Characterization of columns employed in chromatographic study

Name	Characterization of packed membrane	Column dimension	Layers
PBT-pGMA-DEA column	Heat grafted nonwoven at 28% weight gain; Functionalization solution: 30% v/v DEA in aqueous solution	D = 1 cm - L= 0.6 cm	20 layers of modified PBT (weight= 0.153 g) 20 layers of PET Spacers (weight= 0.156 g)
PBT-pGMA-SO_3 column	Heat grafted nonwoven at 29% weight gain; Functionalization solution: Na_2SO_3:IPA:H_2O=2:15:75 %wt.	- D = 1 cm - L= 0.6 cm	20 layers of modified PBT (weight= 0.140 g) 20 layers of PET Spacers (weight= 0.169 g)

The total porosity of the packed PBT-pGMA-SO_3 column was calculated from measurements of the first absolute time moments of pulse injections of nonbinding tracer at different superficial velocities [17]. The porosity was first evaluated for the

column packed with 20 layers of modified PBT alternated with 20 layers of PET spacers, secondly the same experiments were performed with the column packed with 20 layers of PET spacer to evaluate the extra-system volume contribution to consider in porosity calculation. Acetone was chosen as tracer, it is often recommended in pulse injection experiments [59] since it is a small molecule, able to access to all the pores of the chromatographic media, and it shows no electrostatic interactions with the ion exchange functionalized media [17]. The total porosity (ε_t) can be related to the absolute first moment of a pulse injection (μ_1) by Eq 8.

$$\mu_1 = \frac{\int_0^\infty C(L,t)t\,dt}{\int_0^\infty C(L,t)dt} = \frac{L}{u_0}\,\varepsilon_t \qquad \text{Eq. 8}$$

In Eq.8 μ_1 is the first absolute moment (min), C is the concentration of the tracer in the column (mg/ml), t is the time (min), L is the column height (cm), u_o is the superficial velocity (cm/min) and ε_t is the total porosity of the membrane.

Therefore the porosity of the PBT-pGMA-SO_3 membranes is identifiable with the slope of the first moment versus residence time for data presented in Figure 34.

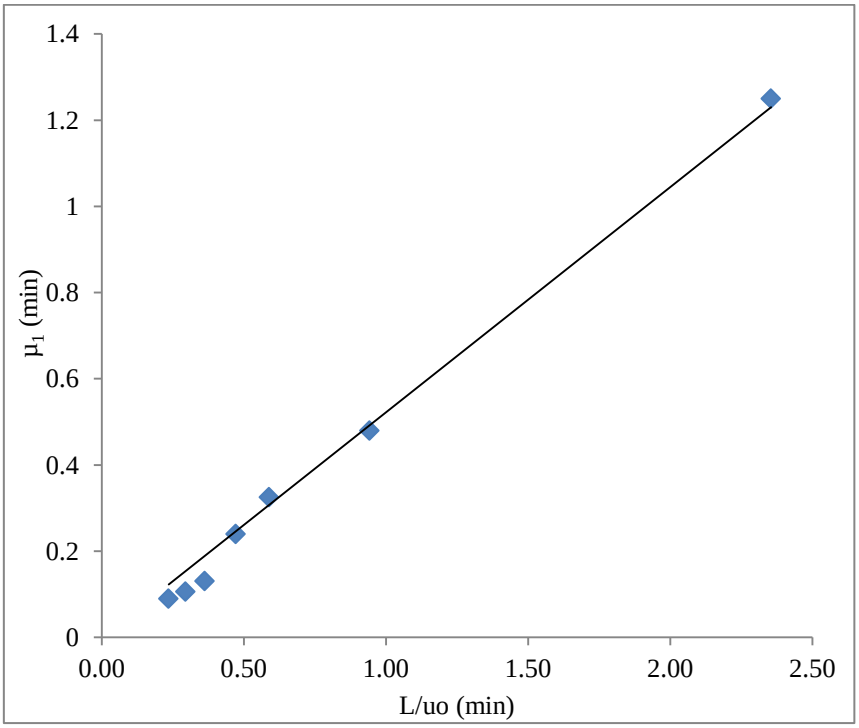

Figure 34. First moment versus L/u_o from acetone pulse injection to PBT-pGMA-SO_3 column at bed height of 0.6 cm. The slope of the fitting line correspond to packed bed porosity of 52%.

The membrane porosity calculated by method of moment was of 0.52.

The average porosity of 20-layers of cation exchange PBT nonwoven not packed into the column can also be calculated using Eq. 9:

$$Porosity = \left(1 - \frac{\rho}{\rho_P}\right) 100\% \qquad \text{Eq. 9}$$

In Eq. 9, ρ is the apparent density of the column, calculated as the ratio of dry mass of the membranes to volume, and ρ_P is the density of the solid polymer (PBT polymer with a density of 1.3 g/cm^3 [60]). Since the apparent density of cation exchange PBT nonwoven calculated is 0.27 g/cm^3, the porosity measured according the Eq. 9 results to be 79%. The values obtained show a drop of the membrane porosity from 79% to 52% when the nonwovens are packed into the column. This decrease is caused by the overlapping of the membranes that produces a blockage of the pores of neighbor membranes. It is important to mention here that the PET spacers were used in order to increase the porosity of the column as it is composed of the fibers with higher diameter (45 μm) and has larger pore size (average pore size ≥ 100 μm) compared to fiber PBT membrane (fiber diameter of 3 μm; average pore size of 8 μm). In order to evaluate the deviation from symmetry condition, the asymmetry factor and the tailing factor were measured. The calculation method was reported in Figure 35.

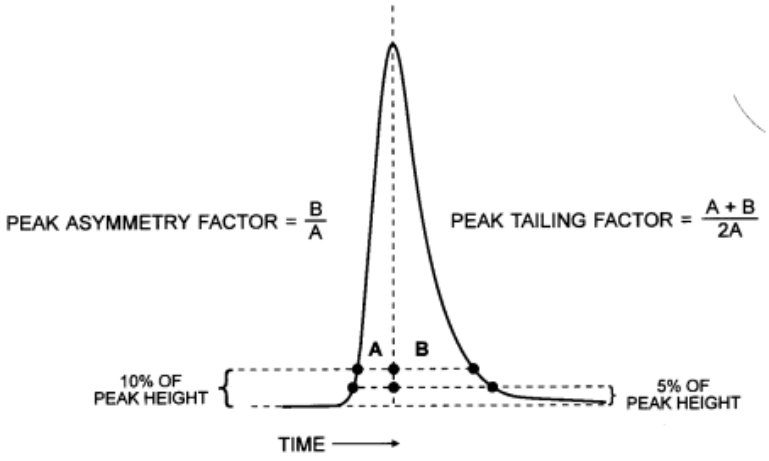

Figure 35. Equations and graphical parameters necessary for calculation of the asymmetry factor and tailing factor.

The asymmetry factor is defined as the ratio between the distance from the center line of the peak to the tail end slope and the distance from the center line of the peak to the front slope, with all measurements made at 10% of the maximum peak height [61].

The tailing factor is defined as the ratio between the distance from the front slope of the peak to the tail end slope and twice the distance from the center line of the peak to the front slope, with all measurements made at 5% of the maximum peak height [61]. These factors are important because they give an indication about the packing of the column and the connected flow distribution. The asymmetry and tailing factor of the PBT-pGMA-SO_3 column tested, corresponding to pulse response at a flow rate of 0.8 ml/min, reported in Figure 36, were showed in Table 6.

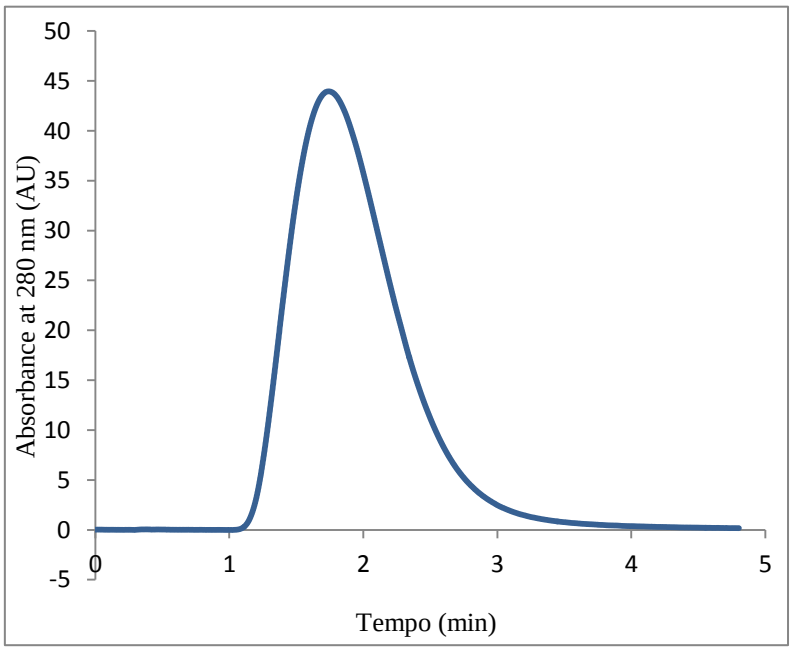

Figure 36. Acetone (2%) pulse injections (20 µl loop) at 0.8 ml/min using nonbinding condition (20 mM Acetate, 1M NaCl pH 5.5. PBT-pGMA-SO_3 column packed with 20 layers of PBT nonwovens grafted at 29% weight gain functionalized using a mass ratio of Na_2SO_3:IPA:H_2O=2:15:75%wt and 20 layers of PET spacers, (column height= 0.6 cm).

Table 6 Asymmetry and tailing factors of the pulses coming from PBT-pGMA-SO_3 column.

Sample	**A_s**	**T_f**
PBT-pGMA-SO_3 column	2.0	1.7

The asymmetry factor results higher than the acceptable range for a well packed column ($0.8 < A_s < 1.2$ [59] and $0.5 < T_f < 2$ [62]). The high asymmetry factor could be due to the heterogeneity of the column packing that causes a mal distribution of the flow in the column [21].

4.2.6 Permeability measurement of HIG nonwovens

Intrinsic permeability of a nonwoven fabric is a characteristic feature of the fabric structure and represent the void capacity through which a fluid can flow [63]. To estimate the flow permeability of cation exchange grafted nonwovens (at 29% weight gain), the pressure drop of PBT-pGMA-SO_3 column was measured. The superficial velocities of the mobile phases were investigated as a function of pressure drop normalized by the column length (L=0.6 cm) and mobile phase viscosity (assumed as water viscosity, μ= 0.001 Pa·s), are illustrated in Figure 37. The pressure drops of cation exchange HIG nonwovens were investigated using a mobile phase with both low ionic strength (20 mM Acetate pH 5.5) and high ionic strength (20 mM Acetate, 1 M NaCl, pH 5.5).

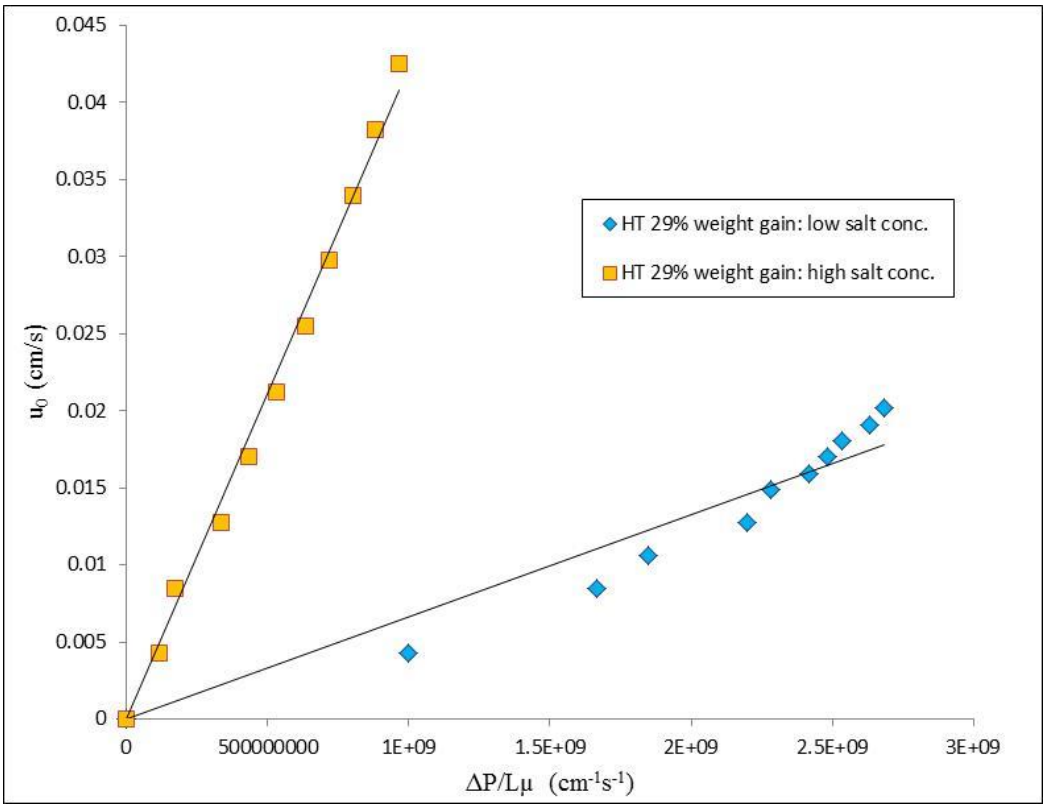

Figure 37 Pressure drop data for PBT-pGMA-SO_3 column packed with heat grafted nonwovens at 29% weight gain. Evaluation with two different mobile phases: low ionic strength (20 mM Acetate pH 5.5) and strong ionic strength (20 mM Acetate, 1 M NaCl, pH 5.5) at different superficial velocities.

Permeability can be calculated with Darcy's law at low Reynold (Eq. 10):

$$u_0 = k\,\frac{\Delta P}{L\mu} \qquad \text{Eq. 10}$$

where u_0 is the superficial velocity of the mobile phase (cm/s), k is the flow permeability (cm^2), Δp is the pressure difference between the inlet and outlet of the column, μ is the mobile phase viscosity (Pa s) and L is the length of the packed bed (cm).

Each data set in Figure 37 was fitted to Eq. 10 to determinate the permeability; for both data set a straight line was found, for the superficial velocities investigated, validating the Darcy's law. The measured permeability coefficients of PBT-pGMA-SO_3 membrane at a mobile phase with low and high ionic strength, are reported in Table 7. The permeability coefficients were calculated considering the contribution of PET spacer.

Table 7 Calculated permeability coefficient for cation exchange PBT membrane grafted at 29% weight gain, functionalized with a mass ratio Na_2SO_3:IPA:H_2O=2:15:75 %wt. evaluated for a mobile phase at low ionic strength and a mobile phase at high ionic strength.

Sample	**$k_{low\ ionic\ strenght}$ (cm^2)**	**$k_{high\ ionic\ strenght}$ (cm^2)**
PBT-pGMA-SO_3 membrane	8×10^{-12}	2×10^{-10}

The permeability, results to be dependent on the ionic strength of the mobile phase.

Permeability coefficient in high ionic strength environment is two order of magnitude higher than in low ionic strength. This behavior is consistent with the results of other published research [54], [30]. Gebauer *at al.* [54] investigated the flow properties of two different type of Sartobind-S (cation exchange membranes) and found a decrease of pressure drops (until 50% lower), increasing ionic strength in mobile phase. This was attributed to a decrease of Deybe length at higher ionic strength that produces a contraction of the three dimensional adsorbing layer and a consequently slightly increasing of pore diameter membrane. This result is consistent also with the study performed by Heller *et al*. [30] who investigated the flow permeability of the ion exchange PBT nonwoven grafted using UV light and heat. Both types of the membranes showed a decrease in pressure drop with an increment of ionic strength in the mobile phase. This effect was resulted more pronounced for UVG membranes due to their structure (extended polymer brushes from the surface) that causes a higher swelling of the bushes due to their electrostatic repulsion in low ionic strength phase.

4.2.7 Protein binding in dynamic conditions for HIG nonwovens

The PBT-pGMA-DEA column and PBT-pGMA-SO_3 column described in Section 3.2.6 were characterized in terms of dynamic binding capacity at saturation ($DBC_{100\%}$) and dynamic binding capacity at 10% breakthrough ($DBC_{10\%}$), using BSA as a target molecule (10 mg/ml BSA in 20 mM Tris-HCl pH 7) for anion exchange HIG membranes and hIgG (10 mg/ml in 20 mM Acetate pH 5.5) for cation exchange HIG membranes. The PET spacers, to separate individual layers of grafted nonwovens, were used in order to increase the porosity of the columns, reducing the pore blockage phenomena due to the overlapping of the PBT layers, and increase consequently the dynamic binding capacity, making a larger part of the membrane available to protein capture [30]. Experiments were performed at three different superficial velocities 0.076, 0.15, 0.25 cm/min, corresponding to residence time to 7.9, 3.9, 2.4 min, in order to study the influence of flow rate on the dynamic binding capacity. In each experiment 50 mg of protein were loaded to the module. The protocol was reported in Table 3 and Table 4 for anion- and cation- exchangers respectively. The
chromatograms obtained from dynamic binding experiments using both PBT-pGMA-DEA and PBT-pGMA-SO_3 columns is presented in Figure 38 and Figure 39 respectively.

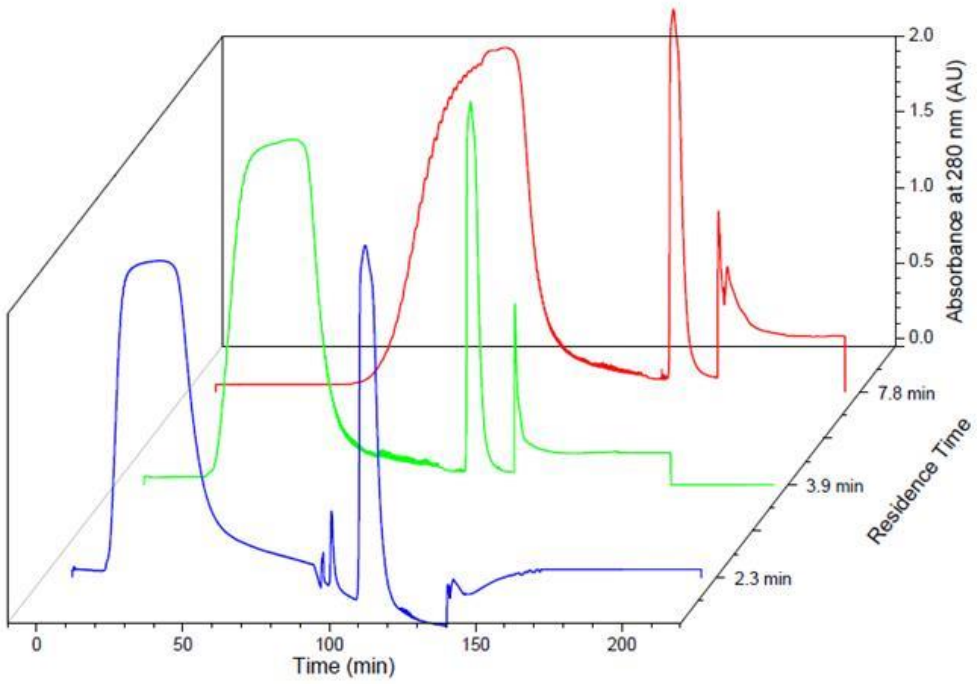

Figure 38 Chromatograms obtained from the dynamic binding of BSA (5ml;10mg/ml) of a column packed with 20 layers of heat grafted PBT nonwovens at 28% weight gain functionalized using 30% (v/v) DEA in aqueous solution, alternated with 20 layers of PET spacer. Superficial velocity = 0.076, 0.15, 0.25 cm/min corresponding to residence time of 7.8,3.9, 2.3 minutes respectively. Binding buffer: 20 mM Tris-HCl pH 7, elution buffer: 20 mM Tris-HCl, 1M NaCl , pH 7.

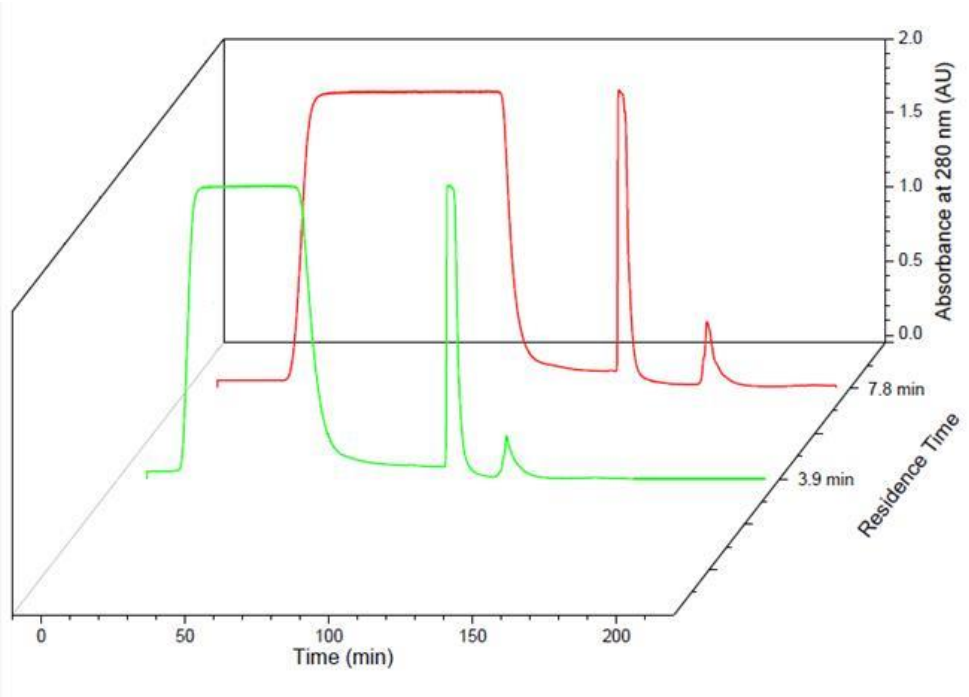

Figure 39 Chromatograms obtained from the dynamic binding of hIgG (5ml;10mg/ml) of a column packed with 20 layers of heat grafted PBT nonwovens at 29% weight gain functionalized using Na_2SO_3:IPA:H_2O=2:15:75 %wt alternated with 20 layers of PET spacer. Superficial velocity = 0.076, 0.15 cm/min corresponding to residence time of 7.9, 3.9 minutes. Binding buffer: 20 mM Acetate pH 5.5, elution buffer: 20 mM Acetate, 1M NaCl , pH 5.5.

The $DBC_{10\%}$, $DBC_{100\%}$ and recovery at different superficial velocities and corresponding residence times τ, of both PBT-pGMA-DEA and PBT-pGMA-SO_3 columns, are reported in Table 8 and Table 9 respectively.

Table 8 Dynamic binding capacity at 10% breakthrough, binding capacity at saturation and % recovery at the superficial velocities investigated for PBT-pGMA-DEA column.

PBT-pGMA-DEA column				
U (cm/min)	**τ (min)**	**$DBC_{10\%}$ (mg/g)**	**$DBC_{100\%}$ (mg/g)**	**% Recovery**
0.076	7.9	168	211	95
0.15	3.9	138	185	99
0.25	2.4	109	144	100

Table 9 Dynamic binding capacity at 10% breakthrough, binding capacity at saturation and % recovery at the superficial velocities investigated for PBT-pGMA-SO3 column.

PBT-pGMA-SO_3 column				
U (cm/min)	**τ (min)**	**$DBC_{10\%}$ (mg/g)**	**$DBC_{100\%}$ (mg/g)**	**% Recovery**
0.076	7.9	107	153	67
0.15	3.9	101	146	69

The recovery was defined as the ratio of the mass of protein eluted and the mass of protein adsorbed. The bound protein was eluted by high ionic strength buffer in order to break electrostatic interactions between protein and the functional groups on membrane surface. Elution buffers were 20 mM Tris-HCl, 1M NaCl pH 7 and 20 mM Acetate, 1 M NaCl pH 5.5 for anion- and cation- exchangers respectively. Elution peaks were collected and their concentrations were measured with UV absorbance at 280 nm. The volume corresponding to the 10% breakthrough point was corrected by subtracting the void volume of the system obtained in nonbinding condition. DBC data shows that, for both the anion and cation exchangers, $DBC_{10\%}$ decreases slightly as the superficial velocity increases.. When the superficial velocity increases from 0.076 cm/min to 0.25 cm/min, the $DBC_{10\%}$ of PBT-pGMA-DEA column decrease from 168 mg/g to 109 mg/g. It is important to underline that the $DBC_{10\%}$ and $DBC_{100\%}$ values only account the mass of modified PBT nonwovens. The PET spacers were not considered in DBC calculation, since no binding contribution, using PET nonwovens, was registered. Therefore, as already mentioned, spacers were used to enhance the flow properties [30].

The calculated recovery is approaching 100% for anion exchange membranes, while is always below 69% for cation exchangers. The ionic strength of the elution buffer was not sufficient to disrupt the electrostatic interactions between the protein and the SO_3^- groups on the PBT-pGMA membranes packed in the column. The low recovery could be attribute to the formation of clusters of hIgG molecules that possess higher affinity for the membrane. To inhibit this interaction, a buffer with higher pH could be utilized in the elution step, and harsher conditions should be used to regenerate the column. Chromatograms from both columns show a second peak, that is principally attributed to an instability of the UV lamp signal and caused by a change of the flow rate from 0.5 to 0.2 ml/min, as confirmed by the measurements of protein concentration in said peak by UV absorbance readings at 280 nm.

The correlation between retention time and protein binding capacity under dynamic and static (equilibrium) condition is shown in Figure 40.

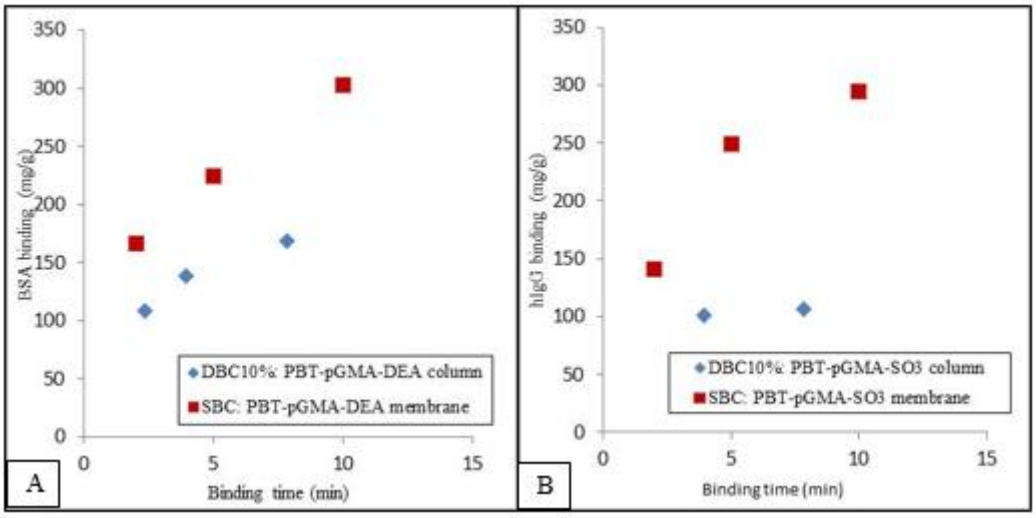

Figure 40. Binding capacity vs retention time for dynamic ($DBC_{10\%}$) and static (SBC) conditions. (A) anion exchange nonwoven, (B) cation exchange nonwoven.

Generally, compared to flow condition, the protein binding capacity in static (Equilibrium) condition is higher. This might be due to the lower porosity of grafted layer on the membranes and the blockage of pores by the neighboring layers. Membranes in static conditions are not limited by the neighboring layers and are able to move. Nevertheless for the short contact time, under flow conditions, the value of BSA bound is pretty similar to the value obtained during binding experiments under the static conditions. The $DBC_{10\%}$ is 109 mg/g and 138 mg/g after exposition of PBT-pGMA-DEA column membranes to BSA solution (10 mg/ml) for 2.3 minutes and 3.9 minutes

compare to a SBS of 165 mg/g and 224 mg/g for a contact time of 2 and 5 minutes respectively. The kinetic study shows that to long retention time is required for the higher protein binding capacity.

4.2.8 Separation of protein mixtures using anion and cation exchange HIG nonwovens

The anion exchange DEA functionalized PBT nonwoven membranes, PBT-pGMA-DEA, were evaluated for their ability to separate BSA from three different mixtures: BSA and lysozyme (5 mg/ml BSA and 5 mg/ml lysozyme), BSA and hIgG (5 mg/ml BSA and 5 mg/ml hIgG) or BSA, lysozyme and hIgG (3.3 mg/ml BSA, 3.3 mg/ml lysozyme, 3.3 mg/ml hIgG). One mL of the protein mixture was loaded onto the column at a superficial velocity of 0.076 cm/min (0.06 ml/min). The protocol is described in Section 3.2.7. A favorable pH condition was maintained (pH 6.5) for the BSA molecules (pI = 4.7) to be adsorbed on the anion exchange membranes (with positive charges), while the polyclonal hIgG (pI=7-9) and lysozyme (pI>10) molecules pass through the column unbound. The chromatograms resulted during the separation of BSA from three different mixtures: BSA and hIgG mixture; BSA and lysozyme; and BSA, hIgG and lysozyme; are presented in Figure 41, Figure 42, Figure 43 respectively. The flow-through, the elution and the regeneration were analyzed by SDS-PAGE.

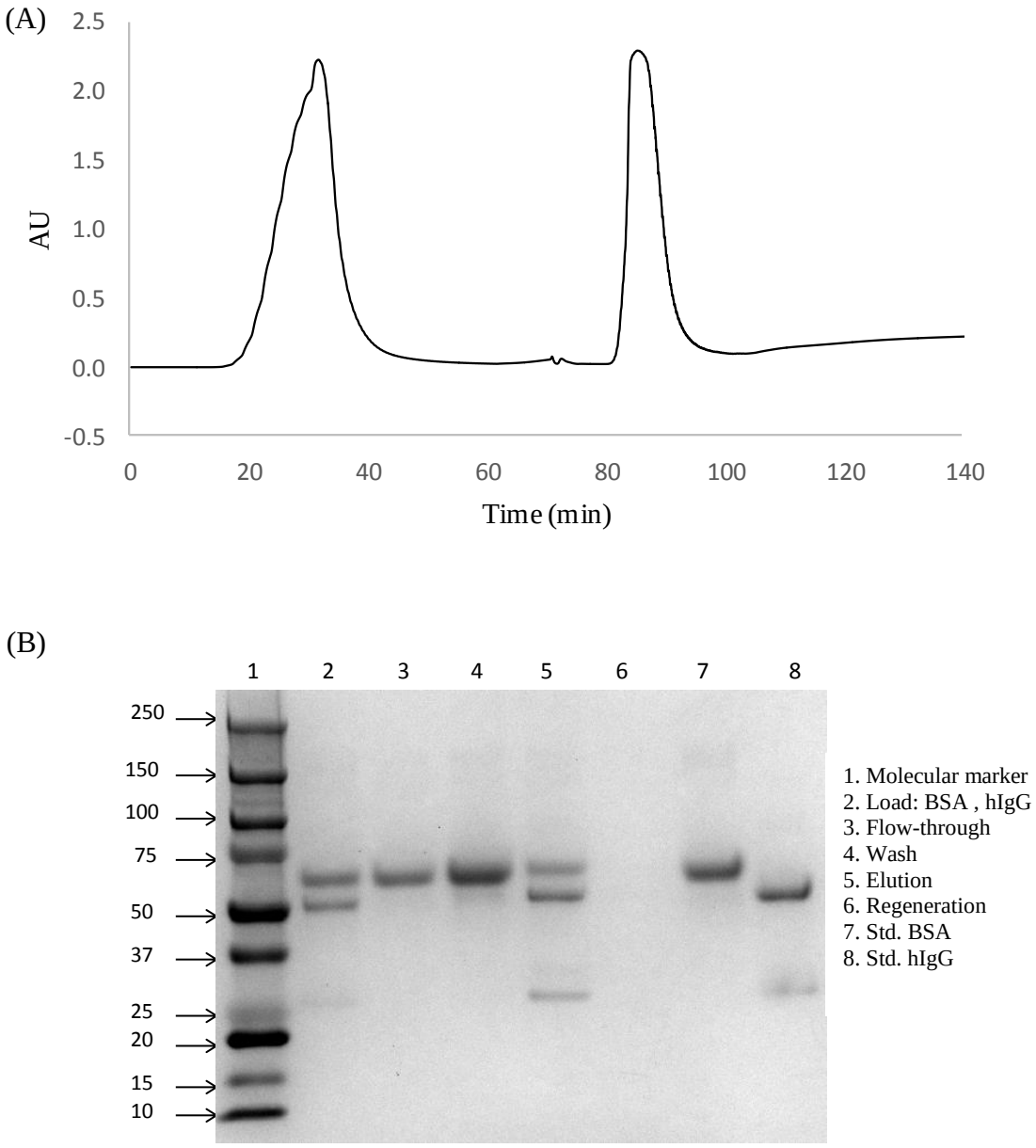

Figure 41. **(A)** Chromatograms for the separation of BSA from the BSA and hIgG mixture separation by PBT-GMA-DEA nonwovens grafted at 28%wt and functionalized with 30%v/v DEA. Column volume (CV): 0.47 ml, injection volume: 1 ml protein solution (5 mg/ml BSA and 5 mg/ml hIgG), RT: 8 min. Binding buffer: 20 mM Tris-HCl pH 6, elution buffer: 20 mM Tris-HCl, 1 M NaCl , pH 6. **(B)** SDS-PAGE (reducing conditions) image corresponds to above chromatogram.

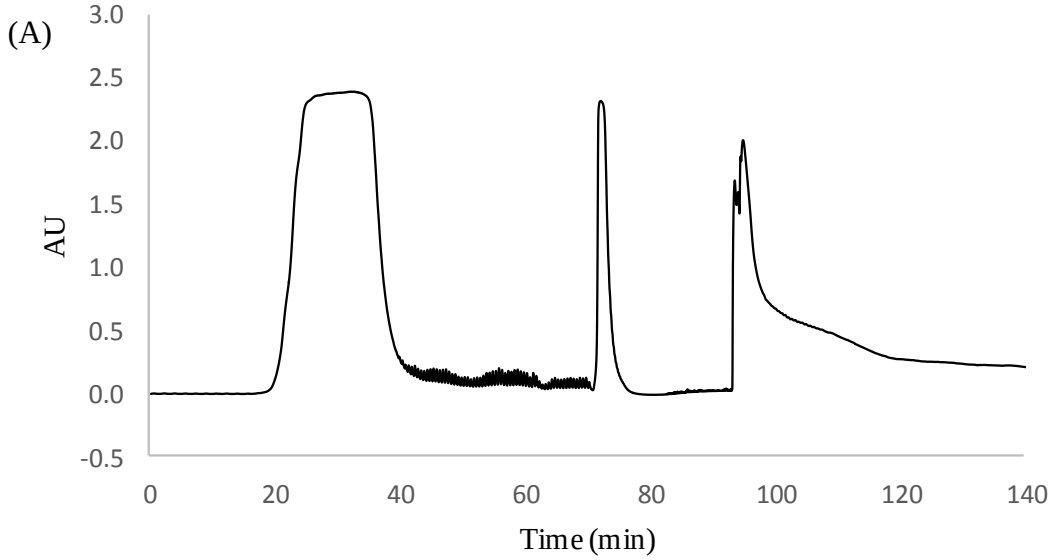

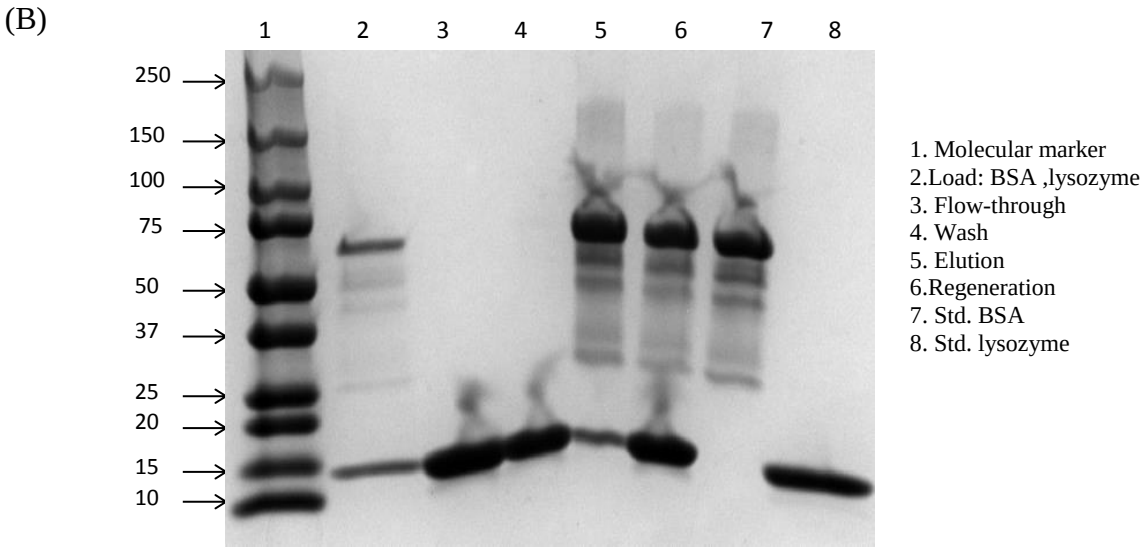

Figure 42. **(A)** Chromatograms for the separation of BSA from the BSA and lysozyme mixture separation by PBT-GMA-DEA nonwovens grafted at 28%wt and functionalized with 30%v/v DEA. Column volume (CV): 0.47 ml, injection volume: 1 ml protein solution (5 mg/ml BSA and 5 mg/ml lysozyme), RT: 8 min. Binding buffer: 20 mM Tris-HCl pH 6, elution buffer: 20 mM Tris-HCl, 1 M NaCl , pH 6. **(B)** SDS-PAGE (reducing conditions) image corresponds to above chromatogram.

(A)

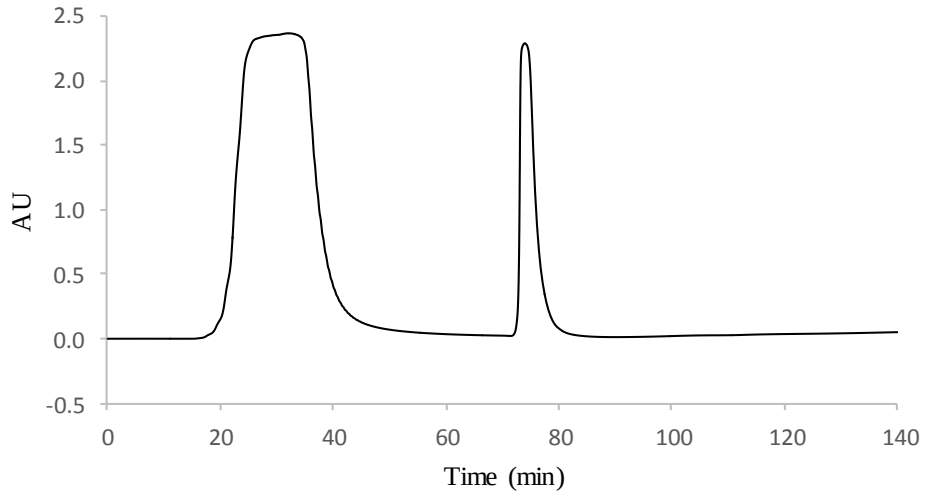

(B)

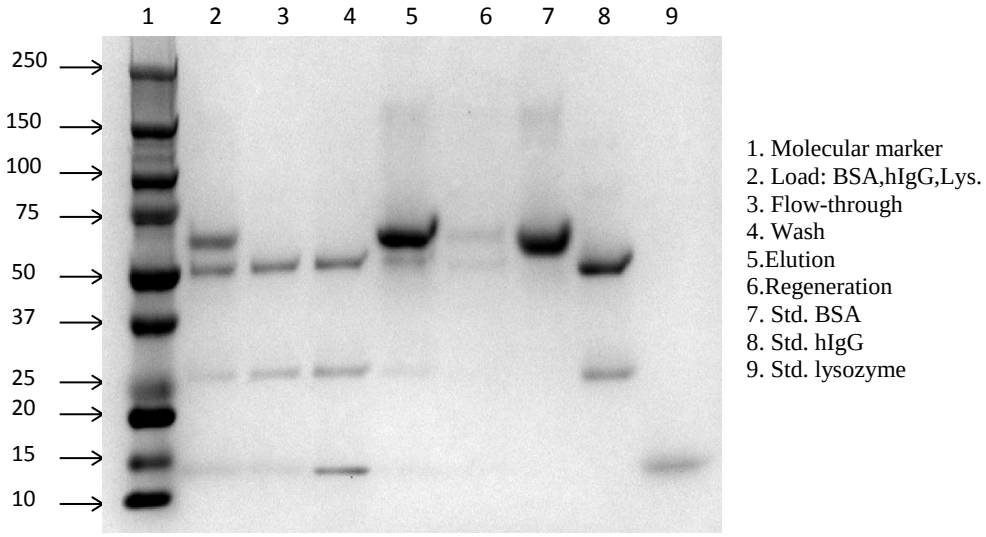

Figure 43. (**A)** Chromatograms for the separation of BSA from the BSA, hIgG and lysozyme mixture separation by PBT-GMA-DEA nonwovens grafted at 28%wt and functionalized with 30%v/v DEA. Column volume (CV): 0.47 ml, injection volume: 1 ml protein solution (3 mg/ml BSA, 3 mg/ml hIgG and 3 mg/ml lysozyme), RT: 8 min. Binding buffer: 20 mM Tris-HCl pH 6, elution buffer: 20 mM Tris-HCl, 1 M NaCl , pH 6. (B) SDS-PAGE (reducing conditions) image corresponds to above chromatogram.**(B)** SDS-PAGE (reducing conditions) image corresponds to above chromatogram.

The chromatograms show a good separation resolution between flow-through peak (the first peak) and elution peak (the second peak). The chromatogram in Figure 42, , shows a third peak, not found in the other chromatograms. This might be due to the presence of impurities, as seen in SDS-PAGE image, in BSA, used , which formed aggregates with BSA and lysozyme. Therefore, the ionic strength of the elution buffer was not sufficient to win their electrostatic interactions with tertiary ammine of the membrane. To inhibit these interactions, buffer with higher pH turned to be necessary (regeneration

buffer: 20mM Tris-HCl, 1 M NaCl, pH 10). The creation of these cluster could explain the lower yield (83%) and lower purity (62%) obtained in this experiment than the values obtained in other experiments (Table 10).

Under reducing conditions lysozyme has a band around 13 kD, hIgG has bands around 50 kD and 25 kD corresponding to the heavy and light chains of hIgG respectively and finally BSA has band around 65 kD. The yield of BSA removed was calculated as the ratio of BSA eluted to total BSA loaded. The BSA purity was determined by densitometric analysis of Coomassie-stained gels by means of ImageJ 1.32j software (National Institutes of Health, Bethesda, MD, USA). The purity of the product was calculated as the fraction of the total area equivalent to the BSA bands at 65 KDa. The purity of the elution fraction for all three separations, was reported in Table 10.

Table 10 Yield and purity of BSA separated from different mixture by PBT-pGMA-DEA column (anion exchange heat grafted nonwovens at 28% weight gain functionalized with 30% v/v DEA)

N°	Protein mixture	BSA Yield	BSA Purity
1	BSA+hIgG (5 mg/ml BSA, 5 mg/ml hIgG	~1	95.4%
2	BSA+ Lysozyme (5 mg/ml BSA, 5 mg/ml lysozyme	83%	62%
3	BSA+ hIgG + Lysozyme (3 mg/ml BSA, 3 mg/ml hIgG, 3 mg/ml lysozyme)	96%	93%

Focusing on the first mixture, the flow-through and wash fractions were found to be pure hIgG using ImgineJ software. Observing the data in the table for one step of purification, anion exchange membranes shows a very good behavior in protein purification.

The cation exchange PBT nonwoven membranes, PBT-pGMA-SO_3, described in Section 3.2.6, were evaluated for their ability to separate the hIgG from BSA and hIgG mixture (5 mg/ml BSA and 5 mg/ml hIgG). One mL of the protein mixture was loaded onto the column at a superficial velocity of 0.076 cm/min (0.06 ml/min). The protocol is described in Section 3.2.7. One millimeter of protein mixture were injected and a binding superficial velocity of 0.076 cm/min (0.06 ml/min) was used for all experiments. The effect of different pH of the binding buffer ranging between pH 5 and

6, were investigated. The protocol is described in Section 3.2.6. Considering the pH of the applied binding buffer, hIgG molecules (pI = 7-9) are positively charged and adsorbed to the cation exchange membranes (with negative charges). Since BSA are molecules (pI = 4.7) show net negative charges at this binding pH conditions, pass thought the column unbound. The flow-through, the elution and the regeneration were analyzed by SDS-PAGE. The chromatograms and the corresponding SDS-PAGE images obtained during the separation of hIgG - BSA mixture with binding buffers of different pH 5.0, 5.5, 6.0, 6.5 are presented in Figure 44, Figure 45, Figure 46, Figure 47 respectively.

(A)

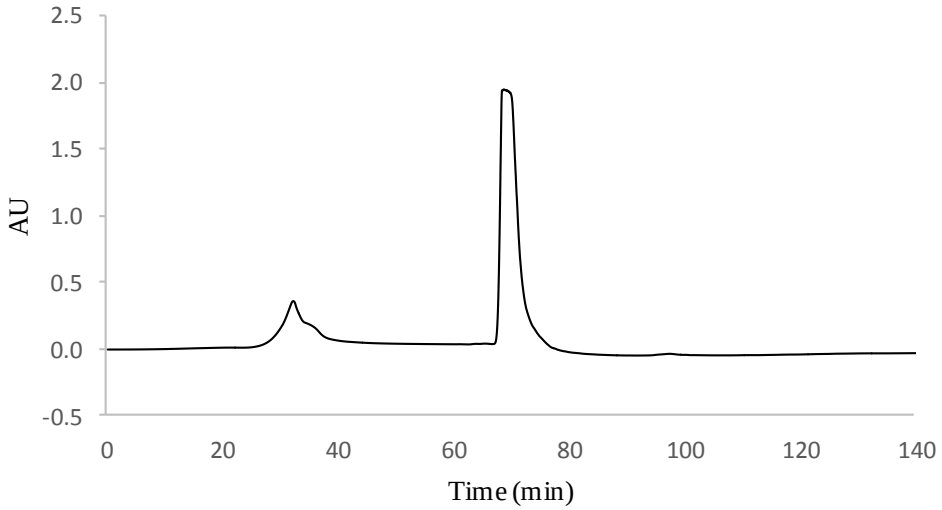

(B)

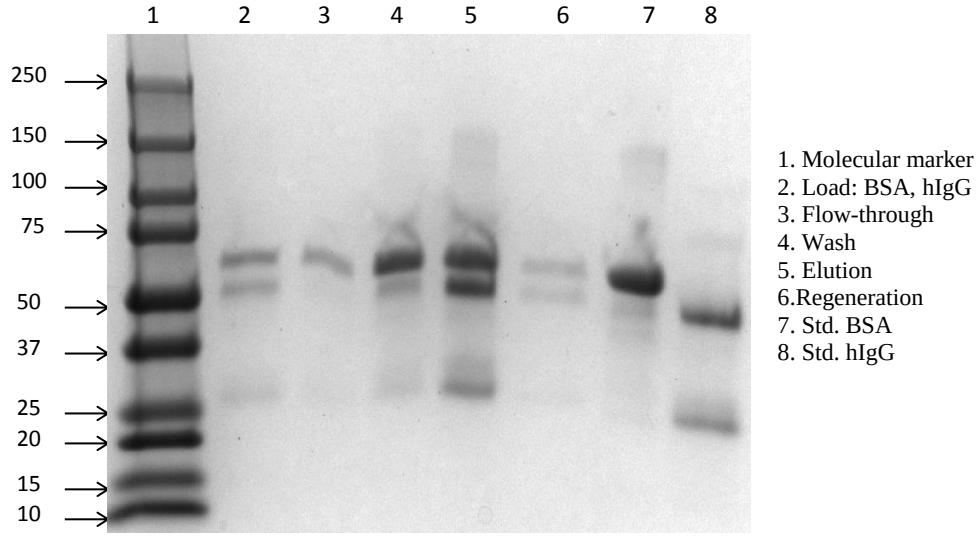

Figure 44. (A) Chromatograms for the separation of BSA and hIgG mixture by PBT-GMA-SO_3 nonwovens grafted at 28%wt and functionalized using 2 mg/ml Na_2SO_3. Column volume (CV): 0.47 ml, injection volume: 1 ml protein solution (5 mg/ml BSA and 5 mg/ml hIgG), RT: 8 min. Binding buffer: 20 mM Acetate pH 5, elution buffer: 20 mM Acetate, 1 M NaCl , pH 5.**(B)** SDS-PAGE (reducing conditions) image corresponds to above chromatogram.

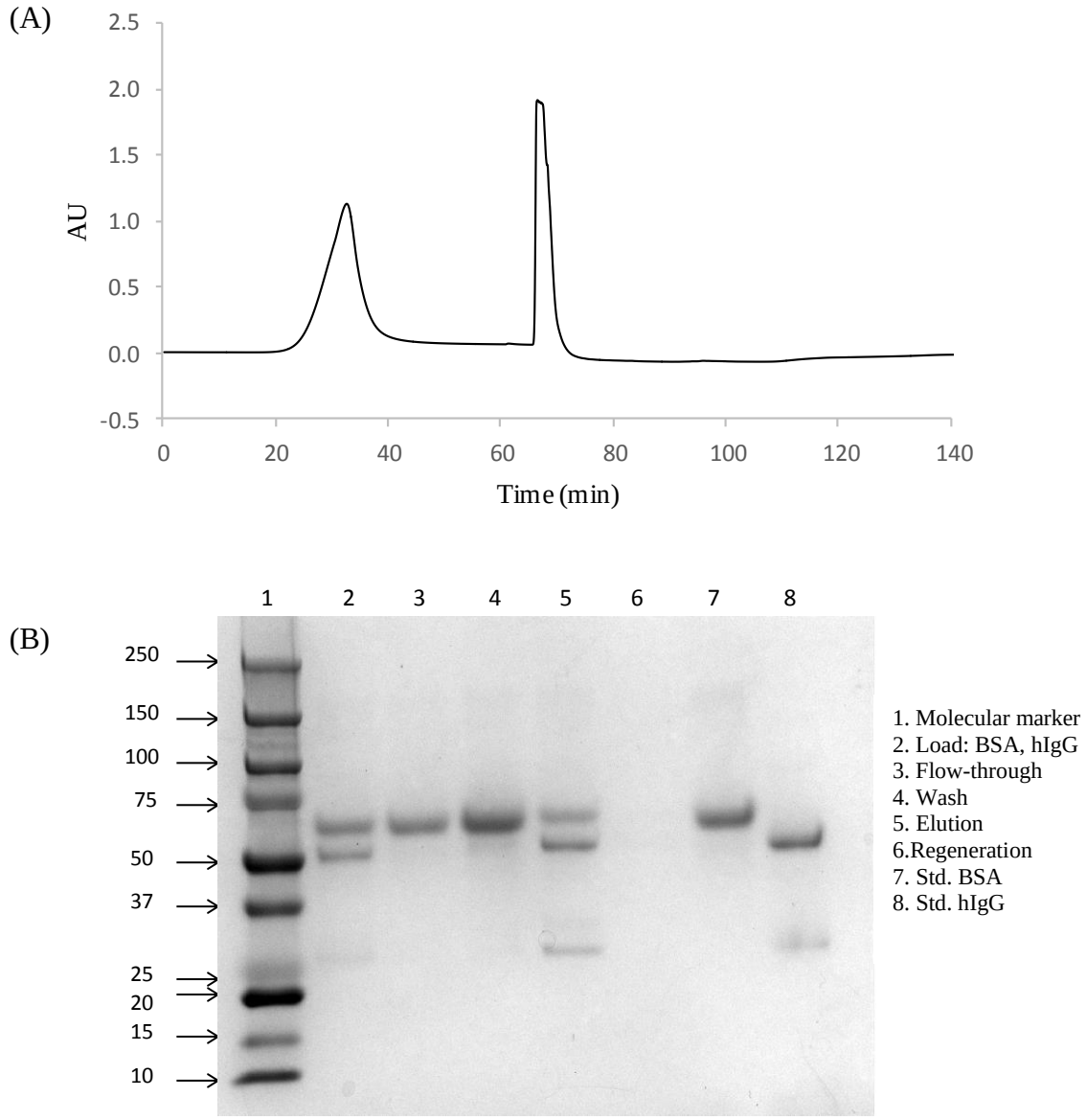

Figure 45. (**A)** Chromatograms for the separation of BSA and hIgG mixture by PBT-GMA-SO_3 nonwovens grafted at 28%wt and functionalized using 2 mg/ml Na_2SO_3. Column volume (CV): 0.47 ml, injection volume: 1 ml protein solution (5 mg/ml BSA and 5 mg/ml hIgG), RT: 8 min. Binding buffer: 20 mM Acetate pH 5.5, elution buffer: 20 mM Acetate, 1 M NaCl , pH 5.5. **(B)** SDS-PAGE (reducing conditions) image corresponds to above chromatogram.

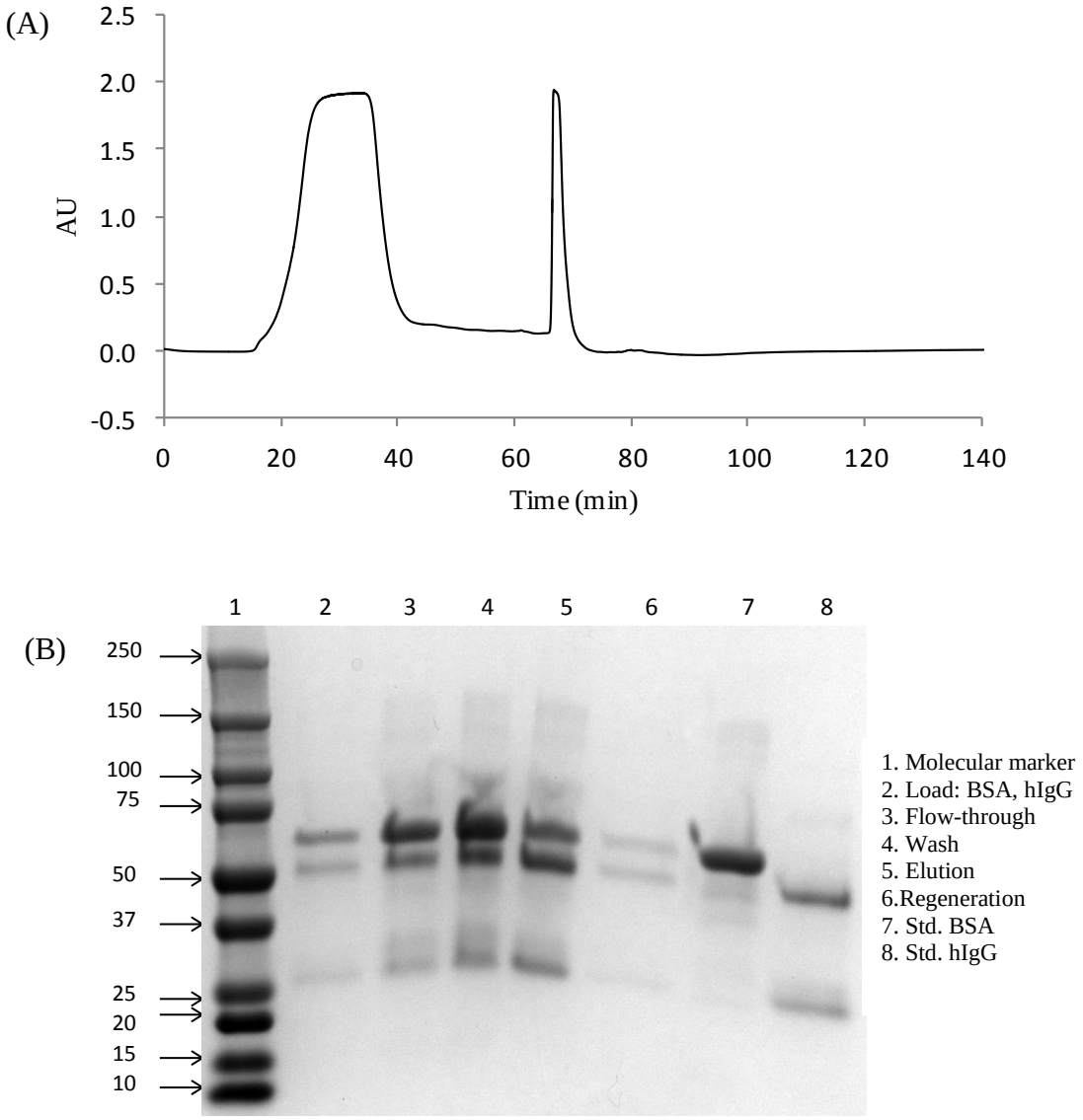

Figure 46. (**A)** Chromatograms for the separation of BSA and hIgG mixture by PBT-GMA-SO_3 nonwovens grafted at 28%wt and functionalized using 2 mg/ml Na_2SO_3. Column volume (CV): 0.47 ml, injection volume: 1 ml protein solution (5 mg/ml BSA and 5 mg/ml hIgG), RT: 8 min. Binding buffer: 20 mM Acetate pH 6, elution buffer: 20 mM Acetate, 1 M NaCl , pH 6. **(B)** SDS-PAGE (reducing conditions) image corresponds to above chromatogram.

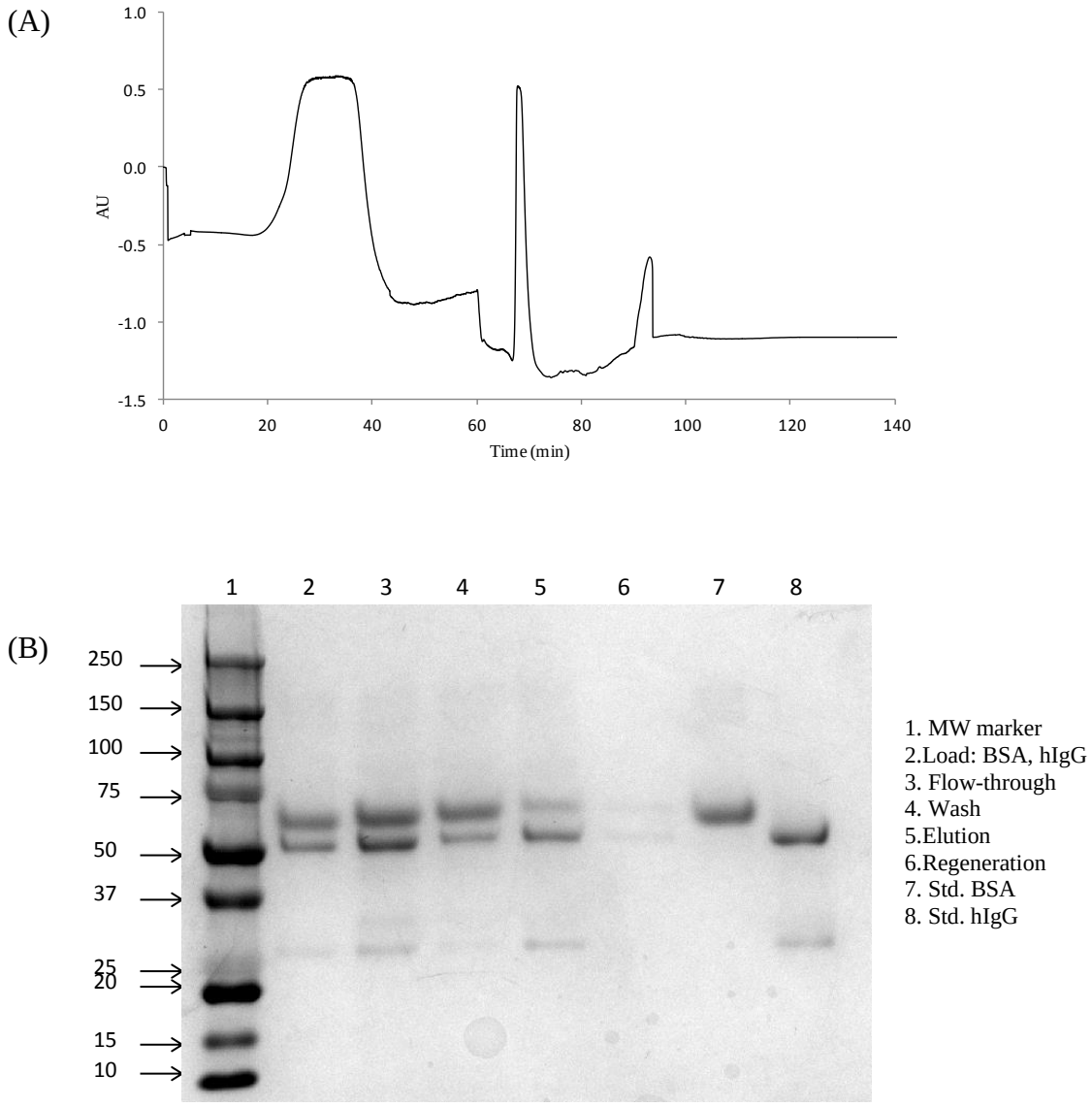

Figure 47. (**A)** Chromatograms for the separation of BSA and hIgG mixture by PBT-GMA-SO_3 nonwovens grafted at 28%wt and functionalized using 2 mg/ml Na_2SO_3. Column volume (CV): 0.47 ml, injection volume: 1 ml protein solution (5 mg/ml BSA and 5 mg/ml hIgG), RT: 8 min. Binding buffer: 20 mM Acetate pH 6.5, elution buffer: 20 mM Acetate, 1M NaCl , pH 6.5. **(B)** SDS-PAGE (reducing conditions) image corresponds to above chromatogram.

The chromatograms presented in Figure 44, Figure 45, Figure 46 show a good separation resolution between flow-through peak (the first peak) and elution peak (the second peak). The yield of hIgG was calculated as the ratio of hIgG eluted to total hIgG loaded. The BSA purity was determined by densitometric analysis of Coomassie-stained gels by means of ImageJ 1.32j software (National Institutes of Health, Bethesda, MD, USA). The purity of the product was calculated as the fraction of the total area

equivalent to the hIgG bands 50 kD and 25 kD, corresponding to the heavy and light chains of hIgG respectively.

The purity of the elution fraction for all four separations was reported in Table 11.

Table 11 Influence of elution pH on yield and purity of IgG purified from BSA and hIgG mixture using PBT-pGMA-SO_3 column (heat grafted nonwovens at 29% weight gain functionalized with mass ratio 2:15:75=Na_2SO_3:IPA:H_2 O %wt.).

Binding buffer pH	hIgG Yield	hIgG Purity
5	90%	70%
5.5	96%	69%
6	80%	74%
6.5	59%	78%

Varying the binding pH from 5 to 6.5, an increment of purity from 70% to 78%, but also a considerably decreasing of yield from 90% to 59% (Table 11) was registered. Increasing the pH, increases the electrostatic repulsion between BSA (pI = 4.7) and ligand with negative charge, resulting in lower amount of BSA bound and higher purity of hIgG eluted. However, a higher amount of hIgG does not bind to the membranes, a significant amount of IgG passed through the column as flow-through and wash wash fractions (e.g. Figure 46 B, Lanes 3-4). Since the pI of hIgG is estimated to be 7-9, moving the pH closer to this range, increases the intensity of negative patches on hIgG causing the leak of the hIgG in the flow-through and wash step due to the electrostatic repulsion with the negative charge of ligand (SO_3^-). In general, the values reported in Table 12 are lower than the values obtained in protein purification by anion exchange chromatography. PBT-pGMA-SO_3 column is packed with membranes characterized by a strong negative charge (the charge in the anion exchangers is weaker) which might be responsible to a stronger electrostatic interaction with the cluster of protein. As consequence the cluster of protein is difficult to divide in single proteins. To further improve the recovery of IgG, the effect of ionic strength of the elution buffer on IgG yield and purity was evaluated. The effect of ionic strength of the elution buffer was studied in terms of NaCl concentration in a linear salt gradient from 20 mM Acetate pH 5.5 to 20 mM Acetate, 1 M NaCl, pH 5.5. Figure 48 shows the typical chromatograms and SDS-PAGE results of the runs using linear salt gradient, while Table 12 reports the values of IgG yield and purity.

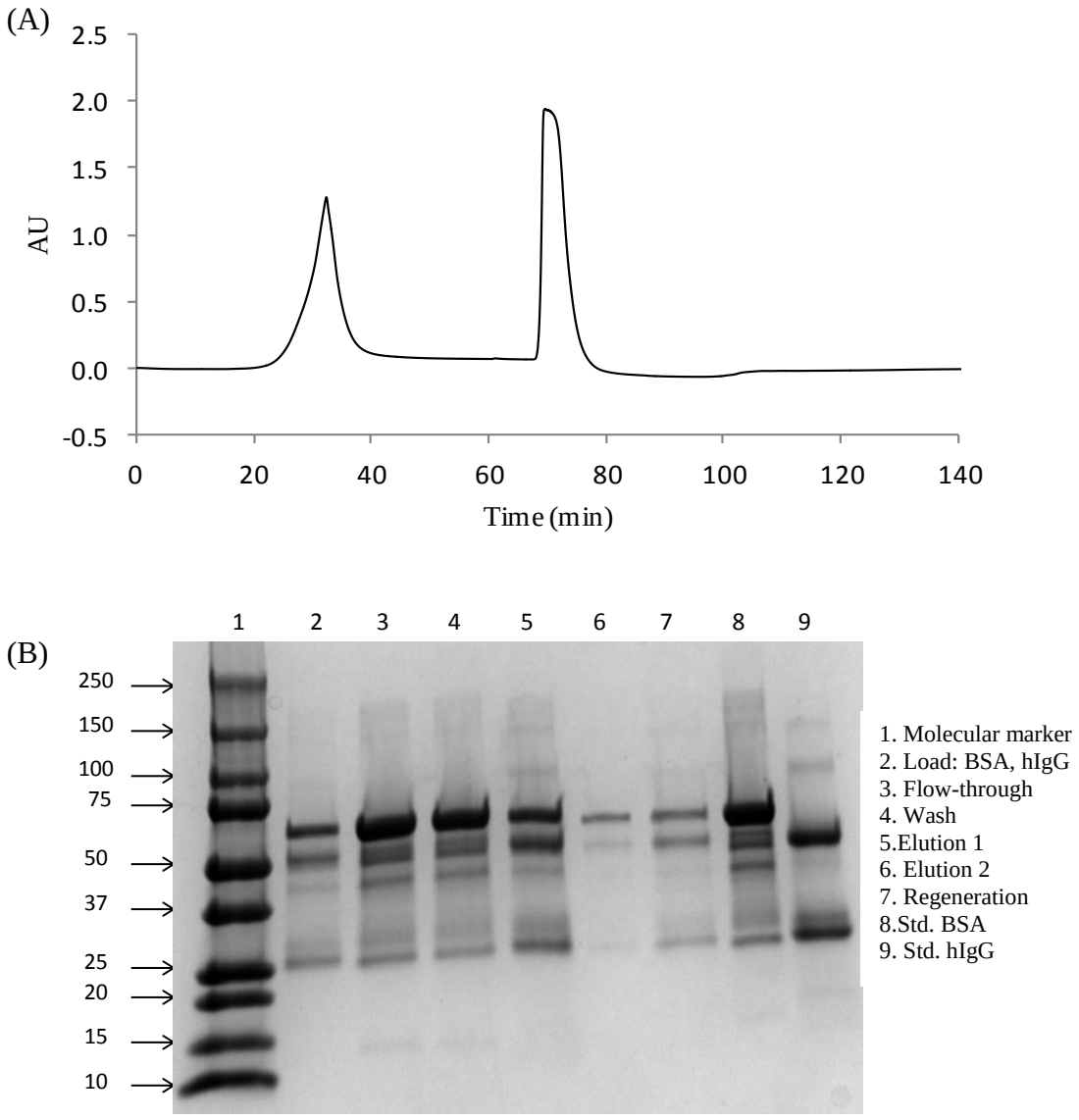

Figure 48. (**A)** Chromatograms for separation of BSA and hIgG mixture by PBT-GMA-SO_3 nonwovens grafted at 28%wt and functionalized using 2 mg/ml Na_2SO_3. Column volume (CV): 0.47 ml, injection volume: 1 ml protein solution (5 mg/ml BSA and 5 mg/ml hIgG), RT: 8 min. Binding buffer: 20 mM Acetate pH 5.5, elution buffer: linear gradient from 20 mM Acetate pH 5.5 to 20 mM Acetate, 1 M NaCl, pH 5.5. **(B)** SDS-PAGE (reducing conditions) image corresponds to above chromatogram.

Table 12. Yield and purity of IgG separated from BSA and hIgG mixture by PBT-pGMA-SO_3 column (heat grafted nonwovens at 29% weight gain functionalized with mass ratio 2:15:75=Na_2SO_3:IPA:H_2 O %wt.) using a linear salt gradient.

Elution mode	hIgG Yield	hIgG Purity
Linear salt gradient from 20 mM Acetate pH 5.5 to 20 mM Acetate pH 5.5 + 1 M NaCl	90%	70%

It can be observed from the SDS-PAGE (Figure 48) that linear increment of NaCl concentration did not help to obtain separate elution peaks for BSA and hIgG. No significant advantages achieved from the gradient elution over the step elution approach.

Chapter 5

Conclusions and future work

PBT nonwovens were successfully grafted with polyGMA using heat induced grafting (HIG) method and UV induced grafting (UVG) method. PBT-pGMA nonwovens were then functionalized with DEA to become weak anion exchangers and with sulfonic acid groups to become strong cation exchangers, respectively. The conclusions can be found as follows:

- For HIG nonwovens, a polymerization temperature of 80 °C and the use of thermal initiator BPO exclusively in initiator solution were found to be the conditions to fabricate membranes with high protein binding capacity.
- For HIG nonwovens, the desirable DEA ligand density on the grafted layer can not be controlled changing the DEA concentration in the functionalization solution, however, it is possible through the % weight gain that is reachable using different polymerization time.
- For HIG nonwovens, even no correlation found between BSA binding capacity and ligand density as well as between % (v/v) DEA and ligand density were registered, the EBC values can be altered by varying the DEA concentration in the functionalization solution.
- Equilibrium binding capacity as high as 673 mg/g was observed for the HIG nonwovens grafted at 28% weight gain and functionalized using 30% v/v DEA in aqueous solution (corresponding to ligand density of 1.54 mmol/g) as anion exchangers for BSA binding.
- For the cation exchange HIG nonwoven it was found that the higher the SO_3 ligand density on the nonwovens, the higher the protein bound. Additionally, it was observed that varying SO_3 concentration in the functionalization solution it is possible to have the control of ligand density on the grafted layer, reaching the highest value using a mass ratio of Na_2SO_3:IPA:H_2O=2:15:75 %wt. among the all % weight gain investigated. Equilibrium binding capacity as high as 675 mg/g was observed for HIG nonwovens at 29% weight gain functionalized as cation exchanger (ligand density of 0.47 mmol/g) for the binding of hIgG.

- No positive effect were observed reducing ligand concentration in the functionalization solution for UVG nonwovens, where the maximum binding capacities of 1209 mg/g and 1563 mg/g were achieved for UV grafted membranes at 19 % weight gain, functionalized with 70% v/v DEA or a mass ratio of Na_2SO_3:IPA:H_2O=10:15:75 %wt. as anion- and cation- exchangers respectively.
- This different behavior between HIG and UVG nonwovens is due to the structural differences between the two grafting methods. It is believed that UVG nonwoven is characterized by a network of independent free moving brushes which rearrange in case of steric hindrance due to electrostatic repulsion during the interactions between ligand and protein. This rearrangement is not possible for HIG nonwovens due to the cross-linking structure, favoring the functionalization condition of low ligand concentration during the that permit to reach the best binding state.
- The performance of ion exchange of HIG PBT nonwovens were evaluated under flow conditions. Rigid PET nonwoven spacers were used to separate individual PBT nonwoven layers in order to increase the total flow porosity of the columns that were determined experimentally to be 52% for PBT-pGMA-SO_3 column. The pressure drops of the heat grafted PBT nonwoven ion exchangers demonstrated to be dependent on the ionic strength of the mobile phase due to partial swelling of the grafted layer causing the blocking of the pores. The dynamic binding capacities valuated at 10% of breakthrough, for BSA capture, using the anion exchange HIG nonwovens grafted at 28% weight gain and functionalized with 30% v/v DEA, increase from 109 mg/g to 168 mg/g , increasing the residence time from 2.4 to 7.9 minutes. The $DBC_{10\%}$ for hIgG capture using the cation exchange HIG nonwovens grafted at 29% weight gain were approximately 100 mg/g for residence time of 3.9 and 7.9 minutes. The anion-and cation- exchange HIG PBT nonwovens were evaluated for their ability to selectively adsorb and selectively elute BSA or hIgG from a mixture of proteins. While with cation exchange nonwovens was not reached a good protein separation, anion exchange HIG nonwovens were able to absorb and elute BSA with high purity and yield in a single step of purification.

The results of the research encourage a further characterization of the modules examined. In particular, a mathematical model needs to be developed and validated with the experimental data obtained, capable to determine the ligand density, using as input variables the % weigh gain of the sample, volume of the solution, weight of the sample and the ligand concentration used in functionalization step. Other aspect that need further investigation could be the effect of the number of PET spacer in the column on the dynamic binding capacity. The research group of Professor R.G. Carbonell has continued the study on these membranes, obtaining excellent results regarding the protein purification. Good dynamic binding capacity and high purity of hIgG, were achieved using a column packed exclusively with cation exchange PBT membranes, modified with conditions such as to achieve the best performance of these membrane and my dissertation has helped to define the optimum conditions to achieve the excellent improvement. In order to further decrease any nonspecific protein adsorption on the membranes, a copolymer grafted layer (using as second polymer HEMA) is under consideration. It is believed that reducing the charge density on the membranes, possible by copolymerization with HEMA having hydroxyl group, lead to decrease the binding of unwanted localized charge pockets on the protein.

References

[1] R. M. Price, A. Sadana, "ENGINEERING PROCESS CONTROL OF BIOSEPARATION PROCESSES," in *Handbook of Bioseparations* , vol. 2, Separation Science and Technology, 2000, pp. 659-665.

[2] D. C. Andersen, L. Krummen, "Recombinant protein expression for therapeutic applications," *Current Opinion in Biotechnology,* vol. 13, p. 117–123, 2002.

[3] G. Z.-P. J. H. Chon, "Advances in the production and downstream processing of antibodies," *New Biotechnology,* vol. 28, no. 5, pp. 458-463, 2011.

[4] E. Fiedler 1, M. Fiedler, G. Proetzel, T. Scheuermann, U. Fiedler, R. Rudolph, "Affilin™ Molecules: Novel Ligands for Bioseparation," *Food and Bioproducts Processing,* vol. 86, pp. 3-8, 2006.

[5] P.Y. Huang, R.G. Carbonell, "Affinity purification of proteins using ligands derived from peptide libraries.," *Biotechnol Bioeng.,* vol. 47(3), pp. 288-97, 1995.

[6] T. Vicentea, M. F.Q. Sousaa, C. Peixotoa, J.P.B. Motab, P. M. Alvesa, M.J.T. Carrondoa, "Anion-exchange membrane chromatography for purification of rotavirus-like particles," *Journal of Membrane Science,* vol. 311, p. 270–283, 2008.

[7] D. P.-J. M. B. M. B. M. R. G. R. C. J. M. Nova, "Elaboration, characterization and study of a new hybrid chitosan/ceramic membrane for affinity membrane chromatography," *Journal of Membrane Science,* vol. 321 , p. 81–89, 2008.

[8] R. Ghosh, "Protein separation using membrane chromatography: opportunities and challenges," *Journal of Chromatography A,* pp. 13-27, 2002.

[9] X. Zeng, E. Ruckenstein, "Membrane Chromatography: Preparation and Applications to Protein Separation," *Biotechnol. Prog.,* vol. 15, p. 1003−1019, 1999.

[10] A. A. Shuklaemail, U. Gottschalk, "Single-use disposable technologies for biopharmaceutical manufacturing," *Trends in Biotechnology,* vol. 31, p. 147–154, 2013.

[11] "Global Biopharmaceuticals Market Growth, Trends & Forecasts (2014 - 2020)," August 2016. [Online]. Available: http://www.mordorintelligence.com/industry-reports/global-biopharmaceuticals-market-industry. [Accessed 23 August 2016].

[12] B. Sekhon, "Biopharmaceuticals: an overview," *Thai J. Pharm. Sci*, vol. 34, pp. 1-19, 2010.

[13] F. Li, B. Lee, J. X. Zhou, T. Tressel, X. Yang, "Current therapeutic antibody production and process optimization," *Bioprocessing Journal,*, pp. 1-8, 2005.

[14] G. Healthcare, Ion Exchange Chromatography & Chromatofocusing. Principles and Methods, Sweden, 2010.

[15] Ion Exchange Chromatography. Principles and Methods, Amersham Biosciences.

[16] Ion Exchange Chromatography.Principles and Methods, Amersham pharmacia biotech .

[17] F.H. Arnold, H.W. Blanch, C.R. Wilke, "Analysis of Affinity Separations I: Predicting the Performance of Affinity Adsorbers," *The Chemical Engineering Journal*, vol. 30, pp. B9-B23, 1985.

[18] I. Sellick, "Capturing large biomolecules with membrane chromatography," *Innovations in Pharmaceutical Technology*, pp. 50-56, 2006.

[19] L. Crossley, "Membrane Chromatography:Not Just for Viral Clearance Anymore?," Nysa Membrane Technologies, 20 February 2007. [Online]. Available: https://www.wpi.edu/Images/CMS/BEI/lisacrossley.pdf. [Accessed 23 August 2016].

[20] S.M. Cramer, M.A. Holstein, "Downstream bioprocessing: Recent advances and future promise," *Current Opinion in Chemical Engineering*, vol. 1, pp. 27-37, 2011.

[21] S. Dimartino, *Studio sperimentale e modellazione della separazione di proteine con membrane di affinità*, Bologna: Tesi di dottorato, Alma Mater Studiorum, Università di Bologna, 2009.

[22] L. Z. M. M.-Y. C. P. C. V. Orr, "Recent advances in bioprocessing application of membrane chromatography," *Biotechnology Advances*, vol. 31, p. 450–465, 2013.

[23] technicaltextile.net, "Nonwoven Manufacturing," technical textile, [Online]. Available: http://www.technicaltextile.net/articles/nonwoven-textiles/detail.aspx?article_id=7188&pageno=1. [Accessed 20 August 2016].

[24] S. Russell, Handbook of nonwovens, WOODHEAD PUBLISHING LIMITED.

[25] I. Hutten, Handbook of Non-Woven Filter Media, Elsevier Science & Technology Books, 2007.

[26] W. Albrecht, H. Fuchs, W. Kittelmann, Nonwoven Fabrics: Raw Materials, Manufacture, Applications, Characteristics, Testing Processes, WILEY-VCH, 2003.

[27] Y. Zheng, H. Liu, P.V.Gurgel, R.G. Carbonell, "Polypropylene nonwoven fabrics with conformal grafting of poly(glycidyl methacrylate) for bioseparations," *Journal of membrane science*, 2010.

[28] G. Tanchis, The nonwovens, Fondazione ACIMIT, 2008.

[29] G.S. Bhat, S.R. Malkan, "Extruded continuous filament nonwovens: Advances in scientific aspects," *Journal of Applied Polymer Science,* vol. 83, p. 572–585 , 2002.

[30] M. Heller, *Polymer Grafted Nonwoven Membrane for Bioseparations*, Raleigh, North Carolina: PhD Thesis, 2015.

[31] A. D. W. G. C. W. M. F. S. B. C. J. Ellison, "Melt blown nanofibers: Fiber diameter distributions and onset of fiber breakup," *Polymer,* vol. 48, pp. 3306-3316, 2007.

[32] I. C. D.H. Reneker, "Nanometre diameter fibres of polyme, produced by electrospinning," *Nanotechnology*, vol. 7, p. 216–223, 1996.

[33] [Online]. Available: http://www.kasen.co.jp/english/product/line/work.html.

[34] S. R. M. G. S. Bhat, "Extruded continuous filament nonwovens: Advances in scientific aspects," *JournalofAppliedPolymerScience*, vol. 83, p. 572–585, 2002.

[35] A. Durany, N. Anantharamaiah, B. Pourdeyhimi, "High surface area nonwovens via fibrillating spunbonded nonwovens comprising Islands-in-the-Sea bicomponent filaments: structure–process–property relationships," *J Mater Sci* , vol. 44, p. 5926–5934, 2009.

[36] H. Liu, Y. Zheng, P. V. Gurgel, R. G. Carbonell, "Affinity membrane development from PBT nonwoven by photo-induced graft polymerization, hydrophilization and ligand attachment," *Journal of Membrane Science,* p. 562–575, 2013.

[37] S. Kalia, B. S.Kaith, I. Kaur, "Chemical Functionalization of Cellulose Derived from Nonconventional Sources," in *Cellulose Fibers: Bio- and Nano-Polymer Composites. Green Chemistry and Technology*, Springer, 2011, pp. 42-60.

[38] K. Kato, E. Uchida, E.T. Kang, Y. Uyama, Y. Ikada, "Polymer surface with graft chains," *Progress in Polymer Science,* vol. 28, p. 209–259, 2003.

[39] F. S. T. H. M. S. T. T. J. X. Zhou, "Viral Clearance Using Disposable Systems in

Monoclonal Antibody Commercial Downstream Processing," *Biotechnology and Bioengineering*, vol. 100, no. 3, pp. 488-496, 2008.

[40] J. X. Zhou, T. Tressel, "Basic Concepts in Q Membrane Chromatography for Large-Scale Antibody," *Biotechnol. Prog.*, vol. 22, p. 341−349, 2006.

[41] Z. Xu, L. Wan, X. Huang, "Surface Modification by Graft Polymerization," in *Surface Engineering of Polymer Membranes*, Berlin, Germany: Springer Berlin Heidelberg, 2009.

[42] H. Liu, P.V. Gurgel, R.G. Carbonell, "Preparation and characterization of anion exchange adsorptive nonwoven membranes with high protein binding capacity," *Journal of Membrane Science,* vol. 493, p. 349–359, 2015.

[43] E. G. Vlakh, T. B. Tennikova, "Preparation of methacrylate monoliths," *Journal of separation science,* pp. 30(17), 2801–2813, 2007.

[44] H. Liu, *Surface modified nonwoven membranes for bioseparations,* Raleigh, NC: PhD Thesis, 2010.

[45] J. Brandrup, E.H. Immergut, E.A. Grulke, Polymer Handbook 4th Edition, NY: John Wiley, 1999.

[46] G. Odian, Principles of Polymerization Fourth Edition, NJ: Wiley and Sons, 2004.

[47] H. Ma, R.H. Davis, C.N. Bowman, "A novel sequential photoinduced living graft polymerization," *Macromolecules,* pp. 33(2), 331-335, 1999.

[48] G.Odian, "Radical Chain Polymerization," in *Principles of Polymerization*, 4 ed., Hoboken, NJ: Wiley and Sons, 2004.

[49] R. Molenaar, J.J. ten Bosch, J.R. Zijp, "Determination of Kubelka–Munk scattering and absorption coefficients by diffuse illumination," *AppliedOptics,* pp. 38(10), 2068-2077, 1999.

[50] M.Kim, K.Saito, S. Furusaki, T. Sugo, J. Okamoto, "Water flux and proteinadsoprion of a hollowfiber modified with hydroxyl groups," *Journal of Membrane Science,* pp. 56(3), 289-302, 1991.

[51] C. Wolf, W.r Burchard, "Branching in Free Radical Polymerization due to chain transfer. Application to poly(vinyl acetate)," *Makromol. Chem.*, vol. 177, pp. 2519-2538, 1976.

[52] S. Ge, K. Kojio, A. Takahara, T. Kajiyama , "Bovine serum albumin adsorption onto immobilized organotrichlorosilane surface: Influence of the phase separation

on protein adsorption patterns," *Journal of Biomaterials Science,* vol. 9, no. 2, pp. 131-150, 1998.

[53] A. I. Liapis, E. Riccardi, J.Wang, "Effects on the dynamic utilization of the adsorptive capacity of chromatographic columns induced by non-uniform ligand density distributions," *Journal of Separation Science,* vol. 33, no. 17-18, p. 2749–2756, 2010.

[54] K.H. Gebauer, J. Thömmes, M.R. Kula, "Breakthrough performance of high-capacity membrane adsorbers in protein chromatography," *Chemical Engineering Science,* vol. 52, no. 3, pp. 405-419, 1997.

[55] K. Wrzosek, M. Gramblicka, M. Polakovic, "Influence of ligand density on antibody binding capacity of cation-exchange adsorbents," *Journal of Chromatography A,* vol. 1216 , no. 25, p. 5039–5044, 2009.

[56] S.Tsuneda, K.i Saito, T. Sugo, K. Makuuchi, "Protein adsorption characteristics of porous and tentacle anion-exchange membrane prepared by radiation-induced graft polymerization," *Radiation Physics and Chemistry,* vol. 46, no. 2, pp. 239-245, 1995.

[57] L. Bai, S.r Burman, L. Gledhill, "Development of ion exchange chromatography methods for monoclonal antibodies," *Journal of Pharmaceutical and Biomedical Analysis,* vol. 22, p. 605–611, 2000.

[58] A. M. ,. M. R. P. ,. P. R. L. G.Denton, "Direct isolation of monoclonal antibodies from tissue culture supernatant using the cation-exchange cellulose Express-Ion S," *Journal of Chromatography A,* vol. 908, p. 223–234, 2001.

[59] GE Healthcare, *Application note 28-9372-07 AA*, Uppsala, Sweden, 2010.

[60] Dupont, *Product information: DuPont™ Crastin® 6130NC010,* Wilmington, DE, 2004.

[61] Z. Papai, T.L. Pap , "Analysis of peak asymmetry in chromatography," *Journal of Chromatography A,* vol. 953, p. 31–38, 2002.

[62] S. Levin, "High Performance Liquid Chromatography (HPLC) in the pharmaceutical analysis," Feb 2010. [Online]. Available: http://www.forumsci.co.il/HPLC/WEB-Pharm_Review/HPLC_pharma_WEB_15-2-10.html. [Accessed 7 August 2016].

[63] N. Mao, S. J. Russell, "Characterisation, testing and modelling of nonwoven

fabrics," in *Handbook of Nonwovens*, 2007, pp. 401-514.

[64] J. Garnett, "Grafting," *Radiation Physics and Chemistry*, pp. 14(1-2), 79-99, 1979.

[65] C. Harinarayan, J. Mueller, A. Ljunglof, R. Fahrner,J. Van Alstine, R. van Reis, "An Exclusion Mechanism in Ion Exchange Chromatography," *Biotechnology and Bioengineering*, vol. 95, no. 5, pp. 775-87, 2006.

[66] A. L. Zydney, C. Harinarayan, R. van Reis, "Modeling electrostatic exclusion effects during ion exchange chromatography of monoclonal antibodies," *Biotechnology and Bioengineering*, vol. 102, no. 4, p. 1131–1140, 2008.

[67] S. J. Russell, "Characterisation, testing and modelling of nonwoven fabrics," in *Handbook of nonwovens*, 2006.

[68] J. W. Dolan, *Peak Tailing and Resolution*, Walnut Creek, California, USA: LC Resources Inc.

[69] N. Fedorova, B. Pourdeyhimi, "High Strength Nylon Micro- and Nanofiber Based Nonwovens via Spunbonding," *Journal of Applied Polymer Science*, vol. 104, p. 3434–3442, 2007.